

Universidade do Minho
Escola de Ciências da Saúde

Paulo César Gonçalves Marques

A network approach to brain aging through multimodal neuroimaging

julho de 2015



Universidade do Minho
Escola de Ciências da Saúde

Paulo César Gonçalves Marques

A network approach to brain aging through multimodal neuroimaging

Tese de Doutoramento em Ciências da Saúde

Trabalho realizado sob a orientação do
Professor Doutor Nuno Jorge Carvalho Sousa

julho de 2015

STATEMENT OF INTEGRITY

I hereby declare having conducted my thesis with integrity. I confirm that I have not used plagiarism or any form of falsification of results in the process of the thesis elaboration. I further declare that I have fully acknowledged the Code of Ethical Conduct of the University of Minho.

University of Minho, 30/07/2015

Full name:
Paulo César Gonçalves Marques

Signature:
Paulo César Gonçalves Marques

Acknowledgments

The work presented in this thesis results from the contribution of numerous people to whom these words wont make justice for all the help and support they provided. I am extremely grateful all of you.

I would like to thank my family in the first place. My father Joaquim and my mother Maria Olinda are the main architects of who I am and what I am today. They have always ensured that I could take my own steps under solid foundations. To my brother Marco for all the arguments and partnership.

To Professor Nuno Sousa, my supervisor, for all the mentorship, support, guidance, clear insights and for encouraging me to take challenges. I deeply appreciate the availability and all the precious time spent in talking and discussing whatever was necessary. You are the main engineer of this work.

To Eng. José Miguel Soares for bringing me into the neuroimaging research topic, for teaching me everything he could, for all the help, wise and pragmatic advises, for the scientific discussions but also for the friendship and fun. To Pedro Moreira and Ricardo Magalhães for all the time spent together inside and outside the "neuroimaging lab", for helping me in acquiring, analyzing and discussing all the data and findings and for their major scientific contributions.

To Professor Victor Alves for all the assistance, advices and profitable collaborations since my masters degree.

To Carlos Portugal Nunes, Liliana Amorim and Teresa Castanho for your precious contribution to the Switchbox project and scientific discussions but mainly for your friendship, partnership and for being there for whatever was necessary

To Professor Nadine Santos, for all the support, contributions and assistance. This project would not be possible without your help.

To Professor Patricio Costa, for all the help and counseling in statistical analyses and also for all the enlightening discussions.

To all my friends and colleagues at ICVS, namely Pedro Morgado, Hugo Almeida, João Cerqueira, Vitor Hugo Pereira and many others for all the help and encouragement in my short scientific career.

To the School of Health Sciences and Life and Health Sciences Research Institute for accepting me into the PhD program in Health Sciences and providing the necessary tools.

To the staff from the Clinical Academic Center and the Imaging department of Hospital de Braga for the assistance in acquiring the data.

To all the participants from the Switchbox project.

To all my friends, in particular João Vieira and Hugo Costa, for all the conversations, laughs and relaxing moments.

Last, but definitely not the least, to my fiancée Emmanuelle for all the love, care and support. For being always by my side and encouraging me into this challenge, you are also a major contributor of this work.

This work was supported by a grant of the project SwitchBox-FP7-HEALTH-2010-grant 259772-2;

Abstract

Healthy aging is a dynamic and inevitable process characterized by cognitive declines and inter-individual variability. Even though these declines seem to be inevitable or hard to revert, some individuals are known decline slower than others, both functionally and cognitively. Alterations in brain structure and function, cognitive changes and other factors such as lifestyle, occupation or education are known to interact with each other and mutually contribute for the heterogeneity observed along the aging process. Although, the neuroscience research community has put a lot of effort in understanding the structural and functional changes that take place in the human brain along aging, most studies have precluded the fact that the human brain is complex network (connectome) with interactions between different brain regions/structures and where both passive and reactive processes take place. The main goal of the present thesis was to provide new insights on how the human brain network ages and try to identify biomarkers of overall good cognitive healthy aging.

Results indicate that older individuals with overall good cognitive performance present lower levels of macro and micro-structural indicators of white matter (WM) lesioning/degeneration than poor performers while WM volumetry does not account for inter-individual variability in performance. At the functional level, overall good cognitive performance is associated with increased local and global network segregation and integration revealing that both specialization of clusters in particular functions as well as efficient information flow through the entire brain network play important roles in cognition. We also revealed for the first time the brain networks whose functional connectivity (FC) levels are associated with important contributors for inter-individual variability in cognitive performance, namely education level and cognitive reserve (CR). These factors were associated with local and global changes in network characteristics and we have demonstrated that CR is associated with higher global efficiency of the FC-derived brain connectome. Finally we demonstrated through a longitudinal analysis that aging is associated with both decreases and increases in FC. Local network alterations that occur in aging have a negative impact mostly in frontal regions accompanied by local rearrangements possibly reflecting compensatory mechanisms that ultimately lead to no alterations in global network properties. Furthermore we revealed that changes in local clustering of the putamen and hippocampus are biomarkers of longitudinal trajectories of learning and recall, respectively.

Concluding, we revealed that better cognitive performance in aging reflects both preserved brain structure as well as more efficient and segregated brain networks with education and CR playing important roles in brain network function in aging. Aging itself produces rearrangements in brain network properties, possibly reflecting both detrimental effects and compensatory mechanisms, and changes in local network properties associate with changes in cognition. This also suggests that network approaches are useful tools to assess brain function providing new biomarkers of successful aging.

Uma abordagem de redes ao envelhecimento cerebral através de técnicas neuroimagiológicas multimodais

Resumo

O envelhecimento saudável é um processo dinâmico e inevitável caracterizado por declínios cognitivos e variabilidade inter-indivíduos. Apesar destes declínios parecerem ser inevitáveis ou difíceis de reverter, alguns indivíduos apresentam maiores declínios do que outros, quer funcionalmente quer cognitivamente. Sabe-se que alterações na estrutura/função cerebral, alterações cognitivas e outros factores como o estilo de vida, a ocupação ou o nível educacional, são fatores conhecidos que interagirem e contribuem mutuamente para a heterogeneidade observada ao longo do envelhecimento. Apesar da comunidade científica de neurociências ter colocado um amplo esforço na tentativa de perceber quais as alterações estruturais e funcionais que acompanham o envelhecimento, a maioria dos estudos negligencia o fato do cérebro ser uma rede complexa (conetoma) com interações entre diferentes estruturas/regiões cerebrais onde vários processos ativos e reativos acontecem. O principal objetivo da presente tese consiste em fornecer novos dados sobre como a rede cerebral humana envelhece na tentativa de identificar novos bio-marcadores de boa cognição geral no envelhecimento saudável.

Os resultados indicam que as pessoas mais velhas com boa performance cognitiva geral apresentam menores níveis de indicadores micro- e macro-estruturais de lesão/degeneração de substância branca (SB) do que indivíduos com má performance cognitiva geral e que a volumetria de SB não parece explicar a variabilidade inter-indivíduos. Ao nível funcional, boa performance cognitiva geral está associada com maior segregação local e integração, revelando que quer a especialização de grupos de regiões em determinadas funções quer um fluxo de informação mais eficientes ao longo de toda a rede cerebral são fatores importantes para a cognição. Nesta tese revelámos pela primeira vez quais as redes cerebrais cujos níveis de conetividade funcional (CF) se associam com fatores que contribuem fortemente para a variabilidade cognitiva inter-indivídual, nomeadamente o nível educacional e a reserva cognitiva (RC). Estes fatores estão associados com alterações topológicas locais e globais e demonstrámos ainda que a RC está associada com uma maior eficiência global da do conetoma cerebral obtido a partir de CF. Por fim, demonstrámos através de uma abordagem

longitudinal que o envelhecimento se encontra associado a decréscimos e aumentos de CF. Alterações locais na rede que acontecem ao longo do envelhecimento afectam negativamente regiões frontais que são acompanhadas por rearranjos topológicos locais, possivelmente refletindo mecanismos compensatórios e que levam a que as propriedades globais da rede não sejam afectadas. Revelámos ainda que alterações no *clustering* local do putâmen e do hipocampo são bio-marcadores das trajetórias longitudinais nos níveis de aprendizagem e de memória, respetivamente.

Em conclusão, foi demonstrado que melhor cognição geral no envelhecimento reflete uma estrutura cerebral preservada bem como uma rede cerebral mais eficiente e especializada, sendo a educação e o RC fatores importantes para a função da rede cerebral no envelhecimento. O envelhecimento, por si, produz rearranjos nas propriedades da rede cerebral, possivelmente refletindo efeitos prejudiciais e compensatórios, e alterações nas propriedades locais da rede cerebral estão associadas com alterações na performance cognitiva. Isto sugere ainda que abordagens de redes são ferramentas úteis no estudo da função cerebral, providenciando novos bio-marcadores de envelhecimento saudável.

Table of Contents

Acknowledgments v

Abstract vii

Resumo ix

Table of Contents xi

List of Abbreviations xv

List of Figures xvii

List of Tables xxi

CHAPTER I 1

THE AGING BRAIN NETWORK AND COGNITION 1

1. Introduction 3

2. Aging and cognitive decline 3

3. Brain Aging 6

   3.1 Structural alterations 6

   3.2 Functional alterations 7

   3.3 Models of cognitive aging 8

4. Neuroimaging in aging 10

   4.1 Structural MRI 11

   4.2 Functional MRI 13

   4.3 The connectomic approach 14

5. Objectives 16

6. References 17

CHAPTER II 31

MACRO- AND MICRO-STRUCTURAL WHITE MATTER DIFFERENCES CORRELATE WITH COGNITIVE PERFORMANCE IN HEALTHY AGING 31

Abstract 34

1. Introduction 35

2. Methods 37

   2.1 Ethics statement 37

2.2 Neurocognitive assessment 37
2.3 Principal Component Analysis and clusters of cognitive performance 38
2.4 Participants 39
2.5 Data acquisition 39
2.6 White matter segmentation and WMSA volume estimation 40
2.7 DWI data pre-processing and tensor fitting 40
2.8 Tract Based Spatial Statistics 41
2.9 Statistical analysis 42
3. Results 43
3.1 Sample characteristics 43
3.2 White matter volumetry 44
3.3 Group by age interactions in DTI metrics 45
3.4 Age effect on DTI metrics 47
3.5 Group effect on DTI metrics 47
4. Discussion 50
5. References 54

CHAPTER III **65**

THE BOUNDS OF EDUCATION IN THE HUMAN BRAIN CONNECTOME **65**

Abstract 68
1. Introduction 68
2. Methods 69
2.1 Participants 69
2.2 Image Acquisition 70
2.3 Image Preprocessing 70
2.4 Network Analysis 71
3. Results 72
3.1 Demographic Characterization 72
3.2 Associations between age and FC networks 73
3.3 Associations between years of formal education and FC networks 73
4. Discussion 78
5. References 80

CHAPTER IV **107**

THE FUNCTIONAL CONNECTOME OF COGNITIVE RESERVE **107**

Abstract 110

1. Introduction 110

2. Methods 112

2.1 Ethics Statement 112

2.2 Participants 112

2.3 Magnetic Resonance Imaging Acquisition 113

2.4 Structural Segmentation 114

2.5 Specification of the Structural Equation Model 114

2.6 Rs-fMRI Data Preprocessing 116

2.7 Network Construction 118

2.8 Network-Based Statistics Analyses 118

2.9 Graph Theory Analysis 119

3. Results 120

3.1 Sample characteristics 120

3.2 Latent Variable Model 121

3.3 Effects of the Cognitive Reserve Latent Variable 121

3.4 Effects of the Demographic Latent Variable 123

3.5 Effects of the Brain Reserve Latent Variable 125

4. Discussion 125

5. References 127

CHAPTER V **133**

CONNECTOMIC FUNCTIONAL BRAIN CHANGES IN HEALTHY AGING AND AGE-RELATED COGNITIVE DECLINE **133**

Abstract 136

1. Introduction 136

2. Methods 139

2.1 Ethics Statement 139

2.2 Participants 139

2.3 Neurocognitive assessment 140
2.4 Magnetic Resonance Imaging Acquisition 141
2.5 Preprocessing of rs-fMRI data 141
2.6 Network construction 142
2.7 Graph theory analysis 142
2.8 Statistical Analysis 143
3. Results 145
3.1 Demographic and cognitive characterization 145
3.2 Differences in network properties between groups of cognitive performance 145
3.3 Age-related trajectories in network properties 148
3.4 Group differences in network properties' trajectories 152
3.5 Associations with cognitive decline 152
4. Discussion 153
5. References 156

CHAPTER VI **163**

GENERAL DISCUSSION **163**

1. Discussion 165
2. Future perspectives 171
3. References 171

List of Abbreviations

A

AAL - Anatomical Automatic Labeling

AD - Axial diffusivity

ANCOVA - Analysis of covariance

ANOVA - Analysis of variance

ASL - Arterial Spin Labeling

B

BOLD - Blood-oxygen-level dependent

BP - Blood Pressure

BR - Brain reserve

C

CLTR - Consistent long term retrieval

COWAT - Controlled oral word association test

CR - Cognitive reserve

CRUNCH - Compensation-related utilization of neural circuits hypothesis

CSF - cerebrospinal fluid

D

DB - Digits Backward

DF - Digits Forward

DMN - Default mode network

DR - delayed recall

DSST - Digit symbol substitution test

DTI - Diffusion tensor imaging

DWI - Diffusion Weighted Imaging

E

EEG - Electroencephalogram

EPI - echo-planar imaging

EXEC - Executive functioning dimension

F

FA - Fractional anisotropy

FC - Functional connectivity

FDR - False discovery rate

FLAIR - Fluid attenuation inversion recovery

fMRI - Functional magnetic resonance imaging

FoV - Field of view

FWE - Family-wise error

G

GDS - Geriatric depression scale

GENEXEC - general executive functioning component

GLM - general linear model

GM - Gray matter

GMC - Gray matter component

GMV - Gray matter volume

H

HAROLD - Hemispheric asymmetry reduction in older adults

I

ICA - Independent component analysis

ICV - Intracranial volume

IQ - Intelligence quotient

L

LTS - Long-term storage

M

MCI - Mild cognitive impairment

MD - Mean diffusivity

MEG - Magneto-encephalogram

MEM - Memory component

MGCFA - Multiple group confirmatory factor analysis

MMSE - Mini-mental state examination

MNI - Montreal neurological institute

mPFC - Medial prefrontal cortex

MPRAGE - Magnetization prepared rapid gradient echo

MRI - Magnetic resonance imaging

MS - Multiple Sclerosis

N

NBS - Network Based Statistic

P

PASA - Posterior-anterior shift with aging

PCA - Principal Component Analysis

PCC - Posterior cingulate cortex

PD - Proton density

PET - Positron emission tomography

PFC - Prefrontal cortex

R

RD - Radial diffusivity

RESTORE - Robust estimation of tensors by outlier rejection

ROI - Region of interest

rs-fMRI - Resting state functional magnetic resonance imaging

RSN - Resting state network

S

SC - Structural connectivity

SD - standard deviation

SE - Spin echo

SMN - Sensorimotor network

SN - Salience Network

SRT - Selective reminding test

STAC - Scaffolding theory of aging and cognition

SW - Stroop words

SWC - Stroop Words Colors

T

TBSS - Tract based spatial statistics

TE - Time of echo

TFCE - Threshold free cluster enhancement

TR - Time of repetition

V

VBM - Voxel based morphometry

W

WM - White matter

WMC - White matter component

WMHI - white matter hyper-intensities

List of Figures

CHAPTER I

Figure 1. Model of interacting dimensions in aging. Aging interacts with several sub-dimensions of cognition, brain structure/function and other factors such as life events or genetic factors. (Adapted from (Grady, 2012))

Figure 2. Overview of human connectome analyses. Whole brain modeling of connectivity can be achieved through pairwise FC (**a**), through co-variances of brain volumes/thickness (**b**) or tractography derived SC (**c**). Analysis can be performed at the edge (**d**), node (**e**) and global network level (**f**).

CHAPTER II

Figure 1. Statistically significant group by age interactions in FA, RD and AD projected maps, before (A, C, E) and after (B, D, F) controlling for WMSA volume. Significance threshold was set to $p < 0.05$ (FWE corrected for multiple comparisons). Blue/light-blue gradient indicates lower age slopes for good cognitive performers when compared to poor cognitive performers. Red/yellow gradient indicates higher age slopes for the good cognitive performance group.

Figure 2. Statistically significant associations between age and FA, RD and AD maps, before (A, C, E) and after (B, D, F) controlling for WMSA volume. Blue/light-blue gradient indicates negative associations with age. Red/yellow gradient indicates positive. All results were considered significant at $p < 0.05$ (FWE corrected for multiple comparisons).

Figure 3. Statistically significant group differences in FA, RD and AD maps, before (A, C, E) and after (B, D, F) controlling for WMSA volume. Blue/light-blue gradient indicates lower values for good cognitive performers when compared to poor cognitive performers. Red/yellow gradient indicates higher values for the good cognitive performance group. All results were considered significant at $p < 0.05$ (FWE corrected for multiple comparisons).

CHAPTER III

Figure 1. Functional connectivity matrices and edge length distribution of the edges surviving the primary thresholding procedure. Both positive and negative associations with age survive the three ($p < 0.01$, $p < 0.005$, $p < 0.001$) primary thresholds of the NBS analysis (a). Positive associations with age occur mainly in short-range connections while negative associations can be found in medium to long-range edges (b). Similarly, positive and negative associations with years of formal education survive the application of the primary thresholds (c) and the supra-threshold edges span a large range of lengths (d).

Figure 2. Networks showing significant associations between functional connectivity (FC) and age. A large sub-network was found to display a negative association between FC and aging using primary thresholds of $p < 0.01$ and $p < 0.005$ but not with a primary threshold of $p < 0.001$ (a). Younger subjects presented moderate positive mean FC values in this network while older subjects presented mean FC values close to zero along the network (b). In the upper panel (a), black dots represent AAL brain regions and blue edges denote edges with negative associations with age. Bottom panel (b) presents scatter plots of the mean FC of the statistically significant networks in function of age.

Figure 3. Networks showing significant associations between functional connectivity (FC) and years of education. A large sub-network showed a positive association between FC and years of formal education using primary thresholds of $p < 0.01$, $p < 0.005$ and $p < 0.001$. A focal sub-network displayed a negative association with years of education using a primary threshold of $p < 0.005$ and $p < 0.001$ (a). In the network that evidenced a positive association with FC, less educated subjects presented moderately low positive FC values while more educated subjects presented moderately high positive FC values (b). In the network with a negative association with years of formal education, mean FC ranges from low positive FC values to moderate negative mean FC values from individual with lower years of formal education to individuals with higher number of years of formal education (b). In the top panel (a) black dots represent AAL brain regions and blue and red edges denote edges with negative and positive associations with years of education, respectively. Bottom panel (b) presents scatter plots of the mean FC of the statistically significant networks in function of years of education.

CHAPTER IV

Figure 1. Structural equation model used in order to decompose memory (MEM) and general executive functioning (GENEXEC) factors into independent variables of demographic characteristics influence (DEM), brain reserve capacity measures (BR) and cognitive reserve (CR). DEM was mainly accounted for school years ($r = 0.88$) but also by sex ($r = 0.26$). Sex and school years were also correlated ($r = 0.35$). Intracranial Volume (ICV) correlated strongly ($r = 0.85$) with gray matter volume (GMV). As expected, the latent gray matter component (GMC) was significantly modeled by GMV ($r = 0.48$) and the latent white matter component (WMC) was almost entirely ($r = 0.97$) modeled by the volume of white matter signal abnormalities (WMSA). GMC positively accounted for BR ($r = 0.69$) and WMC negatively accounted for BR ($r = -0.73$) due to the inverse relationship between white matter lesioning and BR. BR was the greatest predictor of GENEXEC ($r = 0.66$), followed by CR ($r = 0.65$) and then BR ($r = 0.30$). MEM was mostly predicted by CR ($r = 0.88$), then by DEM ($r = 0.37$) and BR ($r = 0.28$).

Figure 2. Associations between CR and FC networks using primary thresholds of $p < 0.01$ (a), $p < 0.005$ (b) and $p < 0.001$ (c). Adjacency matrices after the application of the primary thresholds are presented in the middle of each panel. Edges from the networks revealing positive association are presented in red and from negative associations are presented in blue. Associations between CR and local efficiency (d), strength (e), clustering (f) and betweenness centrality (g). Statistically significant associations ($p < 0.05$, FDR corrected) are presented in filled bars and associations surviving an uncorrected threshold of $p < 0.05$ are reported for completeness using unfilled bars.

Figure 3. Scatter plots highlighting significant positive associations between CR and network global efficiency (a) and between DEM (b) and network transitivity.

Figure 4. Associations between DEM and FC networks using primary thresholds of $p < 0.01$ (a), $p < 0.005$ (b) and $p < 0.001$ (c). Adjacency matrices after the application of the primary thresholds are presented in the middle of each panel. Edges from the networks revealing positive association are presented in red and edges from negative associations are presented in blue. Associations between DEM and local efficiency (d), strength (e), clustering (f) and betweenness centrality (g). Statistically significant associations ($p < 0.05$, FDR corrected) are presented in filled bars and associations surviving an uncorrected threshold of $p < 0.05$ are reported for completeness using unfilled bars

Figure 5. Associations between BR and FC networks using primary thresholds of $p < 0.01$ (a), $p < 0.005$ (b) and $p < 0.001$ (c). Adjacency matrices after the application of the primary thresholds are presented in the middle of each panel. Edges from the networks revealing positive association are presented in red and edges from negative associations are presented in blue. Associations between BR and local efficiency (d), strength (e), clustering (f) and betweenness centrality (g). Statistically significant associations ($p < 0.05$, FDR corrected) are presented in filled bars and associations surviving an uncorrected threshold of $p < 0.05$ are reported for completeness using unfilled bars.

CHAPTER V

Figure 1. Significant group differences between good and poor cognitive performers in nodal network metrics. AAL regions showing significant ($p < 0.05$, FDR corrected for multiple comparisons) group effects in strength (a), clustering coefficient (b) and betweenness centrality (c). Red dots represent nodes where the metric is higher in good than poor cognitive performers and blue dots represent nodes where the metric is lower in good performers compared to poor performers. Grey dots represent nodes without a significant effect.

Figure 2. Scatter plots of global network measures of each group at each assessment. Good performers presented (a) higher mean clustering coefficient and (b) global efficiency than poor

performers, while (c) no differences were found in assortativity (c). Good performers are represented in red, poor performers are represented in blue. Asterisks (*) denote significant group differences at $p < 0.001$.

Figure 3. Significant differences in sub-networks of FC. From the baseline assessment to the follow-up, a small sub-network evidenced increased FC (a) while another sub-network evidenced decreases in FC (b). Red lines represent connections showing increased FC and blue lines represent connections evidencing decreased FC. The size of each node is proportional to the number of connections involving that particular node.

Figure 4. Significant differences in local metrics between moments of assessment. Significant decreases ($p < 0.05$, FDR corrected for multiple comparisons) in (a) strength, (b) clustering coefficient, (c) local efficiency and (d) betweenness centrality (d) were found in several nodes. Red dots represent nodes showing increases in local metrics and blue dots represent nodes evidencing decreases in the same metrics from baseline to the follow-up assessment. Grey dots represent nodes without a significant effect.

Figure 5. Associations between changes in local clustering and changes cognitive dimensions. Changes in clustering coefficient of left putamen correlated positively with changes in Consistent Long-Term Retrieval (CLTR) (a) while reductions in Delayed Recall (DR) scores correlated negatively with changes in the clustering coefficient of the left hippocampus.

List of Tables

CHAPTER II

Table I. Basic characteristics of the study's sample.

Table II. White matter ROIs presenting statistically significant negative associations with age (results FDR corrected at $p < 0.05$).

CHAPTER III

Table I. Demographic and cognitive characteristics of the participants

CHAPTER IV

Table I. Demographic and cognitive characterization of the sample assessed in the study.

CHAPTER V

Table I. Demographic and cognitive characterization of the sample assessed in the study.

Table II. Comparison of nodal properties between groups. The table presents the direction of the results for each metric, the node label, F-statistic and corresponding uncorrected p-value. Results fully corrected for multiple comparisons using the FDR criterion ($p<0.05$).

Table III. Comparison of local metrics between moments of assessment. The table presents the direction of the results for each metric, the node label, F-statistic and corresponding uncorrected p-value. Results fully corrected for multiple comparisons using the FDR criterion ($p<0.05$).

CHAPTER I

The aging brain network and cognition

1. Introduction

Every year the number and proportion of older people increases. The societal impact of this change is notorious. The labor force of older people is lower, social security coverage needs to be higher, the risk of social isolation and economic dependence increases. Thus, for modern societies, the goal is not only to increase the life expectancy but also to ensure that everyone can age with security and dignity while actively participating in society (UN, 2010).

Even though aging is inevitable, some individuals seem to decline slower than others, both functionally and cognitively. This raises the question of which factors trigger changes in the homeostatic mechanisms - the ability of the human body to maintain an internal state of equilibrium while interacting and adjusting to changes in the external environment (Miller-Keane and O'Toole, 2003). This ability to cope with change plays an important role in healthy aging where internal and external signals need to be appropriately received, processed and integrated in order to produce adaptive responses. Triggers such as stress and adverse life events are known to cause disturbances in such mechanisms, induce maladaptive responses and predispose to cognitive impairment (McEwen, 2007;Dias-Ferreira et al., 2009;Sousa and Almeida, 2012). A better understanding of how these factors facilitate the maintenance of health through life is needed.

At the brain level, several functional and structural take place with aging and neuroimaging techniques have the potential to provide insights on how these brain changes relate with cognition. This is important to promote healthy brain aging and, consequently, well-being (Williams and Kemper, 2010;Abrahamson et al., 2012).

2. Aging and cognitive decline

The “normal” aging process is characterized by a natural and progressive cognitive decline (Brickman et al., 2005;Salthouse, 2009). Alterations in two major cognitive dimensions are commonly reported in aging studies – memory and executive functioning. Memory is commonly defined as the ability to encode, store and retrieve information; while, executive functioning refers to the ability to regulate and control cognitive processes (Melton, 1963).

Specifically, regarding the memory domain, cross-sectional studies have shown that older adults perform worse in episodic memory (Nyberg et al., 2003;Ronnlund et al., 2005), verbal (Nicholas et al., 1985) and non-verbal retrieval (Grady et al., 2002), when compared to younger adults. Declines in short-term memory in longitudinal assessments have also been evidenced (Hultsch et al., 1992). On the executive functioning domain, older adults also present age-associated differences in working memory (Hasher and Zacks, 1988), attention (Madden et al., 2005;Salthouse and Madden, 2008) and task switching (Kray and Lindenberger, 2000). Nonetheless, also of note, some cognitive domains such as semantic memory (i.e. vocabulary) and priming seem to be rather preserved (Bäckman et al., 2000;Ronnlund et al., 2005;Singh-Manoux et al., 2012), or even improved, with aging (Nyberg et al., 2003;Goh et al., 2012).

Although cognitive decline is one of the most notorious hallmark of aging, intra- and inter-individual variability is also evident. Intra-individual variability is used to refer to the observed variability in the performance of one individual across different tasks (Hilborn et al., 2009). Although initial investigations suggested that intra-individual variability could be a marker of neurological dysfunction, subsequent research suggests that this variability is normal in neurobiologically healthy individuals (Schretlen et al., 2003). Moreover, inter-individual variability also exists through the entire lifespan (Salthouse, 2012). In fact, cognitive decline is less pronounced in some individuals, with this effect being associated with a multitude of factors (MacDonald et al., 2003;Paulo et al., 2011;Santos et al., 2014). Some individuals actually seem to present preservation in domains where others evidence marked declines (Wilson et al., 2002;de Frias et al., 2009). These findings suggest that cognitive decline with aging is not a uniform phenomenon and distinct cognitive abilities may be more affected by aging (Goh et al., 2012). As such, one of the current challenges in geriatric/cognitive neurosciences is to understand which mechanisms underlie good or poor cognitive performance in older adults (Grady, 2012).

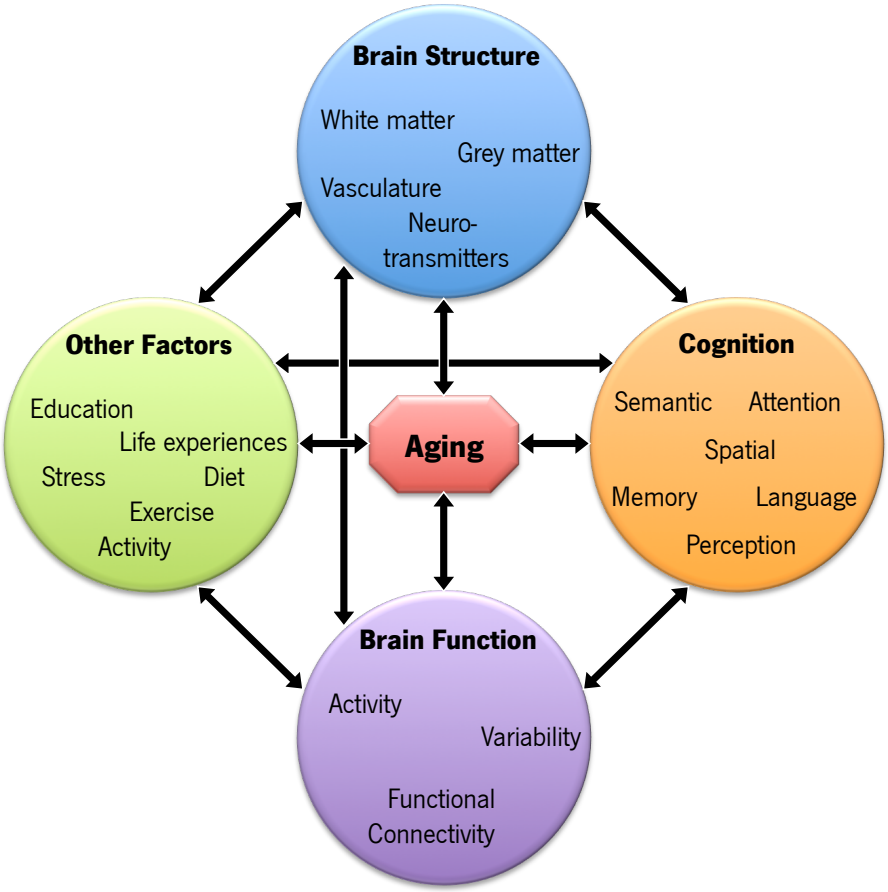


Figure 1. Model of interacting dimensions in aging. Aging interacts with several sub-dimensions of cognition, brain structure/function and other factors such as life events or genetic factors. (Adapted from (Grady, 2012))

In summary, aging is a rather complex phenomenon that influences and is influenced by a multitude of factors. Declines in cognition along aging are intrinsically associated to both brain aging in itself (functionally and structurally) and to other factors such as life experiences or genetic factors, which altogether can be mediators of age-related trajectories in cognition (Figure 1). These factors probably interact with each other and contribute for inter-individual variability in aging. Thus, multidimensional studies incorporating several of these factors can contribute greatly for the understanding of the aging process (Grady, 2012).

3. Brain Aging

Healthy aging is significantly determined by age-related cognitive decline. The relationship between brain structure/function and aging is bidirectional in the sense that the aging process impacts on brain properties and brain alterations have the potential to accelerate age-related cognitive decline. Yet, brain alterations observed in older individuals are not yet fully understood and several complementary and concurrent models have been purposed.

3.1 Structural alterations

One of the most reported findings in brain-aging studies is cortical atrophy. Similar to cognitive decline, age-related brain (macro) structural changes also present inter-individual variability and are not uniform across the whole brain. Some studies have reported global brain atrophy (Good et al., 2001;Sullivan et al., 2004) while others have shown that volumetric reductions occur primarily in frontal regions (Fjell et al., 2009). Some researchers have also explored associations between cognitive measures and brain volumes in older adults (Kaup et al., 2011;O'Shea et al., 2015). Kaup and colleagues (2011) tried to aggregate results from several studies and found that positive associations between brain volumetry and cognition were common, but inconsistent. The most consistent findings were the association between the hippocampus volume and memory and global cognition and between frontal volumes and executive function. They also highlighted that longitudinal studies were still scarce at the time of their review. Similarly to volumetric reductions, cortical thinning has also been reported to occur with aging (Hutton et al., 2009;Lemaitre et al., 2012).

Besides cortical (gray matter) changes, white matter (WM) alterations are also commonly associated with aging. Increased number of white matter hyperintensities (WMHI – localized findings that have bright appearance in T2-weighted Magnetic Resonance Imaging (MRI) images and absence of signal in T1-weighted MRI images) is quite common in aged individuals, especially in subcortical and periventricular areas. These well-known findings are commonly designated as white matter signal abnormalities (WMSA) or WMHI and may reflect ischemic lesions, perivascular spaces, gliosis or axonal degeneration/demyelination (Garde et al., 2000;De Leeuw et al., 2001;Wang et al., 2011). WMSA are usually unnoticed until an MRI

screening, but are associated with poorer cognition and functional status (Inzitari et al., 2009;Lockhart et al., 2014). Some age-related WM microstructural changes have also been described in Diffusion Tensor Imaging (DTI) studies. Although not directly measuring WM integrity, DTI indices suggest that aging is associated with axonal loss and demyelination (Pfefferbaum and Sullivan, 2003;Salat et al., 2005;Madden et al., 2009).

3.2 Functional alterations

Structural alterations at the brain level explain only part of the differences in cognitive functioning in older adults. A bigger challenge is to assess what are the brain activation levels and/or patterns associated with the decline in cognitive functioning. In human studies, insights regarding these features arise from several techniques such as positron emission tomography (PET), functional Magnetic Resonance Imaging (fMRI), electroencephalogram (EEG) or magnetoencephalogram (MEG).

Studies reporting reduced brain metabolism and blood flow in aging and associations to cognitive decline (Mosconi et al., 2008) could lead to the hypothesis that aging would be associated with decreased brain activation. However, one of the most surprising observations in aging studies is the greater regional activation level in older adults when compared to younger adults during the execution of given tasks (Dennis and Cabeza, 2008). This overactivation in older individuals has been mostly described in frontal regions during the execution of memory tasks (Cabeza et al., 1997;Madden et al., 1999). Additionally, some studies have observed this pattern to be accompanied by reductions in occipital activity and overactivation in frontal regions has been interpreted as a compensatory mechanism for reduced activation in occipital regions (Grady et al., 1994;Davis et al., 2008). Within older adults, but not in younger adults, increased activation has been associated with better performance. However, in some studies overactivation was not associated with better performance (Morcom et al., 2007), and associations between increased prefrontal cortex (PFC) activation and poorer memory have also been reported (de Chastelaine et al., 2011). Another common finding in task-related neuroimaging studies in aging is the increase bilateral pattern of activation found in older adults, when compared to younger ones who tend to present more unilateral activations (Cabeza et al., 1997;Reuter-Lorenz et al., 2000).

In resting conditions, reductions in inter-correlated patterns of activity - functional connectivity (FC) – between several brain regions are the most common finding (Ferreira and Busatto, 2013). Most of these findings concern the Default Mode Network (DMN) (Damoiseaux et al., 2008;Koch et al., 2010), a group of regions involving the medial prefrontal cortex (mPFC), precuneus/posterior cingulate cortex (PCC) and inferior parietal lobes (Raichle et al., 2001). Although less consistently, negative associations between age and FC have also been reported for the salience network (SN) and sensory-motor network (SMN) and these have been associated with decreased performance in a motor task (Wu et al., 2007;Onoda et al., 2012).

3.3 Models of cognitive aging

As previously described, aging impacts not only cognition but also brain structure and function. Several models have been proposed with the aim of explaining associations between aging, cognition and imaging findings as well as inter-individual differences in cognition.

One of the most well known models of cognitive aging is the Posterior-Anterior Shift with Aging (PASA) (Davis et al., 2008). According to this model older adults display greater activations, especially in frontal regions, compared to younger adults, as a compensatory mechanism to counterbalance the impairments resulting from the aging process. This model is further supported by observations of bilateral activations in the prefrontal cortex (PFC) in older adults, compared to unilateral activations in younger individuals (Reuter-Lorenz et al., 2000), and by reductions in deactivation in midline posterior regions (Davis et al., 2008). Decreased deactivation in such regions has been interpreted as an increased demand to reallocate resources from the DMN. Additionally, the more symmetric pattern of frontal activations in older individuals has gave rise to the Hemispheric Asymmetry Reduction in OLDer adults (HAROLD) (Cabeza, 2002) model, which suggests that this increase in symmetry is due to the recruitment of the contralateral regions in order to compensate for age-related declines. The less lateralized patterns of activation in older individuals, the more diffuse patterns of activation and less selective activations across different tasks, lead some investigators to suggest that, with aging, the brain gets more dedifferentiated (Park et al., 2004).

Another aging model that builds on top of the compensatory mechanism hypothesis is the Compensation-Related Utilization of Neural Circuits Hypothesis (CRUNCH) model (Reuter-Lorenz and Cappell, 2008). According to this model, at low load levels of a certain task, older adults display greater activity than younger adults due to the need to recruit more resources. However, at higher loads, older individuals are not able to compensate properly, reaching a plateau of cognitive load and, thus, explaining why, in some studies, younger adults display greater levels of activation compared to older adults (Schneider-Garces et al., 2010).

One, more recent, alternative aging model is termed Scaffolding Theory of Aging and Cognition (STAC), which tries to accommodate both structural and functional neuroimaging findings (Park and Reuter-Lorenz, 2009;Reuter-Lorenz and Park, 2014). This model posits that a compensatory scaffolding mechanism is continuously engaged and, thus, when deterioration occurs in one circuitry, additional resources are recruited to meet demanding tasks. Additionally, life-course events have the potential to enhance or deplete neural resources.

The previously summarized models were mainly proposed to accommodate imaging findings associated with aging. On the other hand, others have been postulated to account for inter-individual differences in cognition. This variability can be observed both at the cognitive and brain (structural and functional) levels. However, impairment in one level does not necessarily imply impairments in others. In fact, early studies revealed that some individuals without clinically relevant functional impairments presented brain pathology at autopsy (Katzman et al., 1988). The concept of reserve was offered as a strategy to account for these discrepancies. Two models of reserve have been proposed: a passive one – the Brain Reserve (BR) model (Katzman, 1993) – and an active one – the Cognitive Reserve (CR) model (Stern, 2002).

According to the BR model, brain injury affects each subject in the same manner and the effects of brain injury sum together throughout the lifespan. When the sum of these events surpasses a given threshold, functional deficits appear. However, individuals with bigger brains, or higher number of neurons (i.e. proxies of BR), would have a higher brain reserve capacity meaning that, for the same amount of pathology, more BR implicates better functional outcomes (Katzman et al., 1988;Mortimer et al., 2003;Satz et al., 2011). This model is also referred to as the threshold model since it posits that subjects with more BR can accumulate more pathology before reaching the threshold where functional deficits are noticeable. One

popular (but not necessarily correct) example in favor of this theory derives from Alzheimer's Disease subjects, as it is established that individuals with larger brains sustain additional pathology before the emergence of clinical symptoms (Graves et al., 1996).

Although the BR model is simple and intuitive, it fails to explain why bigger brains are not necessarily associated with greater cognitive performance (Salat et al., 2002). In this context, the CR model was proposed to account for the variability that cannot be explained by pathological indices (Stern, 2002; 2009;Barulli and Stern, 2013). This model states that individuals with higher CR capacity make a more efficient or flexible use of the brain's resources in order to perform better at a given task. The rationale for the CR model is that individuals with a richer environment in terms of cognitive activities/demands through the lifespan accumulate strategies that help them to overcome more easily the challenges of everyday life. Common proxies of this higher level of reserve are education level, intelligence quotient (IQ), occupational attainment and involvement in leisure activities (cognitive engagement) (Stern et al., 1992;Alexander et al., 1997;Richards and Sacker, 2003).

The CR model "sits on top" of the BR model and according to it, for any given level of pathology and BR, individuals with higher CR present better cognitive performance. As such, higher CR shifts the threshold of BR so that individuals with lower BR can display intact cognitive functioning. Furthermore, CR also elucidates why, after being diagnosed with Alzheimer's Disease, the pathology seems to progress faster in individuals with higher CR and these patients die earlier (Stern et al., 1995). This is explained by the fact that when the pathology is diagnosed, the disease has progressed more in individuals with higher CR due to their abilities to compensate, meaning that, at the time of diagnose, the disease is closer to fatal levels in such subjects.

4. Neuroimaging in aging

Neuroimaging plays a very important role in the study of the human brain structure and functioning. Prior to the emergence of imaging techniques, such as MRI or PET, the human brain could only be studied post-mortem (e.g. autopsies) or with invasive procedures. The advent of these techniques enabled the study of the healthy and pathological brain *in vivo* with

rather innocuous procedures. MRI in particular, despite still requiring expensive equipment, has the advantage that several complementary acquisitions can be performed within the same scanner and imaging session, enabling the study of both functional and structural correlates of healthy aging and pathology.

4.1 Structural MRI

Structural MRI is the most conventional form of MRI. In fact, MRI was developed to permit the observation of internal organs' anatomy *in vivo*. Several different structural MRI sequences are used in everyday clinical practice (e.g. T1, T2, proton density (PD), (FLAIR)). Since different acquisitions reveal different aspects of anatomy, in the clinical practice, several of these acquisitions are performed at different orientations in the same imaging session, in order to perform a differential diagnosis.

In neuroscience research, T1-weighted acquisitions are typically used to estimate whole-brain or regional brain volumes. While the goal standard is the manual segmentation of the structures of interest (Fischl et al., 2002), these procedures are difficult, time-consuming and require well-trained anatomists. In order to counterbalance this, semi- (Desikan et al., 2006;Destrieux et al., 2010) and fully automated (Mikheev et al., 2008) procedures have been developed. Additionally, voxel-wise analysis can be performed with techniques such as Voxel-Based Morphometry (VBM) to study more focal volumetric alterations without *a priori* bias regarding anatomical boundaries (Ashburner and Friston, 2000). This technique detects regional volumetric alterations through the amount of deformation that is necessary to apply to each voxel in order to match each subject's brain to a brain standard template. Cortical thinning/atrophy is one of major age-related brain structural alterations. These effects can also be studied with T1-weighted MRI images and consistent results in aging have been reported (Salat et al., 2004;Fjell et al., 2009).

T2-weighted imaging is mostly used for the study of brain pathology indices. Specifically, WMSA are generally identified with this kind of sequences and are a common finding among the older adults' brains (de Groot et al., 2000;Dufouil et al., 2003;Maillard et al., 2012).

Micro-structural alterations in aging can also be studied with a particular kind of MRI acquisition called Diffusion Weighted Imaging (DWI) (Le Bihan and Breton, 1985). This kind of acquisition is based on the attenuation that the displacement of water molecules causes in MRI images when they diffuse along the direction of a previously applied gradient. When several gradients are applied along different directions, the 3D mapping of water diffusion can be obtained. This is particular helpful to study WM since the displacement of water in an arranged media, such as the axonal fibers, actually probes its structure. The Diffusion Tensor Imaging (DTI) model (Basser et al., 1994;Pierpaoli et al., 1996), which approximates the water displacement to an ellipsoid, enables the extraction of several indices that characterize WM micro-structural properties (Hagmann et al., 2006). Fractional anisotropy (FA) is probably the most popular DTI index and represents a measure of the existence of a preferential direction for water diffusion. High values of FA represent a highly directional (anisotropic) water displacement, which is commonly observed in axonal fibers where water molecules diffuse more along the axon than radially, while low values of FA represent isotropic water displacements observed in the ventricles, for example, where water molecules diffuse equally/freely in every direction. Three diffusivity measures are also commonly reported: mean diffusivity (MD), which represents the mean displacement along the three directions of the DTI ellipsoid; axial diffusivity (AD), denoting the extension of diffusion along the main direction of the ellipsoid (direction of the axon); and, radial diffusivity (RD) that embodies the mean diffusivity along the radial aspect of the ellipsoid (direction perpendicular to the axon). Lower FA and higher MD are commonly associated with reduced WM integrity and/or pathology (Kochunov et al., 2007;Barrick et al., 2010). RD is commonly associated with myelination levels, with higher RD being commonly interpreted as reduced myelin density (Song et al., 2005). Results on AD are more difficult to be interpreted, with both increases and decreases being associated with aging (Bender and Raz, 2015).

Additionally, DWI acquisitions can be used to reconstruct the main WM tracts through the directionality information obtained from the DTI model – tractography or fiber tracking (Basser et al., 2000). This technique enables both the estimation of a measure of structural connectivity (SC), as the number of reconstructed tracts that reach a given region, as well as the study of the properties of particular WM tracts.

Regardless of the previous description, DTI indices can be affected by other factors than WM integrity (Jones et al., 2013) and, thus, interpretations regarding WM integrity must be taken cautiously.

4.2 Functional MRI

Regarding brain function, two main imaging techniques are typically used: PET and fMRI. Both techniques provide indirect measures of brain activity through measures of blood flow in the brain. However, fMRI has several advantages when compared to PET: PET requires the use of radioactive isotopes while fMRI does not; fMRI enables the acquisition of higher resolution images. Both are expensive, but the PET scanners are much more expensive than MRI scanners, which contributes for the fact that MRI scanners are more prevalent in hospitals and imaging centers and, as a consequence, for the observation that most neuroimaging studies of brain function use fMRI.

The basic principle of fMRI is that brain activity in a given brain region leads to an increase in metabolism and oxygen consumption and this, in turn, leads to an increased supply of oxygenated blood. The imbalance in the relative levels of oxyhemoglobin and deoxyhemoglobin produces an increase in the MRI contrast, also known as Blood-Oxygen-Level Dependent (BOLD) contrast (Ogawa et al., 1990). More recently, other techniques have been used to assess brain activity, such as arterial spin labeling (ASL), which allows the weighting of the MRI signal by cerebral blood flow.

The BOLD contrast has been used to assess brain function in aging while performing memory encoding (Morcom et al., 2003;de Chastelaine et al., 2011), memory retrieval (Morcom et al., 2007), attention control (Milham et al., 2002), working memory (Cappell et al., 2010;Schneider-Garces et al., 2010), face processing (Lee et al., 2011) and emotion perception (Gunning-Dixon et al., 2003), among other fMRI tasks. As previously described, increased activation, mainly in frontal regions (Davis et al., 2008), as well as more symmetric and diffuse patterns of activation (Cabeza, 2002) are the most common findings across task performance in older individuals.

Another type of fMRI acquisition (using the BOLD contrast) commonly used in neuroimaging research is resting-state fMRI (rs-fMRI). This acquisition builds on the same principals as task-related fMRI with the exception that BOLD signals are acquired while individuals are at rest (i.e. not performing a specific task). This type of acquisition has gained popularity due to its simplicity since it is does not require that individuals are able to perform a specific task, it is fast to acquire and results are reliable and easily interpretable (Shehzad et al., 2009). In rs-fMRI studies, the interest is not in relative levels of activity but rather in inter-correlations in fluctuations of BOLD signals of different brain regions that are assumed to reflect functional connectivity (FC) (Biswal et al., 1995). This kind of analysis has enabled the identification of several sets of regions that display high inter-correlations in BOLD signals along time, leading to the emergence of the concept of the Resting-State Networks (RSNs) (Damoiseaux et al., 2006;De Luca et al., 2006). The most studied network is the DMN, both in aging and pathology, but reductions in FC in other RSNs have also been reported to be associated with age (Tomasi and Volkow, 2012;Ferreira and Busatto, 2013).

4.3 The connectomic approach

Brain connectivity defines the way brain regions are functionally and structurally connected. The brain is commonly perceived as a complex and precise network that comprises several different regions that interact with each other at different levels (genes, proteins, neurons, areas, whole-brain). The perception of the brain as a network lead to an increasing interest in its characterization through the use of network analysis methods, such as graph theory (Bullmore and Sporns, 2009;Power et al., 2011), in the exploration of the so-called Human Connectome (Sporns et al., 2005). These methods enable the reliable quantification of brain networks with meaningful and easily computable measures (Deuker et al., 2009), facilitate the establishment of functional and structural connectivity relations (Honey et al., 2010), and are able to reveal connectivity abnormalities under different conditions ((Lynall et al., 2010;Zhang et al., 2011;Wang et al., 2013). The scientific community and governments have recognized the importance and potential of such analysis as indicated by large national and multinational studies in the field such as “The Human Connectome Project” (http://humanconnectome.org) and “The 1000 Functional Connectome Project” (http://fcon_1000.projects.nitrc.org/).

In graph theory analysis, a network is represented as a graph, which is a mathematical model composed by a group of nodes (the elements of the network) connected through edges that represent the relationships between the elements of the network (Gross and Yellen, 2005). At the brain level, the network nodes are commonly the different brain regions, either from a pre-existing atlas or derived from fMRI analysis (Cohen et al., 2008;Wig et al., 2011). The edges are typically functional connectivity measures, such as interdependencies between rs-fMRI signals of the different regions (Smith et al., 2011;Zalesky et al., 2012) (Figure 2.a), or structural connectivity measures such as the co-variance of volumes/thickness across subjects (He et al., 2007;Bernhardt et al., 2011) (Figure 2.b) or the number/fiber density of DTI derived tracts (Hagmann et al., 2008;Gong et al., 2009) (Figure 2.c).

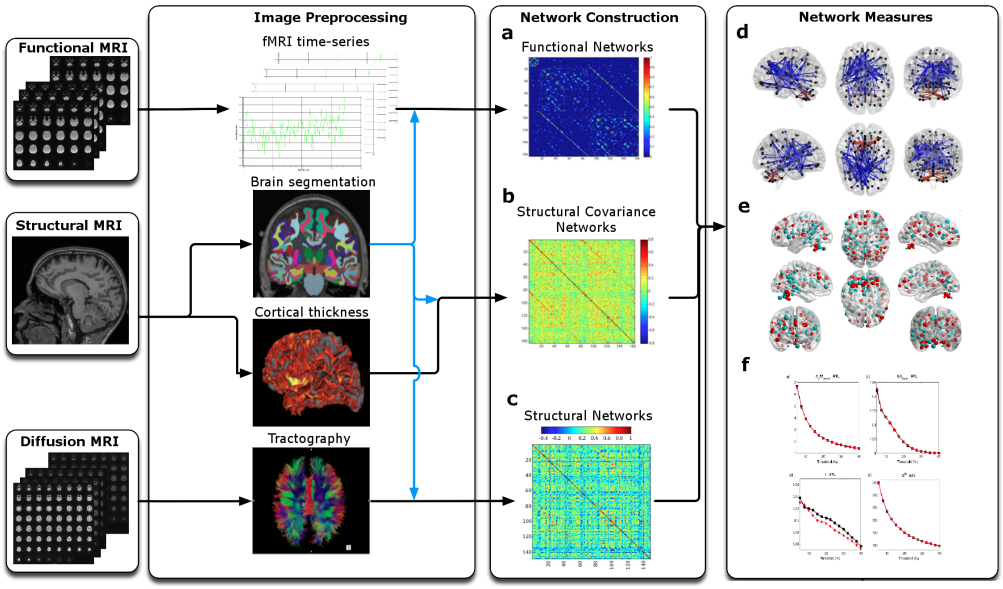


Figure 2. Overview of human connectome analyses. Whole brain modeling of connectivity can be achieved through pairwise FC (**a**), through co-variances of brain volumes/thickness (**b**) or tractography derived SC (**c**). Analysis can be performed at the edge (**d**), node (**e**) and global network level (**f**).

This kind of representation enables the analysis of the brain network at different levels: connection/edge level (Figure 2.d), regional/node level and global network level. At the edge level, simple connectivity analysis enables the exploration of which edges are more important for the network formation or which are more affected in particular conditions/pathologies. At the node level (Figure 2.e), several different metrics can be extracted reflecting centrality (e.g.

betweenness centrality), integration (e.g. global efficiency) or segregation (e.g. clustering coefficient). At the global network level (Figure 2.f), different indices can indicate levels of segregation, integration, centrality and resilience (Rubinov and Sporns, 2010) (Figure 2).

To date, few studies have used connectomic approaches in the study of the aging brain. Comparing young and old individuals, researchers have found that both groups had significantly higher modularity (i.e. propensity for partitioning of the network) than expected for random networks and that in older adults the number of inter-modular connections is lower while the number of small modules is higher in their FC networks (Meunier et al., 2009). It has also been reported that healthy older subjects present less efficient FC networks than younger adults (Achard and Bullmore, 2007). More recently, Sala-Llonch and colleagues found that aging was associated with decreased FC in long-range connections and increased FC in short-range connections, that average clustering and minimum path-length correlated positively with age and that global efficiency correlated negatively with age (Sala-Llonch et al., 2014). Additionally, clustering was negatively associated with memory performance.

Still, studies investigating the impact of aging on brain networks' properties through connectomic approaches are still very limited and the relationships between several cognitive dimensions and those properties remain unknown. Moreover, longitudinal studies, classified as crucial for a better understanding of the age and cognitive decline impact in brain structure/function, are inexistent in the context of graph-theory analysis of the brain network.

5. Objectives

Although intra-individual variability exists in aging, some older individuals seem to perform better across various cognitive domains than others. The focus of this thesis is to provide new insights on how brain networks age in an attempt to identify possible neuronal biomarkers for overall good cognitive aging. Detecting factors that influence the maintenance of good cognitive performance in aging may be helpful in enhancing cognitive functioning and, thus, improving quality of life of the older population.

In order to achieve this overarching objective, multimodal MRI techniques/analyses were used and connectivity patterns were modeled using graph theory to study the network properties of the aging human connectome. Several tasks were designed and performed, within the Switchbox (www.switchbox-online.eu/) project, to investigate:

1 – which WM alterations (both macro- and micro-structural) could distinguish between overall good- and poor-cognitive performers and how these associate across age (Chapter 2);

2 – which FC networks are associated with the major proxy of CR – education level – and which networks and network properties are associated with BR and CR, independently of education level (Chapters 3 and 4);

3 – which are the FC networks and network properties affected by aging and cognitive decline and how opposite cognitive profiles are affected by aging (Chapter 5).

6. References

Abrahamson, K., Clark, D., Perkins, A., and Arling, G. (2012). Does Cognitive Impairment Influence Quality of Life Among Nursing Home Residents? *Gerontologist* 52**,** 632-640.

Achard, S., and Bullmore, E. (2007). Efficiency and cost of economical brain functional networks. *PLoS Comput Biol* 3**,** e17.

Alexander, G.E., Furey, M.L., Grady, C.L., Pietrini, P., Brady, D.R., Mentis, M.J., and Schapiro, M.B. (1997). Association of premorbid intellectual function with cerebral metabolism in Alzheimer's disease: implications for the cognitive reserve hypothesis. *Am J Psychiatry* 154**,** 165-172.

Ashburner, J., and Friston, K.J. (2000). Voxel-based morphometry–the methods. *Neuroimage* 11**,** 805-821.

Bäckman, L., Small, B.J., Wahlin, Å., and Larsson, M. (2000). Cognitive functioning in very old age.

Barrick, T.R., Charlton, R.A., Clark, C.A., and Markus, H.S. (2010). White matter structural

decline in normal ageing: a prospective longitudinal study using tract-based spatial statistics. *Neuroimage* 51**,** 565-577.

Barulli, D., and Stern, Y. (2013). Efficiency, capacity, compensation, maintenance, plasticity: emerging concepts in cognitive reserve. *Trends in Cognitive Sciences* 17**,** 502-509.

Basser, P.J., Mattiello, J., and Lebihan, D. (1994). Estimation of the effective self-diffusion tensor from the NMR spin echo. *J Magn Reson B* 103**,** 247-254.

Basser, P.J., Pajevic, S., Pierpaoli, C., Duda, J., and Aldroubi, A. (2000). In vivo fiber tractography using DT-MRI data. *Magn Reson Med* 44**,** 625-632.

Bender, A.R., and Raz, N. (2015). Normal-Appearing Cerebral White Matter in Healthy Adults: Mean Change over Two Years and Individual Differences in Change. *Neurobiology of Aging*.

Bernhardt, B.C., Chen, Z., He, Y., Evans, A.C., and Bernasconi, N. (2011). Graph-theoretical analysis reveals disrupted small-world organization of cortical thickness correlation networks in temporal lobe epilepsy. *Cereb Cortex* 21**,** 2147-2157.

Biswal, B., Yetkin, F.Z., Haughton, V.M., and Hyde, J.S. (1995). Functional connectivity in the motor cortex of resting human brain using echo-planar MRI. *Magn Reson Med* 34**,** 537-541.

Brickman, A.M., Paul, R.H., Cohen, R.A., Williams, L.M., Macgregor, K.L., Jefferson, A.L., Tate, D.F., Gunstad, J., and Gordon, E. (2005). Category and letter verbal fluency across the adult lifespan: relationship to EEG theta power. *Arch Clin Neuropsychol* 20**,** 561-573.

Bullmore, E., and Sporns, O. (2009). Complex brain networks: graph theoretical analysis of structural and functional systems. *Nat Rev Neurosci* 10**,** 186-198.

Cabeza, R. (2002). Hemispheric asymmetry reduction in older adults: the HAROLD model. *Psychol Aging* 17**,** 85-100.

Cabeza, R., Grady, C.L., Nyberg, L., Mcintosh, A.R., Tulving, E., Kapur, S., Jennings, J.M., Houle, S., and Craik, F.I. (1997). Age-related differences in neural activity during

memory encoding and retrieval: a positron emission tomography study. *J Neurosci* 17**,** 391-400.

Cappell, K.A., Gmeindl, L., and Reuter-Lorenz, P.A. (2010). Age differences in prefontal recruitment during verbal working memory maintenance depend on memory load. *Cortex* 46**,** 462-473.

Cohen, A.L., Fair, D.A., Dosenbach, N.U.F., Miezin, F.M., Dierker, D., Van Essen, D.C., Schlaggar, B.L., and Petersen, S.E. (2008). Defining functional areas in individual human brains using resting functional connectivity MRI. *Neuroimage* 41**,** 45-57.

Damoiseaux, J.S., Beckmann, C.F., Arigita, E.J., Barkhof, F., Scheltens, P., Stam, C.J., Smith, S.M., and Rombouts, S.A. (2008). Reduced resting-state brain activity in the "default network" in normal aging. *Cerebral cortex* 18**,** 1856-1864.

Damoiseaux, J.S., Rombouts, S.A., Barkhof, F., Scheltens, P., Stam, C.J., Smith, S.M., and Beckmann, C.F. (2006). Consistent resting-state networks across healthy subjects. *Proc Natl Acad Sci U S A* 103**,** 13848-13853.

Davis, S.W., Dennis, N.A., Daselaar, S.M., Fleck, M.S., and Cabeza, R. (2008). Que PASA? The posterior-anterior shift in aging. *Cereb Cortex* 18**,** 1201-1209.

De Chastelaine, M., Wang, T.H., Minton, B., Muftuler, L.T., and Rugg, M.D. (2011). The effects of age, memory performance, and callosal integrity on the neural correlates of successful associative encoding. *Cereb Cortex* 21**,** 2166-2176.

De Frias, C.M., Dixon, R.A., and Strauss, E. (2009). Characterizing Executive Functioning in Older Special Populations: From Cognitively Elite to Cognitively Impaired. *Neuropsychology* 23**,** 778-791.

De Groot, J.C., Oudkerk, M., Gijn, J.V., Hofman, A., Jolles, J., and Breteler, M. (2000). Cerebral white matter lesions and cognitive function: the Rotterdam Scan Study. *Annals of neurology* 47**,** 145-151.

De Leeuw, F., De Groot, J.C., Achten, E., Oudkerk, M., Ramos, L., Heijboer, R., Hofman, A., Jolles, J., Van Gijn, J., and Breteler, M. (2001). Prevalence of cerebral white matter

lesions in elderly people: a population based magnetic resonance imaging study. The Rotterdam Scan Study. *Journal of Neurology, Neurosurgery & Psychiatry* 70**,** 9-14.

De Luca, M., Beckmann, C., De Stefano, N., Matthews, P., and Smith, S.M. (2006). fMRI resting state networks define distinct modes of long-distance interactions in the human brain. *Neuroimage* 29**,** 1359-1367.

Dennis, A.N., and Cabeza, R. (2008). "Neuroimaging of Healthy Cognitive Aging," in *Handbook of aging and cognition,* ed. F.I.M.C.T.A. Salthouse. Mahwah, NJ: Erlbaum).

Desikan, R.S., Segonne, F., Fischl, B., Quinn, B.T., Dickerson, B.C., Blacker, D., Buckner, R.L., Dale, A.M., Maguire, R.P., Hyman, B.T., Albert, M.S., and Killiany, R.J. (2006). An automated labeling system for subdividing the human cerebral cortex on MRI scans into gyral based regions of interest. *Neuroimage* 31**,** 968-980.

Destrieux, C., Fischl, B., Dale, A., and Halgren, E. (2010). Automatic parcellation of human cortical gyri and sulci using standard anatomical nomenclature. *Neuroimage* 53**,** 1-15.

Deuker, L., Bullmore, E.T., Smith, M., Christensen, S., Nathan, P.J., Rockstroh, B., and Bassett, D.S. (2009). Reproducibility of graph metrics of human brain functional networks. *Neuroimage* 47**,** 1460-1468.

Dias-Ferreira, E., Sousa, J.C., Melo, I., Morgado, P., Mesquita, A.R., Cerqueira, J.J., Costa, R.M., and Sousa, N. (2009). Chronic stress causes frontostriatal reorganization and affects decision-making. *Science* 325**,** 621-625.

Dufouil, C., Alpérovitch, A., Ducros, V., and Tzourio, C. (2003). Homocysteine, white matter hyperintensities, and cognition in healthy elderly people. *Annals of neurology* 53**,** 214-221.

Ferreira, L.K., and Busatto, G.F. (2013). Resting-state functional connectivity in normal brain aging. *Neurosci Biobehav Rev* 37**,** 384-400.

Fischl, B., Salat, D.H., Busa, E., Albert, M., Dieterich, M., Haselgrove, C., Van Der Kouwe, A., Killiany, R., Kennedy, D., Klaveness, S., Montillo, A., Makris, N., Rosen, B., and Dale, A.M. (2002). Whole brain segmentation: automated labeling of neuroanatomical

structures in the human brain. *Neuron* 33**,** 341-355.

Fjell, A.M., Westlye, L.T., Amlien, I., Espeseth, T., Reinvang, I., Raz, N., Agartz, I., Salat, D.H., Greve, D.N., and Fischl, B. (2009). High consistency of regional cortical thinning in aging across multiple samples. *Cerebral cortex***,** bhn232.

Garde, E., Mortensen, E.L., Krabbe, K., Rostrup, E., and Larsson, H.B. (2000). Relation between age-related decline in intelligence and cerebral white-matter hyperintensities in healthy octogenarians: a longitudinal study. *The Lancet* 356**,** 628-634.

Goh, J.O., An, Y., and Resnick, S.M. (2012). Differential Trajectories of Age-Related Changes in Components of Executive and Memory Processes. *Psychology and Aging* 27**,** 707-719.

Gong, G., He, Y., Concha, L., Lebel, C., Gross, D.W., Evans, A.C., and Beaulieu, C. (2009). Mapping anatomical connectivity patterns of human cerebral cortex using in vivo diffusion tensor imaging tractography. *Cereb Cortex* 19**,** 524-536.

Good, C.D., Johnsrude, I.S., Ashburner, J., Henson, R.N., Friston, K.J., and Frackowiak, R.S. (2001). A voxel-based morphometric study of ageing in 465 normal adult human brains. *Neuroimage* 14**,** 21-36.

Grady, C. (2012). BRAIN AGEING The cognitive neuroscience of ageing. *Nature Reviews Neuroscience* 13**,** 491-505.

Grady, C.L., Bernstein, L.J., Beig, S., and Siegenthaler, A.L. (2002). The effects of encoding task on age-related differences in the functional neuroanatomy of face memory. *Psychology and Aging* 17**,** 7-23.

Grady, C.L., Maisog, J.M., Horwitz, B., Ungerleider, L.G., Mentis, M.J., Salerno, J.A., Pietrini, P., Wagner, E., and Haxby, J.V. (1994). Age-related changes in cortical blood flow activation during visual processing of faces and location. *J Neurosci* 14**,** 1450-1462.

Graves, A.B., Mortimer, J.A., Larson, E.B., Wenzlow, A., Bowen, J.D., and Mccormick, W.C. (1996). Head circumference as a measure of cognitive reserve - Association with severity of impairment in Alzheimer's disease. *British Journal of Psychiatry* 169**,** 86-92.

Gross, J.L., and Yellen, J. (2005). *Graph theory and its applications.* CRC press.

Gunning-Dixon, F.M., Gur, R.C., Perkins, A.C., Schroeder, L., Turner, T., Turetsky, B.I., Chan, R.M., Loughead, J.W., Alsop, D.C., and Maldjian, J. (2003). Age-related differences in brain activation during emotional face processing. *Neurobiology of aging* 24**,** 285-295.

Hagmann, P., Cammoun, L., Gigandet, X., Meuli, R., Honey, C.J., Wedeen, V., and Sporns, O. (2008). Mapping the structural core of human cerebral cortex. *Plos Biology* 6**,** 1479-1493.

Hagmann, P., Jonasson, L., Maeder, P., Thiran, J.P., Wedeen, V.J., and Meuli, R. (2006). Understanding diffusion MR imaging techniques: from scalar diffusion-weighted imaging to diffusion tensor imaging and beyond. *Radiographics* 26 Suppl 1**,** S205-223.

Hasher, L., and Zacks, R.T. (1988). Working memory, comprehension, and aging: A review and a new view. *Psychology of learning and motivation* 22**,** 193-225.

He, Y., Chen, Z.J., and Evans, A.C. (2007). Small-world anatomical networks in the human brain revealed by cortical thickness from MRI. *Cereb Cortex* 17**,** 2407-2419.

Hilborn, J.V., Strauss, E., Hultsch, D.F., and Hunter, M.A. (2009). Intraindividual variability across cognitive domains: investigation of dispersion levels and performance profiles in older adults. *J Clin Exp Neuropsychol* 31**,** 412-424.

Honey, C.J., Thivierge, J.P., and Sporns, O. (2010). Can structure predict function in the human brain? *Neuroimage* 52**,** 766-776.

Hultsch, D.F., Hertzog, C., Small, B.J., Mcdonaldmiszczak, L., and Dixon, R.A. (1992). Short-Term Longitudinal Change in Cognitive Performance in Later Life. *Psychology and Aging* 7**,** 571-584.

Hutton, C., Draganski, B., Ashburner, J., and Weiskopf, N. (2009). A comparison between voxel-based cortical thickness and voxel-based morphometry in normal aging. *Neuroimage* 48**,** 371-380.

Inzitari, D., Pracucci, G., Poggesi, A., Carlucci, G., Barkhof, F., Chabriat, H., Erkinjuntti, T.,

Fazekas, F., Ferro, J.M., and Hennerici, M. (2009). Changes in white matter as determinant of global functional decline in older independent outpatients: three year follow-up of LADIS (leukoaraiosis and disability) study cohort. *Bmj* 339**,** b2477.

Jones, D.K., Knosche, T.R., and Turner, R. (2013). White matter integrity, fiber count, and other fallacies: the do's and don'ts of diffusion MRI. *Neuroimage* 73**,** 239-254.

Katzman, R. (1993). Education and the prevalence of dementia and Alzheimer's disease. *Neurology*.

Katzman, R., Terry, R., Deteresa, R., Brown, T., Davies, P., Fuld, P., Renbing, X., and Peck, A. (1988). Clinical, pathological, and neurochemical changes in dementia: a subgroup with preserved mental status and numerous neocortical plaques. *Ann Neurol* 23**,** 138-144.

Kaup, A.R., Mirzakhanian, H., Jeste, D.V., and Eyler, L.T. (2011). A review of the brain structure correlates of successful cognitive aging. *The Journal of neuropsychiatry and clinical neurosciences* 23**,** 6-15.

Koch, W., Teipel, S., Mueller, S., Buerger, K., Bokde, A.L., Hampel, H., Coates, U., Reiser, M., and Meindl, T. (2010). Effects of aging on default mode network activity in resting state fMRI: does the method of analysis matter? *NeuroImage* 51**,** 280-287.

Kochunov, P., Thompson, P.M., Lancaster, J.L., Bartzokis, G., Smith, S., Coyle, T., Royall, D.R., Laird, A., and Fox, P.T. (2007). Relationship between white matter fractional anisotropy and other indices of cerebral health in normal aging: tract-based spatial statistics study of aging. *Neuroimage* 35**,** 478-487.

Kray, J., and Lindenberger, U. (2000). Adult age differences in task switching. *Psychology and Aging* 15**,** 126-147.

Le Bihan, B., and Breton, E. (1985). Imagerie de diffusion in vivo par résonance magnétique nucléaire. *C. R. Acad. Sci.: Paris* 301**,** 1109-1112.

Lee, Y., Grady, C.L., Habak, C., Wilson, H.R., and Moscovitch, M. (2011). Face processing changes in normal aging revealed by fMRI adaptation. *Journal of cognitive*

neuroscience 23**,** 3433-3447.

Lemaitre, H., Goldman, A.L., Sambataro, F., Verchinski, B.A., Meyer-Lindenberg, A., Weinberger, D.R., and Mattay, V.S. (2012). Normal age-related brain morphometric changes: nonuniformity across cortical thickness, surface area and gray matter volume? *Neurobiol Aging* 33**,** 617 e611-619.

Lockhart, S.N., Roach, A.E., Luck, S.J., Geng, J., Beckett, L., Carmichael, O., and Decarli, C. (2014). White matter hyperintensities are associated with visual search behavior independent of generalized slowing in aging. *Neuropsychologia* 52**,** 93-101.

Lynall, M.E., Bassett, D.S., Kerwin, R., Mckenna, P.J., Kitzbichler, M., Muller, U., and Bullmore, E.T. (2010). Functional Connectivity and Brain Networks in Schizophrenia. *Journal of Neuroscience* 30**,** 9477-9487.

Macdonald, S.W., Hultsch, D.F., and Dixon, R.A. (2003). Performance variability is related to change in cognition: evidence from the Victoria Longitudinal Study. *Psychology and aging* 18**,** 510.

Madden, D.J., Bennett, I.J., and Song, A.W. (2009). Cerebral white matter integrity and cognitive aging: contributions from diffusion tensor imaging. *Neuropsychol Rev* 19**,** 415-435.

Madden, D.J., Turkington, T.G., Provenzale, J.M., Denny, L.L., Hawk, T.C., Gottlob, L.R., and Coleman, R.E. (1999). Adult age differences in the functional neuroanatomy of verbal recognition memory. *Hum Brain Mapp* 7**,** 115-135.

Madden, D.J., Whiting, W.L., Spaniol, J., and Bucur, B. (2005). Adult age differences in the implicit and explicit components of top-down attentional guidance during visual search. *Psychology and Aging* 20**,** 317-329.

Maillard, P., Carmichael, O., Fletcher, E., Reed, B., Mungas, D., and Decarli, C. (2012). Coevolution of white matter hyperintensities and cognition in the elderly. *Neurology* 79**,** 442-448.

Mcewen, B.S. (2007). Physiology and Neurobiology of Stress and Adaptation: Central Role of

the Brain. *Physiological Reviews* 87**,** 873-904.

Melton, A.W. (1963). Implications of Short-Term-Memory for a General-Theory of Memory. Journal of Verbal Learning and Verbal Behavior 2, 1-21.

Meunier, D., Achard, S., Morcom, A., and Bullmore, E. (2009). Age-related changes in modular organization of human brain functional networks. *Neuroimage* 44**,** 715-723.

Mikheev, A., Nevsky, G., Govindan, S., Grossman, R., and Rusinek, H. (2008). Fully automatic segmentation of the brain from T1−weighted MRI using Bridge Burner algorithm. *Journal of Magnetic Resonance Imaging* 27**,** 1235-1241.

Milham, M.P., Erickson, K.I., Banich, M.T., Kramer, A.F., Webb, A., Wszalek, T., and Cohen, N.J. (2002). Attentional control in the aging brain: insights from an fMRI study of the stroop task. *Brain and cognition* 49**,** 277-296.

Miller-Keane, and O'toole (2003). "Miller-Keane Encyclopedia & Dictionary of Medicine, Nursing & Allied Health". 7 th ed.: Saunders).

Morcom, A.M., Good, C.D., Frackowiak, R.S., and Rugg, M.D. (2003). Age effects on the neural correlates of successful memory encoding. *Brain* 126**,** 213-229.

Morcom, A.M., Li, J., and Rugg, M.D. (2007). Age effects on the neural correlates of episodic retrieval: increased cortical recruitment with matched performance. *Cereb Cortex* 17**,** 2491-2506.

Mortimer, J.A., Snowdon, D.A., and Markesbery, W.R. (2003). Head circumference, education and risk of dementia: findings from the Nun Study. *Journal of Clinical and Experimental Neuropsychology* 25**,** 671-679.

Mosconi, L., De Santi, S., Li, J., Tsui, W.H., Li, Y., Boppana, M., Laska, E., Rusinek, H., and De Leon, M.J. (2008). Hippocampal hypometabolism predicts cognitive decline from normal aging. *Neurobiol Aging* 29**,** 676-692.

Nicholas, M., Obler, L., Albert, M., and Goodglass, H. (1985). Lexical Retrieval in Healthy Aging. *Cortex* 21**,** 595-606.

Nyberg, L., Maitland, S.B., Ronnlund, M., Backman, L., Dixon, R.A., Wahlin, A., and Nilsson, L.G. (2003). Selective adult age differences in an age-invariant multifactor model of declarative memory. *Psychology and Aging* 18**,** 149-160.

O'shea, D.M., Fieo, R.A., Hamilton, J.L., Zahodne, L.B., Manly, J.J., and Stern, Y. (2015). Examining the association between late-life depressive symptoms, cognitive function, and brain volumes in the context of cognitive reserve. *Int J Geriatr Psychiatry* 30**,** 614-622.

Ogawa, S., Lee, T.-M., Kay, A.R., and Tank, D.W. (1990). Brain magnetic resonance imaging with contrast dependent on blood oxygenation. *Proceedings of the National Academy of Sciences* 87**,** 9868-9872.

Onoda, K., Ishihara, M., and Yamaguchi, S. (2012). Decreased functional connectivity by aging is associated with cognitive decline. *J Cogn Neurosci* 24**,** 2186-2198.

Park, D.C., Polk, T.A., Park, R., Minear, M., Savage, A., and Smith, M.R. (2004). Aging reduces neural specialization in ventral visual cortex. *Proceedings of the National Academy of Sciences of the United States of America* 101**,** 13091-13095.

Park, D.C., and Reuter-Lorenz, P. (2009). The adaptive brain: aging and neurocognitive scaffolding. *Annual review of psychology* 60**,** 173-196.

Paulo, A.C., Sampaio, A., Santos, N.C., Costa, P.S., Cunha, P., Zihl, J., Cerqueira, J., Palha, J.A., and Sousa, N. (2011). Patterns of Cognitive Performance in Healthy Ageing in Northern Portugal: A Cross-Sectional Analysis. *PLoS ONE* 6**,** e24553.

Pfefferbaum, A., and Sullivan, E.V. (2003). Increased brain white matter diffusivity in normal adult aging: relationship to anisotropy and partial voluming. *Magn Reson Med* 49**,** 953-961.

Pierpaoli, C., Jezzard, P., Basser, P.J., Barnett, A., and Di Chiro, G. (1996). Diffusion tensor MR imaging of the human brain. *Radiology* 201**,** 637-648.

Power, J.D., Cohen, A.L., Nelson, S.M., Wig, G.S., Barnes, K.A., Church, J.A., Vogel, A.C., Laumann, T.O., Miezin, F.M., Schlaggar, B.L., and Petersen, S.E. (2011). Functional

network organization of the human brain. *Neuron* 72**,** 665-678.

Raichle, M.E., Macleod, A.M., Snyder, A.Z., Powers, W.J., Gusnard, D.A., and Shulman, G.L. (2001). A default mode of brain function. *Proc. Natl. Acad. Sci.* 98**,** 676-682.

Reuter-Lorenz, P.A., and Cappell, K.A. (2008). Neurocognitive aging and the compensation hypothesis. *Current directions in psychological science* 17**,** 177-182.

Reuter-Lorenz, P.A., Jonides, J., Smith, E.E., Hartley, A., Miller, A., Marshuetz, C., and Koeppe, R.A. (2000). Age differences in the frontal lateralization of verbal and spatial working memory revealed by PET. *J Cogn Neurosci* 12**,** 174-187.

Reuter-Lorenz, P.A., and Park, D.C. (2014). How does it STAC up? Revisiting the scaffolding theory of aging and cognition. *Neuropsychol Rev* 24**,** 355-370.

Richards, M., and Sacker, A. (2003). Lifetime antecedents of cognitive reserve. *J Clin Exp Neuropsychol* 25**,** 614-624.

Ronnlund, M., Nyberg, L., Backman, L., and Nilsson, L.G. (2005). Stability, growth, and decline in adult life span development of declarative memory: Cross-sectional and longitudinal data from a population-based study. *Psychology and Aging* 20**,** 3-18.

Rubinov, M., and Sporns, O. (2010). Complex network measures of brain connectivity: uses and interpretations. *Neuroimage* 52**,** 1059-1069.

Sala-Llonch, R., Junque, C., Arenaza-Urquijo, E.M., Vidal-Pineiro, D., Valls-Pedret, C., Palacios, E.M., Domenech, S., Salva, A., Bargallo, N., and Bartres-Faz, D. (2014). Changes in whole-brain functional networks and memory performance in aging. *Neurobiol Aging* 35**,** 2193-2202.

Salat, D.H., Buckner, R.L., Snyder, A.Z., Greve, D.N., Desikan, R.S., Busa, E., Morris, J.C., Dale, A.M., and Fischl, B. (2004). Thinning of the cerebral cortex in aging. *Cereb Cortex* 14**,** 721-730.

Salat, D.H., Kaye, J.A., and Janowsky, J.S. (2002). Greater orbital prefrontal volume selectively predicts worse working memory performance in older adults. *Cerebral Cortex* 12**,** 494-

505.

Salat, D.H., Tuch, D.S., Greve, D.N., Van Der Kouwe, A.J., Hevelone, N.D., Zaleta, A.K., Rosen, B.R., Fischl, B., Corkin, S., Rosas, H.D., and Dale, A.M. (2005). Age-related alterations in white matter microstructure measured by diffusion tensor imaging. *Neurobiol Aging* 26**,** 1215-1227.

Salthouse, T.A. (2009). Decomposing age correlations on neuropsychological and cognitive variables. *J Int Neuropsychol Soc* 15**,** 650-661.

Salthouse, T.A. (2012). Are individual differences in rates of aging greater at older ages? *Neurobiology of Aging* 33**,** 2373-2381.

Salthouse, T.A., and Madden, D.J. (2008). Information processing speed and aging.

Santos, N.C., Costa, P.S., Cunha, P., Portugal-Nunes, C., Amorim, L., Cotter, J., Cerqueira, J.J., Palha, J.A., and Sousa, N. (2014). Clinical, physical and lifestyle indicators and relationship with cognition and mood in aging: a cross-sectional analysis of distinct educational groups. *Frontiers in Aging Neuroscience* 6.

Satz, P., Cole, M.A., Hardy, D.J., and Rassovsky, Y. (2011). Brain and cognitive reserve: Mediator(s) and construct validity, a critique. *Journal of Clinical and Experimental Neuropsychology* 33**,** 121-130.

Schneider-Garces, N.J., Gordon, B.A., Brumback-Peltz, C.R., Shin, E., Lee, Y., Sutton, B.P., Maclin, E.L., Gratton, G., and Fabiani, M. (2010). Span, CRUNCH, and beyond: working memory capacity and the aging brain. *Journal of cognitive neuroscience* 22**,** 655-669.

Schretlen, D.J., Munro, C.A., Anthony, J.C., and Pearlson, G.D. (2003). Examining the range of normal intraindividual variability in neuropsychological test performance. *Journal of the International Neuropsychological Society* 9**,** 864-870.

Shehzad, Z., Kelly, A.C., Reiss, P.T., Gee, D.G., Gotimer, K., Uddin, L.Q., Lee, S.H., Margulies, D.S., Roy, A.K., and Biswal, B.B. (2009). The resting brain: unconstrained yet reliable. *Cerebral cortex* 19**,** 2209-2229.

Singh-Manoux, A., Kivimaki, M., Glymour, M.M., Elbaz, A., Berr, C., Ebmeier, K.P., Ferrie, J.E., and Dugravot, A. (2012). Timing of onset of cognitive decline: results from Whitehall II prospective cohort study. *British Medical Journal* 344.

Smith, S.M., Miller, K.L., Salimi-Khorshidi, G., Webster, M., Beckmann, C.F., Nichols, T.E., Ramsey, J.D., and Woolrich, M.W. (2011). Network modelling methods for FMRI. *Neuroimage* 54**,** 875-891.

Song, S.-K., Yoshino, J., Le, T.Q., Lin, S.-J., Sun, S.-W., Cross, A.H., and Armstrong, R.C. (2005). Demyelination increases radial diffusivity in corpus callosum of mouse brain. *Neuroimage* 26**,** 132-140.

Sousa, N., and Almeida, O.F. (2012). Disconnection and reconnection: the morphological basis of (mal)adaptation to stress. *Trends Neurosci* 35**,** 742-751.

Sporns, O., Tononi, G., and Kotter, R. (2005). The human connectome: A structural description of the human brain. *PLoS Comput Biol* 1**,** e42.

Stern, Y. (2002). What is cognitive reserve? Theory and research application of the reserve concept. *J Int Neuropsychol Soc* 8**,** 448-460.

Stern, Y. (2009). Cognitive reserve. *Neuropsychologia* 47**,** 2015-2028.

Stern, Y., Alexander, G.E., Prohovnik, I., and Mayeux, R. (1992). Inverse relationship between education and parietotemporal perfusion deficit in Alzheimer's disease. *Ann Neurol* 32**,** 371-375.

Stern, Y., Tang, M.X., Denaro, J., and Mayeux, R. (1995). Increased Risk of Mortality in Alzheimers-Disease Patients with More Advanced Educational and Occupational Attainment. *Annals of Neurology* 37**,** 590-595.

Sullivan, E.V., Rosenbloom, M., Serventi, K.L., and Pfefferbaum, A. (2004). Effects of age and sex on volumes of the thalamus, pons, and cortex. *Neurobiology of aging* 25**,** 185-192.

Tomasi, D., and Volkow, N.D. (2012). Aging and functional brain networks. *Mol Psychiatry* 17**,** 471, 549-458.

Un (2010). *World Population Ageing 2009.* New York: UN.

Wang, J.H., Zuo, X.N., Dai, Z.J., Xia, M.R., Zhao, Z.L., Zhao, X.L., Jia, J.P., Han, Y., and He, Y. (2013). Disrupted Functional Brain Connectome in Individuals at Risk for Alzheimer's Disease. *Biological Psychiatry* 73**,** 472-481.

Wang, L., Goldstein, F.C., Levey, A.I., Lah, J.J., Meltzer, C.C., Holder, C.A., and Mao, H. (2011). White matter hyperintensities and changes in white matter integrity in patients with Alzheimer's disease. *Neuroradiology* 53**,** 373-381.

Wig, G.S., Schlaggar, B.L., and Petersen, S.E. (2011). Concepts and principles in the analysis of brain networks. *Year in Cognitive Neuroscience* 1224**,** 126-146.

Williams, K.N., and Kemper, S. (2010). Interventions to Reduce Cognitive Decline in Aging. *Journal of Psychosocial Nursing and Mental Health Services* 48**,** 42-51.

Wilson, R.S., Beckett, L.A., Barnes, L.L., Schneider, J.A., Bach, J., Evans, D.A., and Bennett, D.A. (2002). Individual differences in rates of change in cognitive abilities of older persons. *Psychology and Aging* 17**,** 179-193.

Wu, T., Zang, Y., Wang, L., Long, X., Hallett, M., Chen, Y., Li, K., and Chan, P. (2007). Aging influence on functional connectivity of the motor network in the resting state. *Neurosci Lett* 422**,** 164-168.

Zalesky, A., Fornito, A., and Bullmore, E.T. (2012). On the use of correlation as a measure of network connectivity. *Neuroimage* 60**,** 2096-2106.

Zhang, J., Wang, J., Wu, Q., Kuang, W., Huang, X., He, Y., and Gong, Q. (2011). Disrupted brain connectivity networks in drug-naive, first-episode major depressive disorder. *Biol Psychiatry* 70**,** 334-342.

CHAPTER II

Paulo César Gonçalves Marques, José Miguel Montenegro Soares, Ricardo José da Silva Magalhães, Nadine Correia Santos, Nuno Jorge Carvalho Sousa (2015)

Macro- and micro-structural white matter differences correlate with cognitive performance in healthy aging

Brain imaging and behavior,1-14, doi: 10.1007/s11682-015-9378-4

Macro- and micro-structural white matter differences correlate with cognitive performance in healthy aging

Paulo César Gonçalves Marques, ME[123] José Miguel Montenegro Soares, PhD[123] Ricardo José da Silva Magalhães, ME[123] Nadine Correia Santos, PhD[123] Nuno Jorge Carvalho Sousa, MD, PhD[123]

[1] Life and Health Sciences Research Institute (ICVS), School of Health Sciences, University of Minho, Campus Gualtar, 4710-057 Braga, Portugal.

[2] ICVS/3B's - PT Government Associate Laboratory, Braga/Guimarães, Portugal.

[3] Clinical Academic Center – Braga, Braga, Portugal

Corresponding Author: Paulo Marques, Life and Health Sciences Research Institute (ICVS), School of Health Sciences, University of Minho, Campus Gualtar, 4710-057 Braga, Portugal. Email: paulo.c.g.marques@ecsaude.uminho.pt. Phone: +351 253 604 925

Abstract

Studies have shown that white matter (WM) volumetric reductions and overall degradation occur with aging. Nonetheless little is known about the WM alterations that may underlie different cognitive status in older individuals. The main goal of the present work was to identify and characterize possible macro and microstructural WM alterations that could distinguish between older healthy individuals with contrasting cognitive profiles (i.e. “poor” vs “good” cognitive performers). Structural and diffusion magnetic resonance imaging was performed in order to quantify local WM volumes, white matter signal abnormalities (WMSA) volume (a measure of lesion burden) and diffusion tensor imaging scalar maps known to probe WM microstructure. A battery of neurocognitive/psychological tests was administered to assess the cognitive performance. Poor performers showed a higher slope for the positive association between WMSA volume and age compared to good performers. Even when controlling for WMSA volume, poor performers also evidenced lower fractional anisotropy, as well as positive associations with age with higher slopes of regression parameters in radial and axial diffusivity. Altogether results suggest that the cognitive performance is related with differences in WM, with poor cognitive performers displaying signs of faster aging in WM.

Keywords: diffusion tensor imaging; aging; cognitive performance; white matter; tract-based spatial statistics

1. Introduction

The normal aging process is characterized by a natural and progressive cognitive decline (Brickman et al., 2005;Salthouse, 2009). Interestingly, the healthy aging pattern seems to be heterogeneous as different individuals age differently. In fact, cognitive decline is less pronounced in some individuals, compared to others, with this effect being associated with a multitude of factors (MacDonald et al., 2003;Paulo et al., 2011;Santos et al., 2014).

Several changes take place at the brain level with normal aging, including: volume alterations; chemical changes, characterized by decreased synthesis of neurotransmitters, neurotransmitter receptors and transporters (Ota et al., 2006); cortical thinning (Salat et al., 2004); and, functional reorganization (Tomasi and Volkow, 2012). Specifically, gray matter (GM) and white matter (WM) alterations in healthy aging have been the scope of many neuroimaging studies (Salat et al., 2009;Lemaitre et al., 2012;Fjell et al., 2013), with some work reporting patterns of WM alterations that accompany cognitive decline in aging. For example, WM degradation in anterior regions has been associated with decreased processing speed and reduced working memory, while degeneration on the posterior parts has been linked to reduced inhibition and higher task switching costs and poor episodic memory with WM degradation in central regions of the brain (Kennedy and Raz, 2009). Moreover, WM atrophy was also associated with the decline in neuropsychological functioning (Brickman et al., 2006).

Another common finding in aging studies is the positive association between aging, cognitive decline and the presence of WM hyperintensities in T2-weighted MRI images, which have been described as ischemic events (Garde et al., 2005;Fischer et al., 2007). These lesions are frequently associated to axonal loss and demyelination (Wang et al., 2011). Similarly to the volumetric results, WM signal abnormalities (WMSA) seem to present an anterior-to-posterior age pattern, even in healthy individuals, and are associated with poorer cognition and functional status (Prins et al., 2005;Wakefield et al., 2010;Maillard et al., 2012). In a recent study, researchers demonstrated that WMSA were associated with slower search performance in aging and this association was independent of the generalized decrease in processing speed (Lockhart et al., 2014).

Diffusion tensor imaging (DTI) studies have brought evidence that WM microstructural alterations also occur with aging and may be associated with cognition (for review see (Madden et al., 2011)). Cross sectional studies have described variations on WM properties associated with cognitive performance such as memory, executive functioning and information processing speed (Deary et al., 2006;Vernooij et al., 2009;Laukka et al., 2013). These have been supported also by longitudinal alterations of perceptual speed and working memory in older adults (Charlton et al., 2010;Lovden et al., 2014). Moreover, studies involving DTI analysis have consistently reported patterns of WM degradation (O'Sullivan et al., 2001), which typically includes both a decrease in Fractional Anisotropy (FA) of normal appearing white matter with increasing age and a decrease in Mean Diffusivity (MD) (Pfefferbaum and Sullivan, 2003;Salat et al., 2005;Kochunov et al., 2007;Barrick et al., 2010). Fewer studies have also reported greater age-related increases in Radial Diffusivity (RD) compared to Axial Diffusivity (AD) (Zhang et al., 2010). A recent longitudinal study showed that AD changes with aging were more consistent than FA and RD changes and that both increases and decreases in AD occur along aging (Bender and Raz, 2015). There is also an anterior-to-posterior gradient of degeneration with more pronounced effects on the anterior regions (Pfefferbaum and Sullivan, 2003;Head et al., 2004;Salat et al., 2005;Grieve et al., 2007). Cognitive impairments associated with WM degradation using DTI metrics have been found in pathological conditions, including Alzheimer Disease and mild cognitive impairment (MCI) (Mielke et al., 2009;Liu et al., 2011), multiple sclerosis (MS) (Roosendaal et al., 2009) and major depressive disorder (Alves et al., 2012).

Still, despite the findings, most of the previously mentioned studies focused either on an individual dimension of WM assessment (e.g. volumetry, WMSA or DTI indices) or on specific dimensions of cognitive performance (e.g. working memory, executive functioning, processing speed). Moreover, a previous study by Santos et al. (2013) assessed a large sample of older healthy adults with an extensive battery of neurocognitive tests that were grouped in cognitive dimensions. Afterwards, clusters of cognitive performance were obtained using these dimensions and mood status. These results pointed to the fact that some individuals that are better in one dimension of cognition (e.g. memory) are also better at other cognitive dimensions (e.g. executive functioning) and the opposite also holds true. Taking this into account, in the present study through a multimodal neuroimaging approach in a cross-sectional design, we aimed at investigating i) which WM properties could discriminate between

overall “good” and “poor” cognitive performance status in healthy older individuals and ii) if age affects each group differently, through a multimodal neuroimaging approach in a cross-sectional design. Specifically, we assessed WM volumetry and WM hypointensities volume (a measure of WMSA volume) through structural MRI and investigated WM microstructural properties through DTI metrics derived from diffusion MRI.

2. Methods

2.1 Ethics statement

The current study was part of the Switchbox (www.switchbox-online.eu/) project. Study goals and tests were explained to all participants. Informed written consent was obtained from all study participants. The study was conducted in accordance with the principles expressed in the Declaration of Helsinki and was approved by the local and national ethics committees.

2.2 Neurocognitive assessment

The selection of participants was based on cognitive data obtained from a representative sample of the general Portuguese older population in terms of age, gender and education [n=1051, after inclusion/exclusion criteria; subjects randomly selected from the Guimarães and Vizela local area health authority registries (Costa et al., 2013;Santos et al., 2013;Santos et al., 2014)]. A team of trained psychologists performed the neurocognitive/neuropsychological assessments. The test battery included the following instruments: digit-span forward and backward test, Stroop color and word test, controlled oral word association test (COWAT, letters F-A-S), selective reminding test (SRT), digit symbol substitution test (DSST), mini-mental state examination (MMSE), geriatric depression scale (GDS, long-version) and the Graffar socio-demographic scale (Santos et al., 2014). Regarding the MMSE scores, recommendations state that the corresponding threshold should be adjusted depending on factors such as age and/or education (Grigoletto et al., 1999;Busch and Chapin, 2008). The following adjusted thresholds for cognitive impairment were calculated and applied: MMSE score < 17 if individual with ≤ 4 years of formal school education and/or ≥

72 years of age, and MMSE score < 23 otherwise [follows the MMSE validation study for the Portuguese population (Guerreiro et al., 1994)].

2.3 Principal Component Analysis and clusters of cognitive performance

In a previous study, Principal Component Analysis (PCA) was performed in a subsample of 487 participants in order to allocate the multiple test variables into composite components/dimensions, thus reducing the data dimensionality with the least possible loss of information (Santos et al., 2013). PCA resulted in the identification of four significant dimensions: memory (MEM) (SRT test variables: consistent long-term retrieval (CLTR), log term storage (LTS) and delayed recall); executive function (EXEC) (FAS admissible parameter; Stroop parameters: words, colors and words/colors; digits parameters: forward and backward); global cognitive status (MMSE) and mood (GDS). Further details regarding factor loadings can be consulted in the original publication of the exploratory factor analysis (Santos et al., 2013).

Finally, a cluster analysis on the PCA-derived dimensions (i.e. MEM, EXEC, MMSE and GDS z-scores) was performed in order to identify groups sharing similar characteristics across these dimensions and a four-cluster membership was considered to provide the best solution (Santos et al., 2013). Further analysis of the resulting clusters (C1 to C4) revealed that the subjects included in C1 had the highest MEM, EXEC and MMSE z-scores, and that the clusters followed a consistent rank order of cognitive performance in all cognitive dimensions (i.e. EXEC, MEM and MMSE): C1 > C2 > C3 > C4. Thus, this ranked order of performance in cognitive dimensions corresponded to “very good”, “good”, “poor” and “very poor” cognitive performers. The clusters differed significantly from each other in all cognitive dimensions (ANOVAs, followed by Games-Howell post hoc tests). GDS scores differed significantly between C1 and C2 clusters and between the C3 and C4 clusters, but not between C1 and C3 and C2 and C4 (Santos et al., 2013).

2.4 Participants

In the Switchbox project, from the considered cohort (Santos et al., 2013), 60 subjects from the cluster exhibiting "very good" (C1) cognitive performance and 60 subjects from the "very poor" (C4) cognitive performers cluster were recruited for MRI screening. Participants were pseudo-randomly selected from each cluster in order to obtain two groups matched for age and gender. Selectivity indexes for these background variables ([Msubsample - Mtotal sample] / SDtotal sample) were -0.131 for age and 0.400 for years of formal school education and the ratio of males/females was 0.533 in the original sample and 0.467 in this sample. The primary exclusion criteria were inability to understand the informed consent, participant choice to withdraw from the study, incapacity and/or inability to attend the MRI session, dementia and/or diagnosed neuropsychiatric and/or neurodegenerative disorder (medical records).

In the present manuscript "very good" and "very poor" cognitive performers will be referred simply as good and poor performers, respectively. This setting enabled to test which WM correlates could distinguish between overall cognitive performance groups. From the 120 subjects initially recruited, nine refused to undergo MRI screening at the time of the evaluation, one subject did not finish the diffusion acquisition from the screening protocol and four subjects had brain lesions/pathology. In total, 106 subjects (ranging from 51 to 87 years of age) participated in the present study: 58 good and 48 poor cognitive performers.

2.5 Data acquisition

All participants underwent the same acquisition protocol implemented on a clinical approved Siemens Magnetom Avanto 1.5 T (Siemens Medical Solutions, Erlangen, Germany) at Hospital de Braga (Braga, Portugal) using a Siemens 12-channel receive-only head coil. The acquisition protocol included a structural 3D T1-weighted magnetization prepared rapid gradient echo (MPRAGE) with the following parameters: repetition time (TR) = 2730 ms, echo time (TE) = 3.48 ms, flip angle = 7°, 176 sagittal slices, in-plane resolution = 1 × 1 mm^2 and slice thickness = 1 mm. A Diffusion Weighted Imaging (DWI) scan was also performed using a spin-echo echo-planar imaging (SE-EPI) sequence: TR = 8800 ms, TE = 99 ms, FoV = 240 x 240 mm, acquisition matrix = 120 × 120, 61 2-mm axial slices with no gap, 30 non-collinear

gradient directions with b=1000 s mm^{-2}, one b = 0 s mm^{-2} acquisition and 1 repetition. Before any data pre-processing, the raw DWI acquisitions from all subjects were visually inspected by the authors, including a certified neuroradiologist, to confirm that none of the participants had brain lesions and/or critical head motion or artifacts that could compromise data quality.

2.6 White matter segmentation and WMSA volume estimation

T1-weighted MPRAGE images were processed using the standard semi-automated workflow implemented in Freesurfer toolkit version 5.1 (http://surfer.nmr.mgh.harvard.edu). The pipeline and procedures employed have been validated against manual segmentations (Fischl et al., 2002) and are considered reliable across sessions, scanner platforms, updates and field strengths (Jovicich et al., 2009). Several improvements were made during the last decade and the technicalities of the procedures are described elsewhere (Fischl et al., 2002;Desikan et al., 2006;Destrieux et al., 2010). Briefly, the entire pipeline involves 31 processing steps which include the spatial normalization to Talairach standard space, skull stripping, intensity normalization, tessellation of GM-WM boundary and cortical, subcortical and WM segmentation. For the present study, only the volumes of regions of interest (ROI) resulting from WM segmentation and total WM hypointensities (i.e. WMSA) volume were considered. Freesurfer labels the WMSA using probabilistic procedures that were extended to WM lesion identification (Fischl et al., 2002). This T1-based WMSA volume estimate has been successfully used as a measure of WM lesion volume (Salat et al., 2012), and showed sensitivity in measuring WM lesions in Alzheimer's disease (Salat et al., 2010), as well as to correlate with estimates based on FLAIR acquisitions and to correlate better with clinical symptoms in MS (Bagnato et al., 2010).

2.7 DWI data pre-processing and tensor fitting

All data pre-processing was performed with tools provided with the FMRIB Software Library (FSL v5.0; http://fsl.fmrib.ox.ac.uk/fsl/). The DWI images were initially corrected for motion and eddy current distortions using FMRIB's Diffusion Toolbox (FDT). The affine transformations used to register each volume were also used to rotate the gradient vectors accordingly using

FSL's fdt_rotate_bvecs script. The first b0 volume of each subject's dataset was then extracted and skull stripped using the BET tool, thus generating a brain mask that was then applied to the remaining volumes in order to remove non-brain structures.

Tensor fitting and scalar maps computation steps were performed with the tools provided with Camino software package (http://cmic.cs.ucl.ac.uk/camino/) which implements the Robust Estimation of Tensors by Outlier Rejection (RESTORE) algorithm (Chang et al., 2005). RESTORE algorithm performs nonlinear least squares fitting with constant weights after rejecting potential outliers with an iteratively reweighted least squares regression and inspection of the reweighted fit residuals. After tensor fitting, scalar maps of FA and AD and RD were generated.

2.8 Tract Based Spatial Statistics

Voxel-wise analysis of scalar maps was performed using the TBSS (Smith et al., 2006) procedures, also implemented in FSL. Initially, the FA maps from all participants were slightly eroded and the end slices were zeroed in order to further remove potential outliers. Next, all FA images were nonlinearly registered into a 1 x1 x 1 mm standard space. In order to perform this, the FA image from each subject was nonlinearly registered to each other in order to find the "most representative one" (i.e. the one that requires the least warping to align all images) that served as the study specific template. This template image was then affine transformed into Montreal Neurological Institute (MNI) 152 standard space and each FA map was transformed into standard space by combining the nonlinear transformation to the FA target with the affine transformation into MNI space. All FA images were then averaged and the resulting image was skeletonized. The skeleton was then thresholded at 0.3 in order to remove from the skeleton regions encompassing multiple tissue types. Finally, all scalar maps (FA, AD and RD) were projected into this FA skeleton using the transformations applied to the FA images.

2.9 Statistical analysis

The main focus of the present work was on the effects of overall cognitive functioning, age and their interactions in relation with WM. Multiple group confirmatory factor analysis (MGCFA) was performed in order to ensure that the cognitive factor structure was valid and invariant across age categories. This can be confirmed by the absence of differences between the fit of unconstrained and constrained models ($\Delta\chi^2 = 8.22$, $\Delta df = 14$, $p=0.877$) supporting metric invariance. [1]

Volumetric data analysis was performed ROI-wise and the statistical analysis was performed with SPSS version 22 (IBM, SPSS, Chicago, IL, USA). For each WM ROI, a general linear model analysis of covariance (ANCOVA) was performed with the ROI volume as the dependent variable, group as the fixed factor and age, sex, years of formal school education and intracranial volume (ICV) as covariates. For the present study, only the main effects of age, group and age by group interaction were considered of interest. Only results surviving a significance level of $p < 0.05$ after correction for multiple comparisons using the false discovery rate (FDR) criterion were reported. Analyses of the WMSA volume, as well as the volumes from the left caudal anterior cingulate and right pars triangularis, rostral anterior cingulate and superior temporal, were performed on natural log transformations of the estimated volume in order to meet the normality assumptions of the residuals of the ANCOVA models. The reason for this transformation was their positively skewed distribution. Systolic and diastolic blood pressure (BP) did not differ between groups (Table I) and it was not a significant predictor of WMSA volume. For these reasons, and in order to reduce the number of independent variables in the models, we did not control for BP.

Statistical analysis of the skeletonized maps of FA, AD and RD was performed using the permutation methods employed in "randomise", distributed with FSL. In total, 4 models were used. In the first model we tested for the group by age interaction; thus, testing if the slopes of

[1] Analysis performed on another sample of 435 subjects, similar to the sample used in (Santos et al., 2013) in terms of age and gender (data not published). The sample was divided in age categories (i.e. 50-60, 60-70, 70 or more years of age) for the MGCFA.

the age associations for each group differed significantly. In the second model, regions with significant interactions were masked out, thus enabling the estimation of the main effects of group and age. The third and fourth models were similar to the first two but with an additional regressor for the estimated volume of WMSA. These models enabled the estimation of the same effects as the previous two while controlling for a measure of WM lesion. Sex and years of formal school education were always entered in the models as covariates. 10000 random permutations were used in the inference of the contrasts of interest. Threshold-free cluster enhancement (TFCE) was used to detect widespread differences and family-wise error (FWE) correction at $p < 0.05$ was used to correct for multiple comparisons. The projected regions showing significant results were then labeled according to the John Hopkins University ICBM-DTI-81 WM labels atlas (Hua et al., 2008) distributed with FSL. For visualization purposes, the significant results were dilated with tbss_fill tool (distributed with FSL).

3. Results

3.1 Sample characteristics

Table I presents a basic demographic, cognitive and physiological characterization of the two cognitive performance groups enrolled in the present study.

Table I. Basic characteristics of the study's sample.

	Poor		**Good**		
	Mean (SD)	**Range**	**Mean (SD)**	**Range**	**Test statistic**
Males/Females (n)	32/26		20/28		$X^2_{(104)}=1.917$
Age (years)	66.19 (7.84)	52 – 87	64.41 (8.66)	51 – 82	$T_{(104)}=-1.094$
Education (years)	3.65 (1.99)	0 – 12	6.84 (4.33)	2 – 17	$T_{(104)}=4.720$ ($p<0.001$)
MMSE score	24.02 (3.56)	18 – 29	28.52 (1.78)	23 – 30	$T_{(104)}=8.439$ ($p<0.001$)
ZMEM	-0.723 (0.525)	-1.603 – 0.638	1.339 (0.664)	0.512 – 3.314	$T_{(104)}=17.449$ ($p<0.001$)
ZEXEC	-1.062 (0.581)	-2.341 – 0.326	1.083 (0.900)	-0.4681 – 2.703	$T_{(104)}=14.234$ ($p<0.001$)
ZMMSE	-0.427 (0.918)	-3.013 – 0.8587	0.734 (0.460)	-0.690 – 1.117	$T_{(104)}=8.439$ ($p<0.001$)
ICV (mm^3)	1453651 - (159935)	1173954 – 1898374	1484486 - (153998)	1134670 – 1834778	$T_{(104)}=1.008$ ($p=0.316$)
Systolic BP	142.10 (18.32)	102 - 191	139.95 (17.41)	93 - 181	$T_{(104)}=0.620$ ($p=0.537$)
Diastolic BP	82.52 (8.20)	63 - 107	80.97 (8.01)	60 -98	$T_{(104)}=0.984$ ($p=0.327$)

3.2 White matter volumetry

Analysis of WM regional volumes yielded no significant effects for group by age interactions. Similarly, no statistically significant differences were found between good and poor cognitive performers. However, several WM regions showed statistically significant (FDR corrected at $p < 0.05$) negative associations with age in both hemispheres (Table II). Lateral Orbitofrontal, Superior Frontal, Inferior Temporal, Fusiform and the Posterior Cingulate appeared to show the largest age differences.

Table II. White matter ROIs presenting statistically significant negative associations with age (results FDR corrected at $p < 0.05$).

White Matter Region	T-statistic	p-value	White Matter Region	T-statistic	p-value
Right Hemisphere			*Left Hemisphere*		
Lateral orbitofrontal	-5.44976	<0.001	Inferior temporal	-7.31238	<0.001
Fusiform	-5.21978	<0.001	Superior frontal	-5.50838	<0.001
Posterior cingulate	-5.15511	<0.001	Lateral orbitofrontal	-5.26034	<0.001
Inferior parietal	-5.07018	<0.001	Rostral middle frontal	-4.7374	<0.001
Middle temporal	-4.68758	<0.001	Entorhinal	-4.55841	<0.001
Parahippocampal	-4.67506	<0.001	Middle temporal	-4.55636	<0.001
Superior parietal	-4.60471	<0.001	Posterior cingulate	-4.4679	<0.001
Superior frontal	-4.44204	<0.001	Superior parietal	-4.3474	<0.001
Medial orbitofrontal	-4.24614	<0.001	Superior temporal	-4.1974	<0.001
Post central	-4.21701	<0.001	Fusiform	-4.19575	<0.001
Inferior parietal	-4.01232	<0.001	Postcentral	-4.16346	<0.001
Superior temporal	-3.97203	<0.001	Paracentral	-3.80857	<0.001
Pars orbitalis	-3.94235	<0.001	Precentral	-3.80357	<0.001
Rostral middle frontal	-3.67635	<0.001	Lingual	-3.70006	<0.001
Precentral	-3.63165	<0.001	Parahippocampal	-3.41426	<0.001
Lateral occipital	-3.56865	<0.001	Superior temporal	-3.40162	<0.001
Pars triangularis	-3.40025	<0.001	Pars triangularis	-3.3605	0.001
Entorhinal	-3.23258	0.002	Inferior parietal	-3.23466	0.002
Paracentral	-3.16105	0.002	Supramarginal	-3.22941	0.002
Frontal pole	-3.12296	0.002	Pars triangularis	-3.21845	0.002
Lingual	-2.97717	0.004	Precuneus	-2.92762	0.004
Supramarginal	-2.96515	0.004	Rostral anterior cingulate	-2.8917	0.004
Rostral anterior cingulate	-2.84301	0.005	Pars orbitalis	-2.71792	0.008
Pars opercularis	-2.80929	0.006			

[a] Analyses performed with natural log transformed volumes in order to meet the assumptions of normality of the residuals of the ANCOVA models.

Similarly to other studies, WMSA volumes were non-normally distributed and positively skewed (skewness of 1.843 and 2.150 for good and poor cognitive performers respectively) (Jacobs et al., 2013). Good cognitive performers presented median WMSA volume of 2109.5 (IQR= 1469.25) and poor cognitive performers presented median WMSA volume of 3052.5 (IQR= 4375.5). These values are comparable to other studies assessing healthy individuals with approximate age ranges (Jacobs et al., 2013;Leritz et al., 2013). Analysis of natural log transformed WMSA volume revealed a significant group by age interaction ($F(1,100) = 10.531$; $p = 0.003$; $\eta^2 = 0.095$). Parameter estimates revealed that while WMSA volume has a positive correlation with age in both groups, the slope of the regression parameter is higher in poor cognitive performers (B = 0.072; SE = 0.012; $CI_{95\%}$= [0.047-0.097]) when compared to the slope in good cognitive performers (B = 0.033; SE = 006; $CI_{95\%}$= [0.020-0.046]). As expected, age was a significant predictor of WMSA volume ($F(1,101) = 73.785$; $p < 0.001$; $\eta^2 = 0.422$) and group differences were also significant ($F(1,101) = 8.253$; $p = 0.005$; $\eta^2 = 0.076$).

3.3 Group by age interactions in DTI metrics

Spatial representations of statistically significant interactions between age and group, with and without inclusion of WMSA volume in the model, are presented in Figure 1. Significant interactions between age and group in FA maps were found in the posterior thalamic radiation, splenium of corpus callosum and body of corpus callosum, with all clusters localized in the left hemisphere of the brain (Figure1.A).

Post-hoc analysis revealed that the group with poor cognitive performance had a stronger negative association between FA and age when compared to the group with good cognitive performance. The results presented in Figure 1.B indicate that after the inclusion of WMSA in the regression model, no significant interactions between age and group in FA values remained.

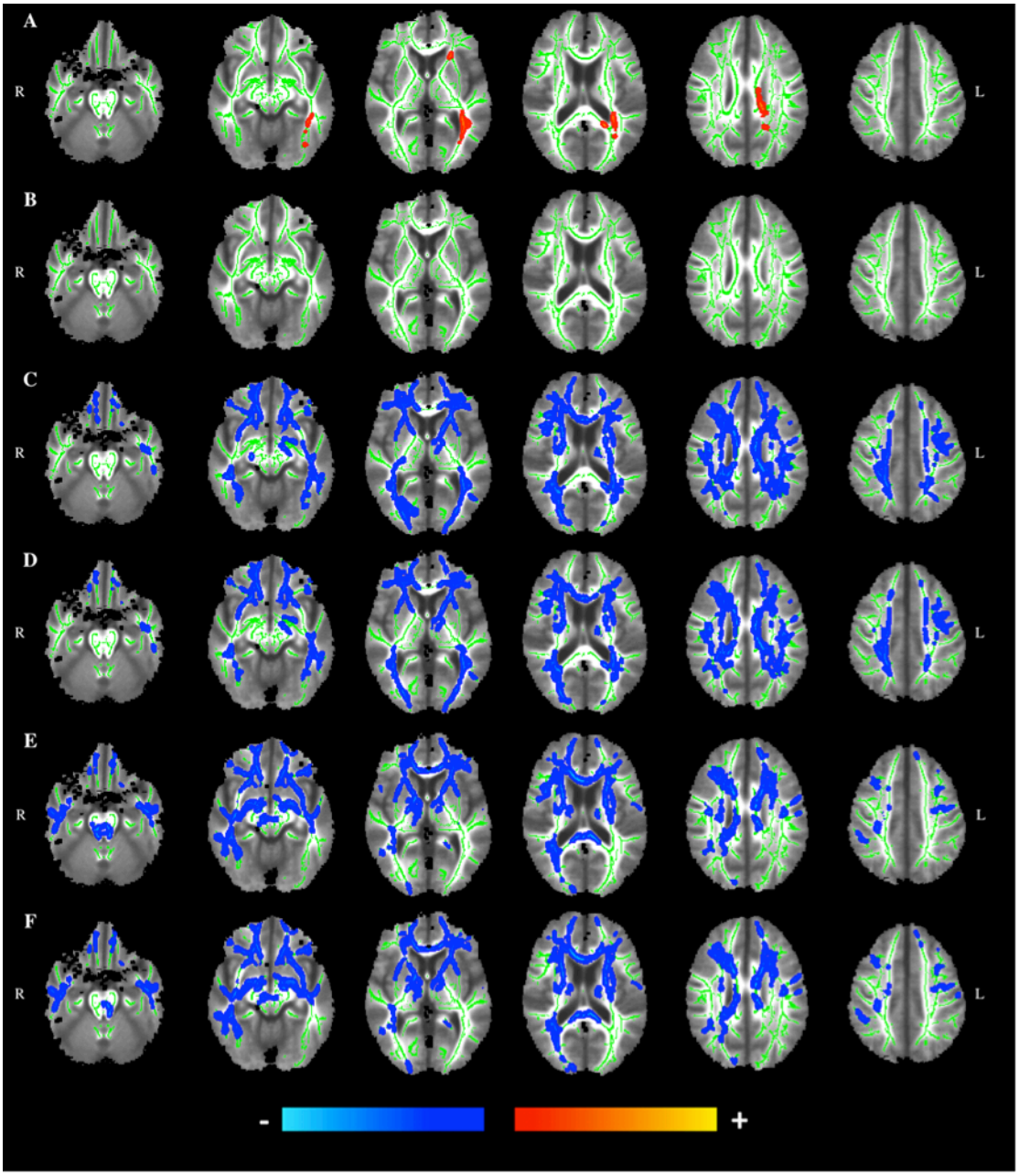


Figure 1. Statistically significant group by age interactions in FA, RD and AD projected maps, before (A, C, E) and after (B, D, F) controlling for WMSA volume. Significance threshold was set to $p < 0.05$ (FWE corrected for multiple comparisons). Blue/light-blue gradient indicates lower age slopes for good cognitive performers when compared to poor cognitive performers. Red/yellow gradient indicates higher age slopes for the good cognitive performance group.

Regarding RD, Figure 1.C shows that several significant interactions could be found between age and group in several widespread clusters and in both hemispheres. Post-hoc analysis revealed an inverse pattern relative to the FA interactions, with the poor cognitive performance

group evidencing a higher slope in the positive association of RD and age. After inclusion of WMSA volume in the model, most of the significant interactions remained, being observed the same pattern of higher slope of the RD association with age in poor cognitive performers when compared to good cognitive performers (Figure 1.D).

Analysis of AD maps showed several widespread significant age by group interactions (Figure1.E). Similarly to the interactions in RD profiles, poor cognitive performers showed higher slopes for the positive association of AD with age when compared to good cognitive performers. As shown in Figure 1.F, after inclusion of WMSA volume in the model, most of the previously described interactions remained.

3.4 Age effect on DTI metrics

Maps of the significant effects of age on FA, RD and AD are presented in Figure 2. These results, were previously masked out with the significant group by age interaction results in order to reflect age effects only. Higher age was associated with lower FA values in almost all the WM tracts (Figure 2.A), and most of those differences remained after controlling for WMSA volume (Figure 2.B). The same pattern, although with a positive correlation with age, was found for RD profiles with and without inclusion of WMSA volume as a covariate (Figure 2.D and Figure 2.C). Age was also positively associated with higher AD values (Figure 2.E). The inclusion of WMSA as covariate seemed to have a low impact in the age effect (Figure 2.F).

3.5 Group effect on DTI metrics

Analysis of group differences while accounting for age, gender and years of formal school education, yielded several statistically significant effects (Figure 3). Similarly to the age effect results, regions where group by age interactions were significant were previously masked out so that the presented results reflect only group differences. Between group analyses of FA maps revealed that good cognitive performers had significantly higher FA values in several wide spread WM tracts when compared with poor cognitive performers (Figure 3.A). Inclusion

of WMSA volume in the regression model accounted for some, but not all, of the described between group differences (Figure 3.B).

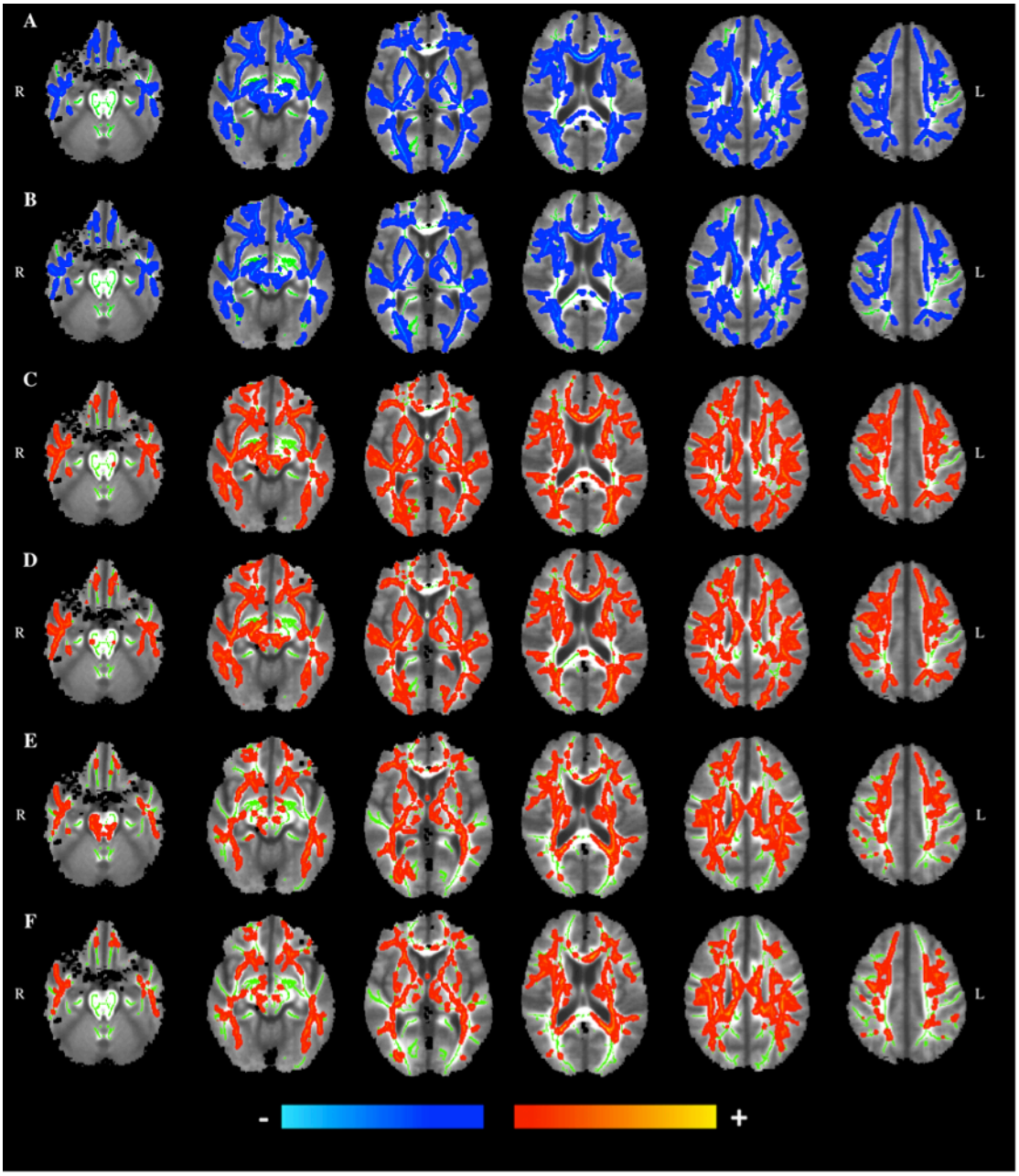


Figure 2. Statistically significant associations between age and FA, RD and AD maps, before (A, C, E) and after (B, D, F) controlling for WMSA volume. Blue/light-blue gradient indicates negative associations with age. Red/yellow gradient indicates positive. All results were considered significant at $p < 0.05$ (FWE corrected for multiple comparisons).

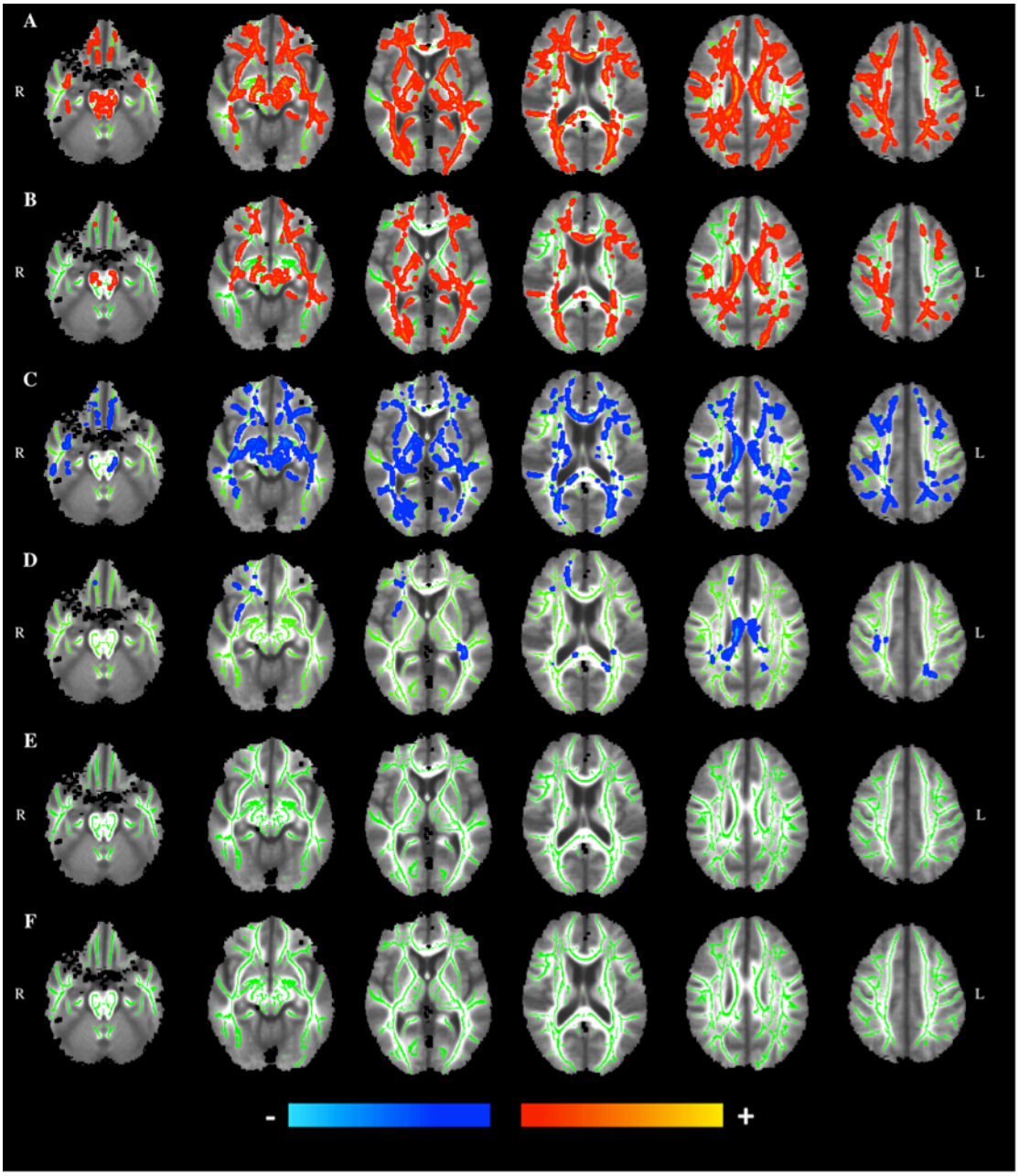


Figure 3. Statistically significant group differences in FA, RD and AD maps, before (A, C, E) and after (B, D, F) controlling for WMSA volume. Blue/light-blue gradient indicates lower values for good cognitive performers when compared to poor cognitive performers. Red/yellow gradient indicates higher values for the good cognitive performance group. All results were considered significant at $p < 0.05$ (FWE corrected for multiple comparisons).

In the same way, several widespread group differences could be found in RD maps, with good cognitive performers showing statistically significant lower values of RD (Figure 3.C). Figure 3.D shows that, after regressing out WMSA volume effect, good cognitive performers still showed

lower values of RD than poor cognitive performers in several white matter tracts. Regarding AD profiles, no group differences were found in AD before (Figure 3.E) and after (Figure 3.F) including WMSA volume as a covariate in the model.

4. Discussion

In the present study we investigated which possible WM correlates could underlie the distinction between two opposite cognitive profiles (i.e. 'good' and 'poor') in older subjects. Considering the effect of age on WM, the results are consistent with the majority of the previously published aging studies. These effects include i) overall volumetric negative associations with age in WM, which are more pronounced in anterior regions (Salat et al., 2009;Westlye et al., 2010), ii) positive associations with volume of WMSAs (Smith et al., 2000;Leritz et al., 2013), and iii) overall lower FA, increased RD and AD in aged individuals, when comparing to younger subjects (Bennett et al., 2010;Leritz et al., 2013). Longitudinal evidence also suggests reduced FA and increased AD and RD with aging (Teipel et al., 2010;Sexton et al., 2014). These results are usually interpreted in the context of axonal injury or loss and demyelination in late stages of life, potentially linked to cognitive decline.

Furthermore, interestingly, when controlling for the effects of age, results indicate that the contrasting cognitive profiles are underlined by differences in WM, which, notably, evolve differently with age. In fact, albeit no volumetric group differences or group by age interactions differences were observed, WMSA volume evidenced a positive association with age. This association had a higher slope in poor cognitive performers in comparison with the slope of association in good cognitive performers. This points to an increased susceptibility for the presence of brain ischemic events in older individuals with poorer cognitive performance, even when these are clinically silent. Moreover, WMSA volume has been shown to be positively associated with vascular risk factors, such as blood pressure (Firbank et al., 2007), as well with executive functioning, processing speed and memory performance (Prins et al., 2005;Maillard et al., 2012;Jacobs et al., 2013). Thus, poorer cognitive performers not only reveal an augmented presence of WM lesions, which potentially results from loss of axonal integrity (Wang et al., 2011), with repercussion in cognitive functions, but they also exhibit

patterns that could reflect an increased vascular risk when compared to those of similar age but overall stronger cognitive performance pattern. However, we did not find differences in BP between groups and BP was not a significant predictor of WMSA. This could be due to the fact that the older Portuguese population is generally hypertensive, independently of cognitive performance, and possibly, other factors may play a role. Some studies suggest that vascular risk factors, including hypertension, affect WM microstructural integrity independently of WMSA (Wang et al., 2015). Additionally, metabolic risk factors could also mediate these effects (Bender and Raz, 2015).

When considering the effect in WM microstructure, good cognitive performers evidenced overall higher FA and lower RD and AD when compared to poorer performers. However, since several group by age interactions were found in all metrics, group differences need to be interpreted in the context of these interactions. Regarding FA, only small significant interactions were found in regions close to the left lateral ventricle that were not significant after the inclusion of WMSA volume as regressor. Nevertheless, the volume of WMSA explained only some of the widespread group differences in FA. Of note, lower values of FA are usually associated with age-related cognitive decline. This is thought to reflect axonal damage and decreased efficiency in communication and consequent disconnection of neural networks (O'Sullivan et al., 2001;Bartzokis et al., 2004;Kochunov et al., 2007). Additionally, longitudinal studies showed that alterations in FA in one tract are associated with similar alterations in other tracts (Lovden et al., 2014) thus indicating that FA changes with aging are not mostly tract specific.

Regarding RD, several widespread group by age interactions were found, with most remaining significant after the inclusion of WMSA in the model. This means that the positive association of RD and age had a higher slope in poor cognitive performers compared to good performers. The group comparisons further revealed that poor cognitive performers already showed significantly higher RD values at the mean age of the population under study. RD is the DTI metric mostly associated with myelination levels with increased RD typically reflecting demyelination (Sun et al., 2006;Klawiter et al., 2011). Taking this into account, our results point to an increased rate of demyelination in older individuals with poor cognitive performance, which is a clinically relevant finding.

When analyzing AD maps, no group differences were found with or without inclusion of WMSA volume as regressor in the model. More interestingly, numerous significant group by age interactions were found with and without inclusion of WMSA volume as a regressor. This suggests that although at the mean age of our sample the groups did not differ significantly in AD after inclusion of WMSA volume, the slopes of the positive associations between AD and age are different, with the poor performance group showing a higher slope in AD compared to the good performance group. Unlike FA and RD, localized or sparse foci of increase (Zhang et al., 2010), decrease (Burzynska et al., 2010) or no effect (Madden et al., 2009) in AD with aging have been reported. Bender & Raz (2015) found, in a longitudinal setting, that aging was associated with both decreases and increases in AD. Whereas, RD is typically associated with myelination levels, AD is usually interpreted in the context of axonal pathology. Small decreases of AD have been reported in the presence of axonal injury (Budde et al., 2007;Budde et al., 2009) suggesting that cellular fragments and gliosis would restrict water diffusion. Sun and colleagues suggest, however, that cellular debris could be later removed by microglia, clearing the lesion area and thus leading to an increase in AD (Sun et al., 2008). As such, the increased slopes of the age regressor in AD could reflect the higher presence of axonal damage and the increased slopes of the regression parameter with RD could reflect a higher axonal myelin loss. Wallerian degeneration theory accounts for both axonal injury (primary degeneration) and loss of myelin following the axonal lesioning (secondary degeneration) (Conforti et al., 2014). Taking all of this into account, we hypothesize that the higher slope of the associations of age with AD and RD could reflect that poor cognitive performers could be suffering a higher rate of Wallerian degeneration compared to good cognitive performers.

In summary, older individuals with poor cognitive performance evidenced lower FA and higher slopes in the association of age with RD and AD, controlling for age, education and macrostructural lesioning, when compared to good cognitive performers. In the context of aging, a similar pattern has been suggested to reflect chronic WM degeneration (Burzynska et al., 2010). Longitudinal studies reported that changes in perceptual speed are associated with decreased FA and increased MD in the cortical spinal tract (Lovden et al., 2014) and that working memory declines with aging were associated with decreases in MD but not FA (Charlton et al., 2010). In the present study however, we found differences to affect not only

these tracts but also almost all WM tracts. This may indicate that overall good performance could be the result of overall preserved WM integrity. This is further supported by the results found for WMSA. However, with the present setting, we cannot exclude the hypothesis that this is the result of the summation of the effects of individual cognitive dimensions that are preserved in good performers. Considering that poor cognitive performers evidence higher slopes for the age regression parameters with diffusivity metrics, we speculate that poor cognitive performers display faster WM degeneration. This view is further reinforced by the similarity between the group comparisons results and the cross sectional effects of age. We aim at further investigating this with longitudinal analysis of the same cohort.

The present work presents some limitations that should be considered. One of the main limitation concerns the estimation of WMSA volume that, as in the present study, is estimated from a T1-weighted MPRAGE acquisition. Several different sources of WM lesioning can lead to WMSA and these different sources could not be fully identified with a T1-weighted sequence. Optimally, a combination of T1, T2, proton density (PD) and fluid-attenuated inversion-recovery (FLAIR) sequences should be used (Kim et al., 2008). Another limitation concerns the nature and interpretation of the DTI metrics analyzed. The images acquired in order to estimate those metrics had a limited voxel size of 2 mm. However, these metrics were interpreted as reflecting the properties of WM at the axonal level that has a much smaller scale. This leads to an important issue in inferring WM integrity from DTI scalar metrics. The link between FA, RD and AD and myelination levels or axonal injury is not well established. Other aspects such as crossing fibers, axonal re-arrangement or partial volume effects are known to have some impact on the same metrics (Jones et al., 2013). Nevertheless, the use of multiple DTI and structural metrics, as addressed in this work, may help to overcome part of these limitations. A final limitation of the study is that is has a cross-sectional design. Future work should include a longitudinal perspective of the effects of aging, to clarify how the different groups actually progress with age.

In summary, our results showed that poor cognitive performance in older adults is associated with increased volume of WM lesions and that individuals with a weaker cognitive profile show a higher rate of chronic white matter degeneration. The similarities between the group effects and the age effect suggest that aging has a greater impact in poor cognitive performers compared to stronger performers with similar chronological age.

5. References

Alves, G.S., Karakaya, T., Fusser, F., Kordulla, M., O'dwyer, L., Christl, J., Magerkurth, J., Oertel-Knochel, V., Knochel, C., Prvulovic, D., Jurcoane, A., Laks, J., Engelhardt, E., Hampel, H., and Pantel, J. (2012). Association of microstructural white matter abnormalities with cognitive dysfunction in geriatric patients with major depression. *Psychiatry Res* 203**,** 194-200.

Bagnato, F., Salman, Z., Kane, R., Auh, S., Cantor, F.K., Ehrmantraut, M., Gallo, A., Ikonomidou, V.N., Ohayon, J., Pellicano, C., Stern, S.K., and Mcfarland, H.F. (2010). T1 cortical hypointensities and their association with cognitive disability in multiple sclerosis. *Mult Scler* 16**,** 1203-1212.

Barrick, T.R., Charlton, R.A., Clark, C.A., and Markus, H.S. (2010). White matter structural decline in normal ageing: a prospective longitudinal study using tract-based spatial statistics. *Neuroimage* 51**,** 565-577.

Bartzokis, G., Sultzer, D., Lu, P.H., Nuechterlein, K.H., Mintz, J., and Cummings, J.L. (2004). Heterogeneous age-related breakdown of white matter structural integrity: implications for cortical "disconnection" in aging and Alzheimer's disease. *Neurobiol Aging* 25**,** 843-851.

Bender, A.R., and Raz, N. (2015). Normal-Appearing Cerebral White Matter in Healthy Adults: Mean Change over Two Years and Individual Differences in Change. *Neurobiology of Aging*.

Bennett, I.J., Madden, D.J., Vaidya, C.J., Howard, D.V., and Howard, J.H., Jr. (2010). Age-related differences in multiple measures of white matter integrity: A diffusion tensor imaging study of healthy aging. *Hum Brain Mapp* 31**,** 378-390.

Brickman, A.M., Paul, R.H., Cohen, R.A., Williams, L.M., Macgregor, K.L., Jefferson, A.L., Tate, D.F., Gunstad, J., and Gordon, E. (2005). Category and letter verbal fluency across the adult lifespan: relationship to EEG theta power. *Arch Clin Neuropsychol* 20**,** 561-573.

Brickman, A.M., Zimmerman, M.E., Paul, R.H., Grieve, S.M., Tate, D.F., Cohen, R.A., Williams, L.M., Clark, C.R., and Gordon, E. (2006). Regional white matter and neuropsychological functioning across the adult lifespan. *Biol Psychiatry* 60**,** 444-453.

Budde, M.D., Kim, J.H., Liang, H.F., Schmidt, R.E., Russell, J.H., Cross, A.H., and Song, S.K. (2007). Toward accurate diagnosis of white matter pathology using diffusion tensor imaging. *Magn Reson Med* 57**,** 688-695.

Budde, M.D., Xie, M., Cross, A.H., and Song, S.K. (2009). Axial diffusivity is the primary correlate of axonal injury in the experimental autoimmune encephalomyelitis spinal cord: a quantitative pixelwise analysis. *J Neurosci* 29**,** 2805-2813.

Burzynska, A.Z., Preuschhof, C., Backman, L., Nyberg, L., Li, S.C., Lindenberger, U., and Heekeren, H.R. (2010). Age-related differences in white matter microstructure: region-specific patterns of diffusivity. *Neuroimage* 49**,** 2104-2112.

Busch, R.M., and Chapin, J.S. (2008). Review of normative data for common screening measures used to evaluate cognitive functioning in elderly individuals. *Clin Neuropsychol* 22**,** 620-650.

Chang, L.C., Jones, D.K., and Pierpaoli, C. (2005). RESTORE: robust estimation of tensors by outlier rejection. *Magn Reson Med* 53**,** 1088-1095.

Charlton, R.A., Schiavone, F., Barrick, T.R., Morris, R.G., and Markus, H.S. (2010). Diffusion tensor imaging detects age related white matter change over a 2 year follow-up which is associated with working memory decline. *J Neurol Neurosurg Psychiatry* 81**,** 13-19.

Conforti, L., Gilley, J., and Coleman, M.P. (2014). Wallerian degeneration: an emerging axon death pathway linking injury and disease. *Nature Reviews Neuroscience* 15**,** 394-409.

Costa, P.S., Santos, N.C., Cunha, P., Palha, J.A., and Sousa, N. (2013). The use of bayesian latent class cluster models to classify patterns of cognitive performance in healthy ageing. *PLoS One* 8**,** e71940.

Deary, I.J., Bastin, M.E., Pattie, A., Clayden, J.D., Whalley, L.J., Starr, J.M., and Wardlaw, J.M. (2006). White matter integrity and cognition in childhood and old age. *Neurology* 66**,**

505-512.

Desikan, R.S., Segonne, F., Fischl, B., Quinn, B.T., Dickerson, B.C., Blacker, D., Buckner, R.L., Dale, A.M., Maguire, R.P., Hyman, B.T., Albert, M.S., and Killiany, R.J. (2006). An automated labeling system for subdividing the human cerebral cortex on MRI scans into gyral based regions of interest. *Neuroimage* 31**,** 968-980.

Destrieux, C., Fischl, B., Dale, A., and Halgren, E. (2010). Automatic parcellation of human cortical gyri and sulci using standard anatomical nomenclature. *Neuroimage* 53**,** 1-15.

Firbank, M.J., Wiseman, R.M., Burton, E.J., Saxby, B.K., O'brien, J.T., and Ford, G.A. (2007). Brain atrophy and white matter hyperintensity change in older adults and relationship to blood pressure. Brain atrophy, WMH change and blood pressure. *J Neurol* 254**,** 713-721.

Fischer, P., Krampla, W., Mostafaie, N., Zehetmayer, S., Rainer, M., Jungwirth, S., Huber, K., Bauer, K., Hruby, W., Riederer, P., and Tragl, K.H. (2007). VITA study: white matter hyperintensities of vascular and degenerative origin in the elderly. *J Neural Transm Suppl***,** 181-188.

Fischl, B., Salat, D.H., Busa, E., Albert, M., Dieterich, M., Haselgrove, C., Van Der Kouwe, A., Killiany, R., Kennedy, D., Klaveness, S., Montillo, A., Makris, N., Rosen, B., and Dale, A.M. (2002). Whole brain segmentation: automated labeling of neuroanatomical structures in the human brain. *Neuron* 33**,** 341-355.

Fjell, A.M., Westlye, L.T., Grydeland, H., Amlien, I., Espeseth, T., Reinvang, I., Raz, N., Holland, D., Dale, A.M., Walhovd, K.B., and Alzheimer Disease Neuroimaging, I. (2013). Critical ages in the life course of the adult brain: nonlinear subcortical aging. *Neurobiol Aging* 34**,** 2239-2247.

Garde, E., Mortensen, E.L., Rostrup, E., and Paulson, O.B. (2005). Decline in intelligence is associated with progression in white matter hyperintensity volume. *Journal of Neurology, Neurosurgery & Psychiatry* 76**,** 1289-1291.

Grieve, S.M., Williams, L.M., Paul, R.H., Clark, C.R., and Gordon, E. (2007). Cognitive aging,

executive function, and fractional anisotropy: a diffusion tensor MR imaging study. *AJNR Am J Neuroradiol* 28**,** 226-235.

Grigoletto, F., Zappala, G., Anderson, D.W., and Lebowitz, B.D. (1999). Norms for the Mini-Mental State Examination in a healthy population. *Neurology* 53**,** 315-320.

Guerreiro, M., Silva, A.P., Botelho, M.A., Leitão, O., Castro-Caldas, A., and Garcia, C. (1994). Adaptação à população portuguesa da tradução do Mini Mental State Examination (MMSE). *Revista Portuguesa de Neurologia* 1**,** 9-10.

Head, D., Buckner, R.L., Shimony, J.S., Williams, L.E., Akbudak, E., Conturo, T.E., Mcavoy, M., Morris, J.C., and Snyder, A.Z. (2004). Differential vulnerability of anterior white matter in nondemented aging with minimal acceleration in dementia of the Alzheimer type: evidence from diffusion tensor imaging. *Cereb Cortex* 14**,** 410-423.

Hua, K., Zhang, J., Wakana, S., Jiang, H., Li, X., Reich, D.S., Calabresi, P.A., Pekar, J.J., Van Zijl, P.C., and Mori, S. (2008). Tract probability maps in stereotaxic spaces: analyses of white matter anatomy and tract-specific quantification. *Neuroimage* 39**,** 336-347.

Jacobs, H.I., Leritz, E.C., Williams, V.J., Van Boxtel, M.P., Van Der Elst, W., Jolles, J., Verhey, F.R., Mcglinchey, R.E., Milberg, W.P., and Salat, D.H. (2013). Association between white matter microstructure, executive functions, and processing speed in older adults: the impact of vascular health. *Hum Brain Mapp* 34**,** 77-95.

Jones, D.K., Knosche, T.R., and Turner, R. (2013). White matter integrity, fiber count, and other fallacies: the do's and don'ts of diffusion MRI. *Neuroimage* 73**,** 239-254.

Jovicich, J., Czanner, S., Han, X., Salat, D., Van Der Kouwe, A., Quinn, B., Pacheco, J., Albert, M., Killiany, R., Blacker, D., Maguire, P., Rosas, D., Makris, N., Gollub, R., Dale, A., Dickerson, B.C., and Fischl, B. (2009). MRI-derived measurements of human subcortical, ventricular and intracranial brain volumes: Reliability effects of scan sessions, acquisition sequences, data analyses, scanner upgrade, scanner vendors and field strengths. *NeuroImage* 46**,** 177-192.

Kennedy, K.M., and Raz, N. (2009). Aging white matter and cognition: differential effects of

regional variations in diffusion properties on memory, executive functions, and speed. *Neuropsychologia* 47**,** 916-927.

Kim, K.W., Macfall, J.R., and Payne, M.E. (2008). Classification of white matter lesions on magnetic resonance imaging in elderly persons. *Biol Psychiatry* 64**,** 273-280.

Klawiter, E.C., Schmidt, R.E., Trinkaus, K., Liang, H.F., Budde, M.D., Naismith, R.T., Song, S.K., Cross, A.H., and Benzinger, T.L. (2011). Radial diffusivity predicts demyelination in ex vivo multiple sclerosis spinal cords. *Neuroimage* 55**,** 1454-1460.

Kochunov, P., Thompson, P.M., Lancaster, J.L., Bartzokis, G., Smith, S., Coyle, T., Royall, D.R., Laird, A., and Fox, P.T. (2007). Relationship between white matter fractional anisotropy and other indices of cerebral health in normal aging: tract-based spatial statistics study of aging. *Neuroimage* 35**,** 478-487.

Laukka, E.J., Lovden, M., Kalpouzos, G., Li, T.Q., Jonsson, T., Wahlund, L.O., Fratiglioni, L., and Backman, L. (2013). Associations between white matter microstructure and cognitive performance in old and very old age. *PLoS One* 8**,** e81419.

Lemaitre, H., Goldman, A.L., Sambataro, F., Verchinski, B.A., Meyer-Lindenberg, A., Weinberger, D.R., and Mattay, V.S. (2012). Normal age-related brain morphometric changes: nonuniformity across cortical thickness, surface area and gray matter volume? *Neurobiol Aging* 33**,** 617 e611-619.

Leritz, E.C., Shepel, J., Williams, V.J., Lipsitz, L.A., Mcglinchey, R.E., Milberg, W.P., and Salat, D.H. (2013). Associations between T(1) white matter lesion volume and regional white matter microstructure in aging. *Hum Brain Mapp*.

Liu, Y., Spulber, G., Lehtimaki, K.K., Kononen, M., Hallikainen, I., Grohn, H., Kivipelto, M., Hallikainen, M., Vanninen, R., and Soininen, H. (2011). Diffusion tensor imaging and tract-based spatial statistics in Alzheimer's disease and mild cognitive impairment. *Neurobiol Aging* 32**,** 1558-1571.

Lockhart, S.N., Roach, A.E., Luck, S.J., Geng, J., Beckett, L., Carmichael, O., and Decarli, C. (2014). White matter hyperintensities are associated with visual search behavior

independent of generalized slowing in aging. *Neuropsychologia* 52**,** 93-101.

Lovden, M., Kohncke, Y., Laukka, E.J., Kalpouzos, G., Salami, A., Li, T.Q., Fratiglioni, L., and Backman, L. (2014). Changes in perceptual speed and white matter microstructure in the corticospinal tract are associated in very old age. *Neuroimage* 102 Pt 2**,** 520-530.

Macdonald, S.W., Hultsch, D.F., and Dixon, R.A. (2003). Performance variability is related to change in cognition: evidence from the Victoria Longitudinal Study. *Psychology and aging* 18**,** 510.

Madden, D.J., Bennett, I.J., Burzynska, A., Potter, G.G., Chen, N.K., and Song, A.W. (2011). Diffusion tensor imaging of cerebral white matter integrity in cognitive aging. *Biochimica et biophysica acta*.

Madden, D.J., Spaniol, J., Costello, M.C., Bucur, B., White, L.E., Cabeza, R., Davis, S.W., Dennis, N.A., Provenzale, J.M., and Huettel, S.A. (2009). Cerebral white matter integrity mediates adult age differences in cognitive performance. *J Cogn Neurosci* 21**,** 289-302.

Maillard, P., Carmichael, O., Fletcher, E., Reed, B., Mungas, D., and Decarli, C. (2012). Coevolution of white matter hyperintensities and cognition in the elderly. *Neurology* 79**,** 442-448.

Mielke, M.M., Kozauer, N.A., Chan, K.C., George, M., Toroney, J., Zerrate, M., Bandeen-Roche, K., Wang, M.C., Vanzijl, P., Pekar, J.J., Mori, S., Lyketsos, C.G., and Albert, M. (2009). Regionally-specific diffusion tensor imaging in mild cognitive impairment and Alzheimer's disease. *Neuroimage* 46**,** 47-55.

O'sullivan, M., Jones, D.K., Summers, P.E., Morris, R.G., Williams, S.C., and Markus, H.S. (2001). Evidence for cortical "disconnection" as a mechanism of age-related cognitive decline. *Neurology* 57**,** 632-638.

Ota, M., Yasuno, F., Ito, H., Seki, C., Nozaki, S., Asada, T., and Suhara, T. (2006). Age-related decline of dopamine synthesis in the living human brain measured by positron emission tomography with L-[beta-11C]DOPA. *Life Sci* 79**,** 730-736.

Paulo, A.C., Sampaio, A., Santos, N.C., Costa, P.S., Cunha, P., Zihl, J., Cerqueira, J., Palha, J.A., and Sousa, N. (2011). Patterns of Cognitive Performance in Healthy Ageing in Northern Portugal: A Cross-Sectional Analysis. *PLoS ONE* 6**,** e24553.

Pfefferbaum, A., and Sullivan, E.V. (2003). Increased brain white matter diffusivity in normal adult aging: relationship to anisotropy and partial voluming. *Magn Reson Med* 49**,** 953-961.

Prins, N.D., Van Dijk, E.J., Den Heijer, T., Vermeer, S.E., Jolles, J., Koudstaal, P.J., Hofman, A., and Breteler, M.M. (2005). Cerebral small-vessel disease and decline in information processing speed, executive function and memory. *Brain* 128**,** 2034-2041.

Roosendaal, S.D., Geurts, J.J., Vrenken, H., Hulst, H.E., Cover, K.S., Castelijns, J.A., Pouwels, P.J., and Barkhof, F. (2009). Regional DTI differences in multiple sclerosis patients. *Neuroimage* 44**,** 1397-1403.

Salat, D.H., Buckner, R.L., Snyder, A.Z., Greve, D.N., Desikan, R.S., Busa, E., Morris, J.C., Dale, A.M., and Fischl, B. (2004). Thinning of the cerebral cortex in aging. *Cereb Cortex* 14**,** 721-730.

Salat, D.H., Greve, D.N., Pacheco, J.L., Quinn, B.T., Helmer, K.G., Buckner, R.L., and Fischl, B. (2009). Regional white matter volume differences in nondemented aging and Alzheimer's disease. *NeuroImage* 44**,** 1247-1258.

Salat, D.H., Tuch, D.S., Greve, D.N., Van Der Kouwe, A.J., Hevelone, N.D., Zaleta, A.K., Rosen, B.R., Fischl, B., Corkin, S., Rosas, H.D., and Dale, A.M. (2005). Age-related alterations in white matter microstructure measured by diffusion tensor imaging. *Neurobiol Aging* 26**,** 1215-1227.

Salat, D.H., Tuch, D.S., Van Der Kouwe, A.J., Greve, D.N., Pappu, V., Lee, S.Y., Hevelone, N.D., Zaleta, A.K., Growdon, J.H., Corkin, S., Fischl, B., and Rosas, H.D. (2010). White matter pathology isolates the hippocampal formation in Alzheimer's disease. *Neurobiol Aging* 31**,** 244-256.

Salat, D.H., Williams, V.J., Leritz, E.C., Schnyer, D.M., Rudolph, J.L., Lipsitz, L.A., Mcglinchey, R.E., and Milberg, W.P. (2012). Inter-individual variation in blood pressure is associated with regional white matter integrity in generally healthy older adults. *Neuroimage* 59**,** 181-192.

Salthouse, T.A. (2009). Decomposing age correlations on neuropsychological and cognitive variables. *J Int Neuropsychol Soc* 15**,** 650-661.

Santos, N.C., Costa, P.S., Cunha, P., Cotter, J., Sampaio, A., Zihl, J., Almeida, O.F., Cerqueira, J.J., Palha, J.A., and Sousa, N. (2013). Mood is a key determinant of cognitive performance in community-dwelling older adults: a cross-sectional analysis. *Age (Dordr)* 35**,** 1983-1993.

Santos, N.C., Costa, P.S., Cunha, P., Portugal-Nunes, C., Amorim, L., Cotter, J., Cerqueira, J.J., Palha, J.A., and Sousa, N. (2014). Clinical, physical and lifestyle indicators and relationship with cognition and mood in aging: a cross-sectional analysis of distinct educational groups. *Frontiers in Aging Neuroscience* 6.

Sexton, C.E., Walhovd, K.B., Storsve, A.B., Tamnes, C.K., Westlye, L.T., Johansen-Berg, H., and Fjell, A.M. (2014). Accelerated changes in white matter microstructure during aging: a longitudinal diffusion tensor imaging study. *J Neurosci* 34**,** 15425-15436.

Smith, C.D., Snowdon, D.A., Wang, H., and Markesbery, W.R. (2000). White matter volumes and periventricular white matter hyperintensities in aging and dementia. *Neurology* 54**,** 838-842.

Smith, S.M., Jenkinson, M., Johansen-Berg, H., Rueckert, D., Nichols, T.E., Mackay, C.E., Watkins, K.E., Ciccarelli, O., Cader, M.Z., Matthews, P.M., and Behrens, T.E. (2006). Tract-based spatial statistics: voxelwise analysis of multi-subject diffusion data. *Neuroimage* 31**,** 1487-1505.

Sun, S.W., Liang, H.F., Cross, A.H., and Song, S.K. (2008). Evolving Wallerian degeneration after transient retinal ischemia in mice characterized by diffusion tensor imaging. *Neuroimage* 40**,** 1-10.

Sun, S.W., Liang, H.F., Le, T.Q., Armstrong, R.C., Cross, A.H., and Song, S.K. (2006). Differential sensitivity of in vivo and ex vivo diffusion tensor imaging to evolving optic nerve injury in mice with retinal ischemia. *Neuroimage* 32**,** 1195-1204.

Teipel, S.J., Meindl, T., Wagner, M., Stieltjes, B., Reuter, S., Hauenstein, K.H., Filippi, M., Ernemann, U., Reiser, M.F., and Hampel, H. (2010). Longitudinal changes in fiber tract integrity in healthy aging and mild cognitive impairment: a DTI follow-up study. *J Alzheimers Dis* 22**,** 507-522.

Tomasi, D., and Volkow, N.D. (2012). Aging and functional brain networks. *Mol Psychiatry* 17**,** 471, 549-458.

Vernooij, M.W., Ikram, M.A., Vrooman, H.A., Wielopolski, P.A., Krestin, G.P., Hofman, A., Niessen, W.J., Van Der Lugt, A., and Breteler, M.M. (2009). White matter microstructural integrity and cognitive function in a general elderly population. *Arch Gen Psychiatry* 66**,** 545-553.

Wakefield, D.B., Moscufo, N., Guttmann, C.R., Kuchel, G.A., Kaplan, R.F., Pearlson, G., and Wolfson, L. (2010). White matter hyperintensities predict functional decline in voiding, mobility, and cognition in older adults. *J Am Geriatr Soc* 58**,** 275-281.

Wang, L., Goldstein, F.C., Levey, A.I., Lah, J.J., Meltzer, C.C., Holder, C.A., and Mao, H. (2011). White matter hyperintensities and changes in white matter integrity in patients with Alzheimer's disease. *Neuroradiology* 53**,** 373-381.

Wang, R., Fratiglioni, L., Laukka, E.J., Lovden, M., Kalpouzos, G., Keller, L., Graff, C., Salami, A., Backman, L., and Qiu, C. (2015). Effects of vascular risk factors and APOE epsilon4 on white matter integrity and cognitive decline. *Neurology*.

Westlye, L.T., Walhovd, K.B., Dale, A.M., Bjørnerud, A., Due-Tønnessen, P., Engvig, A., Grydeland, H., Tamnes, C.K., Østby, Y., and Fjell, A.M. (2010). Life-span changes of the human brain white matter: diffusion tensor imaging (DTI) and volumetry. *Cerebral Cortex* 20**,** 2055-2068.

Zhang, Y., Du, A.T., Hayasaka, S., Jahng, G.H., Hlavin, J., Zhan, W., Weiner, M.W., and Schuff,

N. (2010). Patterns of age-related water diffusion changes in human brain by concordance and discordance analysis. *Neurobiol Aging* 31**,** 1991-2001.

CHAPTER III

Paulo César Gonçalves Marques, José Miguel Montenegro Soares, Ricardo José da Silva Magalhães, Nadine Correia Santos, Nuno Jorge Carvalho Sousa (2015)

The bounds of education in the human brain connectome

Manuscript accepted for publication in Scientific Reports

The Bounds Of Education In The Human Brain Connectome

Authors: P Marques[123], JM Soares[123], R Magalhães[123], NC Santos[123], N Sousa[123]*

[1]Life and Health Sciences Research Institute (ICVS), School of Health Sciences, University of Minho, Campus Gualtar, 4710-057 Braga, Portugal.

[2]ICVS/3B's - PT Government Associate Laboratory, Braga/Guimarães, Portugal.

[3]Clinical Academic Center – Braga, Braga, Portugal.

*Corresponding author: Nuno Sousa, Life and Health Sciences Research Institute (ICVS), School of Health Sciences, University of Minho, Campus Gualtar, 4710-057 Braga, Portugal. Email: njcsousa@ecsaude.uminho.pt. Phone: +351 253 604 806.

Abstract

Inter-individual heterogeneity is evident in aging; education level is known to contribute for this heterogeneity. Using a cross-sectional study design and network inference applied to resting-state fMRI data, we show that aging was associated with decreased functional connectivity in a large cortical network. On the other hand, education level, as measured by years of formal education, produced an opposite effect on the long-term. These results demonstrate the increased brain efficiency in individuals with higher education level that may mitigate the impact of age on brain functional connectivity.

1. Introduction

Normal aging is characterized by inter-individual heterogeneity with some individuals showing a marked (cognitive) decline, while others evidence relatively preserved cognition (MacDonald et al., 2003;Santos et al., 2014). One of the factors thought to contribute for this heterogeneity is education level, a factor associated to "cognitive reserve" (CR). CR can be perceived as the brain's capacity to optimize/maximize performance (Stern, 2002). More so, previous studies have shown that older individuals with higher education levels evidence larger brains and lower levels of brain activity during task performance, thus reflecting more efficient brain networks (Sole-Padulles et al., 2009).

One of the recent trends in the neuroimaging field is the use of graph theory models to study the human brain connectome as a network, modeling each brain region as a node and the connections between brain regions as the edges of a graph (Bullmore and Sporns, 2009). Resting-state functional magnetic resonance imaging (rs-fMRI) is one of the most widely used neuroimaging techniques to study the brain's functional connectivity (FC) and has been used in combination with graph theory to study the human functional connectome in health (Zalesky, 2011) and disease (Zhang et al., 2011). Concerning aging, it has been recently shown that it has a negative impact on the FC of several brain networks such as the default mode network (DMN) and the salience network as well as in internetwork connectivity, with these changes being associated with cognitive decline (Onoda et al., 2012). At the connectome level, there is evidence that long-range connections are negatively impacted by aging, while short-range

connection may display higher FC with aging (Sala-Llonch et al., 2014). Comparative studies between older and younger individuals, using graph theory, have shown that aging is associated with decreased network efficiency in frontal and temporal regions and a rearrangement in the modular organization of the brain (Achard and Bullmore, 2007;Meunier et al., 2009).

Yet, to the best of our knowledge, no study has yet characterized the effect of education level, one of the major proxies of CR, in the brain's functional network in aging. We performed rs-fMRI on more than 97 healthy older subjects (without manifestation or diagnosed brain pathology), modeling whole FC patterns and investigating: i) the cross-sectional effects of healthy aging in the human functional connectome, and (ii) the effects of education level in the human connectome as well as possible interactions with the aging effects.

2. Methods

2.1 Participants

The present study was performed with a sample comprising 97 participants (49 males, 48 females; mean age 64.94 ± 8.20, minimum age 51, maximum age 82; mean years of education 5.37 ± 3.83, minimum 0, maximum 17 years of education), after inclusion/exclusion criteria were met. All participants underwent an extensive battery of neuropsychological and neurocognitive tests in order to rule out the presence of Mild Cognitive Impairment and dementia. In the recruitment phase, exclusion criteria including inability to understand informed consent, participant choice to withdraw from the study, incapacity and/or inability to attend the clinical and neuropsychological assessment session(s), dementia and/or diagnosed neuropsychiatric and/or neurodegenerative disorder (including via verification from medical records) were verified by a clinician. Additionally, individuals presenting MMSE scores below the adjusted thresholds for cognitive impairment were not included in the present study. Regarding the MMSE scores, recommendations state that the corresponding threshold should be adjusted depending on factors such as age and/or education. The following adjusted thresholds for cognitive impairment were calculated and applied: MMSE score < 17 if individual with ≤ 4 years of formal school education and/or ≥ 72 years of age, and MMSE

score < 23 otherwise [follows the MMSE validation study for the Portuguese population (Guerreiro et al., 1994)].

This sample is part of a cohort of subjects that was recruited for the SWITCHBOX Consortium project (www.switchbox-online.eu/) and is representative of the Portuguese older population in terms of age, education and sex (Santos et al., 2013). The study goals and tests were explained to all participants, which gave informed written consent. The study was conducted in accordance with the principles expressed in the Declaration of Helsinki and was approved by the Ethics Committee of Hospital de Braga (Portugal).

2.2 Image Acquisition

Imaging was performed at Hospital de Braga on a clinical approved 1.5 T Siemens Magnetom Avanto MRI scanner (Siemens, Erlangen, Germany). A structural T1 scan (176 sagittal slices, TR/TE= 2730/ 3.48 ms, FA = 7°, slice thickness = 1 mm, slice gap = 0 mm, voxel size= 1x1 mm2, FoV = 256 mm) and a functional blood oxygen level dependent (BOLD) sensitive echo-planar imaging (EPI) scan (30 axial slices, TR/TE = 2000/30 ms, FA = 90°, slice thickness = 3.5, slice gap = 0.48 mm, voxel size = 3.5 x 3.5 mm2 FoV = 1344 mm and 180 volumes) were collected. During the resting state scan, the subjects were instructed to remain still, awake, with their eyes closed, as motionless as possible and to think of nothing in particular. None of the participants fell asleep during the acquisition.

2.3 Image Preprocessing

Image pre-processing was performed with tools provided with the FMRIB Software Library (FSL v5.07; http://fsl.fmrib.ox.ac.uk/fsl/). Preprocessing steps included: the removal of the first five volumes of the acquisition; slice-timing correction; motion correction; normalization to MNI standard space; regression of motion parameters, mean WM and CSF signals; band-pass temporal filtering (0.01-0.08Hz). For each subject, mean time-series for 116 cortical, subcortical and cerebellar regions from the Anatomical Automatic Labeling (AAL) atlas (Tzourio-Mazoyer et al., 2002) were then extracted by averaging all voxels composing each region for

each time point. Pearson correlation coefficients were then calculated between the time-series of each pair of regions, resulting in one adjacency matrix per subject. These matrices were then transformed to Z-score matrices by the application of Fisher's r-to-Z transform to the correlation coefficients.

2.4 Network Analysis

Each adjacency matrix represents the entire functional brain network of the corresponding subject, with the vertices of the network being the AAL regions and the edges the correlations between regions' time-series. Herein we aimed at exploring the cross-sectional effects of age and years of education, on brain's functional network. In order to achieve this we built a General Linear Model (GLM) including the linear and quadratic effect of age and the linear effect of years of education as regressors. We decided to include both linear and quadratic effect of age given the relatively large range of age (brain regions are known to follow nonlinear aging effects (Jernigan and Gamst, 2005)). Additionally, we also included MMSE scores in the model in order to check/control for cognition associations. Sex was included as covariate in the model in order to control for its' effect. Additionally, we built a second model in which we added the age*years of education interaction terms in order to investigate if cognitive reserve could be a modulator of the aging effect in FC. Correlations between every pair of regressors were performed in order to check for collinearity issues and none were collinear.

Statistical analysis was performed at the network level through the use of Network-Based Statistics (NBS) (Zalesky et al., 2010). This approach increases statistical power by finding sub-networks that, as whole, display a similar pattern regarding a contrast of interest and enabling inference while controlling for family-wise error (FWE) rate. This procedure is similar to cluster-based inference of the more typical voxel-wise fMRI analysis. Specifically, initially, the model was fitted to every edge of the whole brain network. Then, edges with a p-value less than a primary uncorrected threshold (e.g. $p < 0.005$) obtained for a particular effect (e.g. age effect) were filtered in. Based on these supra-threshold edges, components or sub-networks of interconnected edges were identified and their size was calculated. Then 5000 permutations were performed in order to build a null distribution for the largest sub-network size.

Significance of each sub-network was calculated as the percentage of permutations that originated sub-networks with greater size than the originally identified sub-network.

One of the difficulties in such analysis is the definition of the primary threshold. The authors of the NBS procedures recommend the use of a range of thresholds since effects present at liberal thresholds (e.g. $p<0.01$) are likely to be subtle, yet topologically extended, effects while effects captured using more strict thresholds (e.g. $p < 0.001$) reflect more focal and strong effects. In order to capture both kinds of effects, three primary thresholds ($p< 0.01$, $p<0.005$ and $p < 0.001$) were used in the present work. Networks were considered significant at a corrected level of $p < 0.05$ FWE corrected. BrainNet Viewer (http://www.nitrc.org/projects/bnv/) was used for visualization purposes.

3. Results

3.1 Demographic Characterization

Table I presents the demographic characteristics of the sample under study, separated by sex and also presents the p-value of two-sample T-tests performed between males and females. Males and females were matched for age, with males presenting significantly higher number of years of formal education ($p < 0.001$) and MMSE scores ($p < 0.001$), when compared to females. Additionally, years of formal education were positively correlated with MMSE scores ($r=0.36$; $p<0.001$) and negatively correlated with age ($r=-0.23$; $p = 0.022$).

Table I. Demographic and cognitive characteristics of the participants

	Total Sample	**Males**	**Females**	
	Mean ± SD	**Mean ± SD**	**Mean ± SD**	**p-value**
N	97	49	48	
Age	64.94 ± 8.20	63.73 ± 6.69	66.16 ± 7.90	0.145
Education (years)	5.37 ± 3.83	8.38 ± 4.30	3.91 ± 2.72	< 0.001
MMSE	26.54 ± 3.57	27.80 ± 2.26	24.71 ± 4.17	< 0.001

3.2 Associations between age and FC networks

Several edges revealed associations with aging that survived the three primary thresholds ($p < 0.01$, $p < 0.005$, $p < 0.001$) used in the Network Based-Statistic (NBS) analysis (Figure 1a). Both positive and negative associations survived the thresholding procedure. From these edges, the ones exhibiting positive associations with age were mainly short-range connections while negative associations were found for a wide range of normalized edge lengths (Figure 1b).

Regarding NBS analysis, age presented a linear negative relationship with FC in a large and extent sub-network (Figure 2a) when using the most liberal primary threshold (i.e. $p < 0.01$). This effect was still evident for a more restricted primary threshold (i.e. $p < 0.005$), but was not significant for the most restricted threshold ($p < 0.001$). The bilateral caudate, left frontal superior, left Heshl and left parahippocampal were the brain regions through which most of the connections passed (the complete list of node degrees can be consulted in Supplementary Table S1 and Supplementary Table S2). Although both positive and negative associations between edges and age survived the primary threshold, the edges with positive associations did not survive the NBS procedure (network level inference), meaning that these positive associations do not form a significant network. Furthermore, interpreting the scatter plots between mean FC in the significant networks and age (Figure 2b), younger individuals presented moderate positive mean FC Z-scores while older individuals present mean FC Z-scores of approximately zero.

3.3 Associations between years of formal education and FC networks

Regarding the effects of years of formal education, several edges survived the application of the three primary thresholds (Figure 1c). In Figure 1d it is noted that these edges span a broad range of edge lengths, both in positive and negative associations.

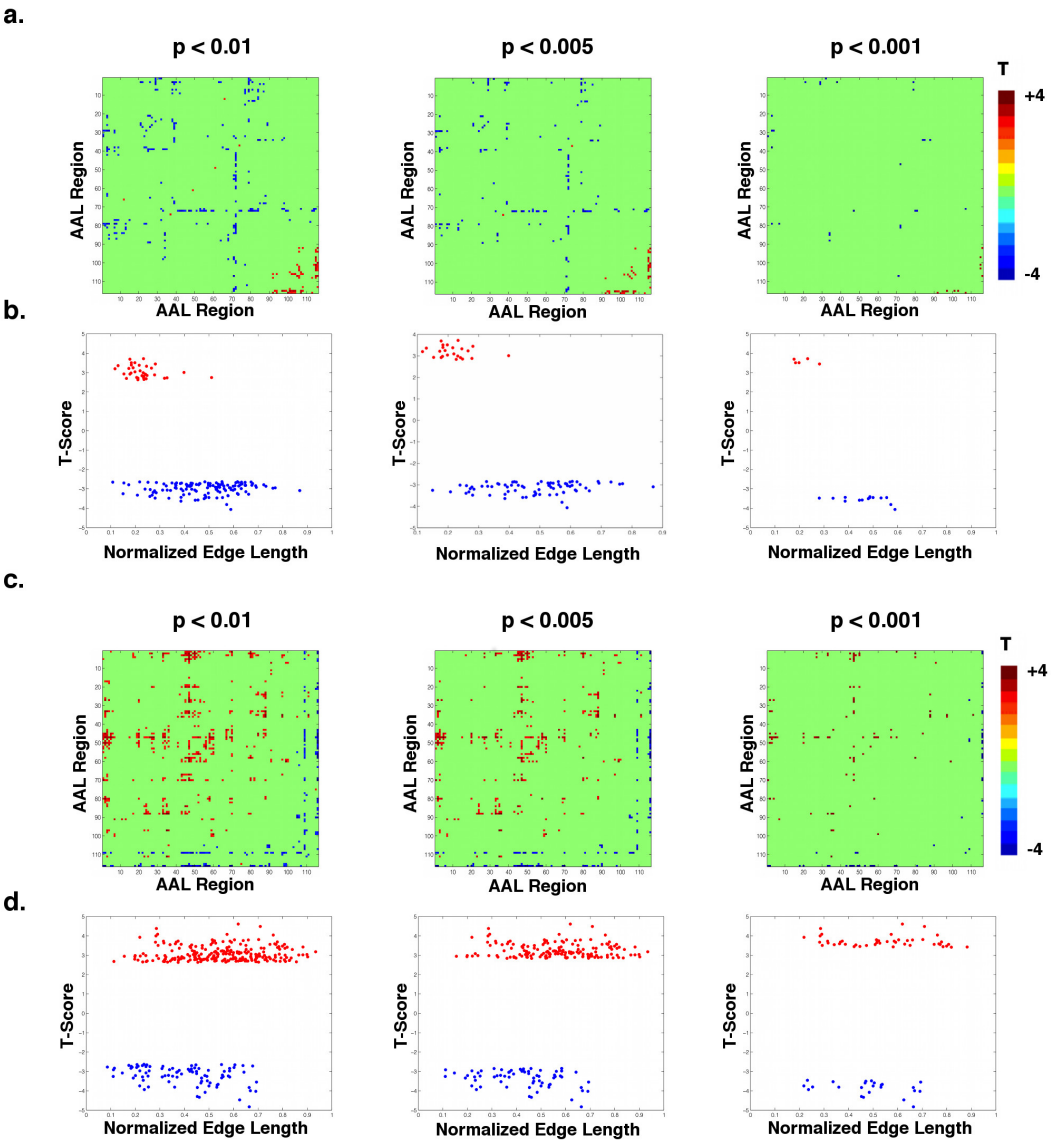


Figure 1. Functional connectivity matrices and edge length distribution of the edges surviving the primary thresholding procedure. Both positive and negative associations with age survive the three ($p < 0.01$, $p < 0.005$, $p < 0.001$) primary thresholds of the NBS analysis (a). Positive associations with age occur mainly in short-range connections while negative associations can be found in medium to long-range edges (b). Similarly, positive and negative associations with years of formal education survive the application of the primary thresholds (c) and the supra-threshold edges span a large range of lengths (d).

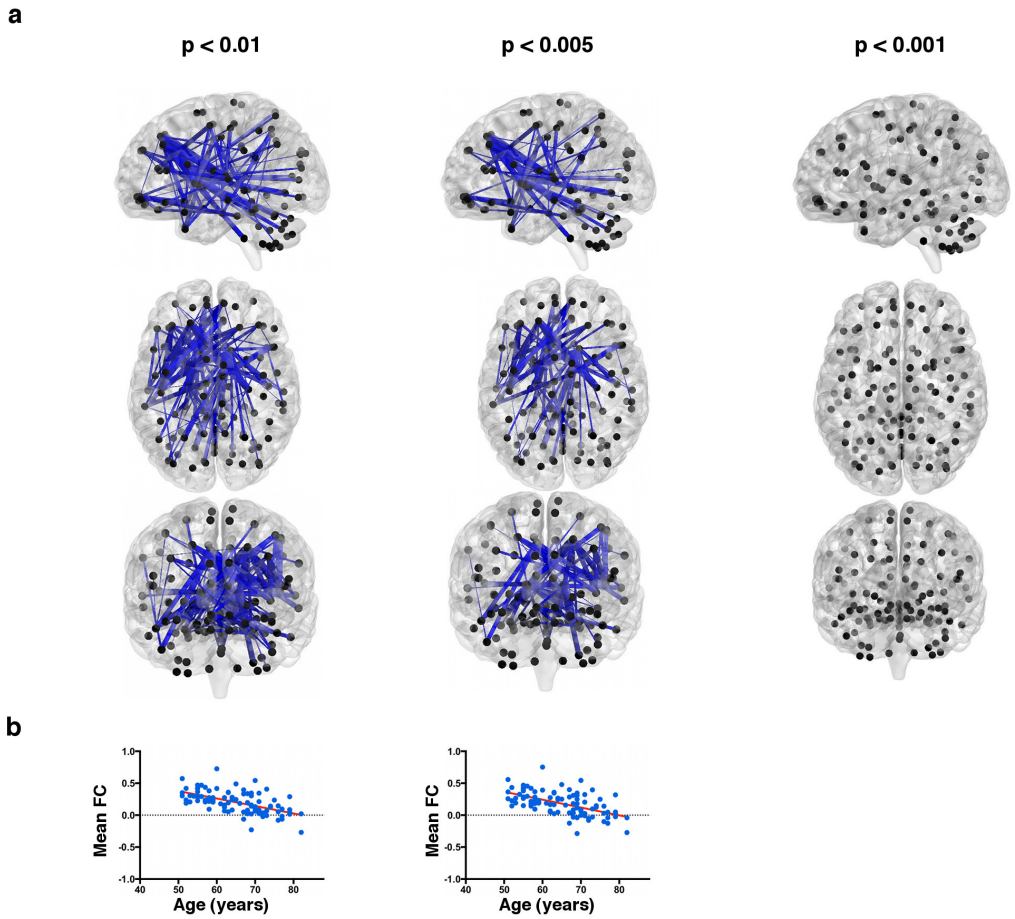


Figure 2. Networks showing significant associations between functional connectivity (FC) and age. A large sub-network was found to display a negative association between FC and aging using primary thresholds of $p < 0.01$ and $p < 0.005$ but not with a primary threshold of $p < 0.001$ (a). Younger subjects presented moderate positive mean FC values in this network while older subjects presented mean FC values close to zero along the network (b). In the upper panel (a), black dots represent AAL brain regions and blue edges denote edges with negative associations with age. Bottom panel (b) presents scatter plots of the mean FC of the statistically significant networks in function of age.

The NBS results for the associations between FC networks and years of formal education are shown in Figure 3a. Results revealed that a large and distributed network showed a positive association between FC and years of formal education when using the most liberal primary threshold ($p < 0.01$). When using a stricter primary threshold ($p < 0.005$), a large sub-part of the previous network still evidenced a positive association with education level. Concerning strong focal effects of education level on FC ($p < 0.001$), a sub-network still revealed a positive

association with education level. Regarding the contribution of each region for this network, the left lingual, left frontal superior, right precentral, left cuneus and the middle right temporal pole middle were some of the main contributors (the complete list of node degrees can be consulted in Supplementary Table S3, Supplementary Table S4 and Supplementary Table S5).

Furthermore, a focal network that was not significant with the most liberal primary threshold used ($p < 0.01$), evidenced a negative association with years of formal education when using the stricter primary thresholds ($p < 0.005$ and $p < 0.001$). This was a highly bilateral network with several connection from/to the Vermis 10 and Vermis 1 2 (full list of node degrees can be found in Supplementary Table S6 and Supplementary Table S7).

Figure 3b reveals that in the network with positive associations with years of education, the mean FC seems to increase from low positive values to high positive values, while in the network evidencing a negative associations with years of formal education, the mean FC seems to decrease from low positive values to moderate negative values.

No interactions were found between years of formal education and age in FC networks.

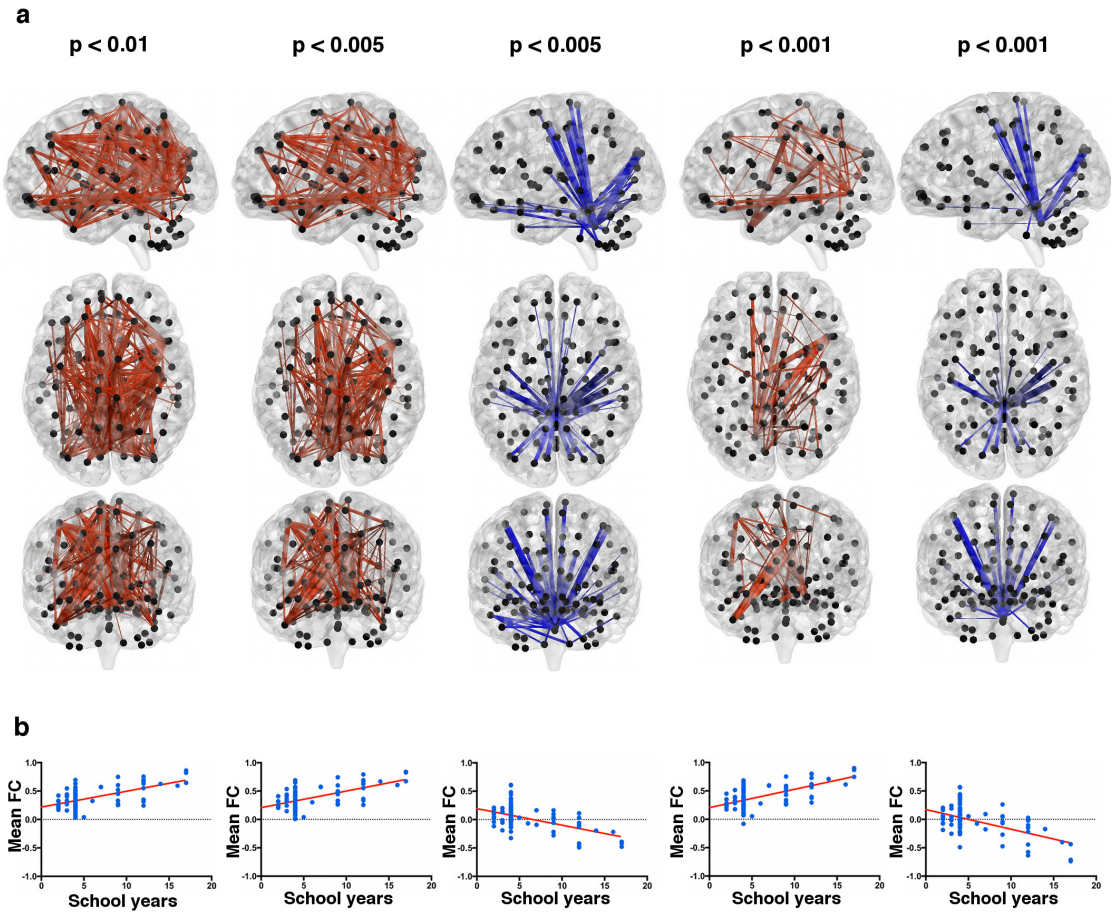


Figure 3. Networks showing significant associations between functional connectivity (FC) and years of education. A large sub-network showed a positive association between FC and years of formal education using primary thresholds of $p < 0.01$, $p < 0.005$ and $p < 0.001$. A focal sub-network displayed a negative association with years of education using a primary threshold of $p < 0.005$ and $p < 0.001$ (a). In the network that evidenced a positive association with FC, less educated subjects presented moderately low positive FC values while more educated subjects presented moderately high positive FC values (b). In the network with a negative association with years of formal education, mean FC ranges from low positive FC values to moderate negative mean FC values from individual with lower years of formal education to individuals with higher number of years of formal education (b). In the top panel (a) black dots represent AAL brain regions and blue and red edges denote edges with negative and positive associations with years of education, respectively. Bottom panel (b) presents scatter plots of the mean FC of the statistically significant networks in function of years of education.

4. Discussion

The present work aimed at exploring the cross-sectional effects of healthy aging and education level in the brain's FC. In order to achieve this, a large cohort of healthy older individuals was screened so to investigate FC patterns with network-based inference applied to rs-fMRI data.

Concerning the aging effect, age was associated with a decrease in FC. This effect was rather global as no sparse or focal sub-network was found to present an increase in FC with increasing age. A recent study analyzed a similar population in terms of mean age and age range finding both increases and decreases in FC (Sala-Llonch et al., 2014). With a similar threshold (i.e. primary threshold of $p < 0.001$), here only a few connections were found to display such pattern; however, when making inferences at the network level, these did not form a significant sub-network. These differences might arise either from the fact that, in the referred study, correction for multiple comparisons was not performed at the network level or, most likely, these connections that display positive associations with age do not form a network at all. Additionally, the magnetic field strength of the MRI scanner and the resolution of acquisition were different from those used in the present study, which could potentially justify part of these discrepancies given the greater signal-to-noise ratio of the 3T MRI scanners (van der Zwaag et al., 2009). Furthermore, here the results are compatible with the cognitive decline commonly associated with the aging pattern (Esposito et al., 1999;O'Sullivan et al., 2001;Salthouse, 2009). Reduced FC might reflect an overall greater disconnection between several brain regions with repercussions in brain function, such as slower processing speed (Salthouse, 2000). Interestingly, findings here are also in line with the posterior-to-anterior shift with aging (PASA) theory (Davis et al., 2008), as a greater disconnection with increasing age in the anterior parts of the brain was found. The PASA pattern is characterized by greater frontal activity in older individuals, compared to younger individuals in order to perform the same task, which is likely to reflect a compensatory mechanism. Additionally, reductions in deactivation in midline posterior regions and increased deactivation in midline anterior regions have also been observed (Davis et al., 2009). Davis et al. (2009) hypothesize that this deactivation shift could reflect an increased demand in older individuals to reallocate resources from the Default Mode Network (DMN) for task performance. Our findings of reduced FC in anterior connections in resting conditions could justify an increased effort in task conditions in order to compensate for a greater FC disconnection.

Regarding the effects of education level (in this work assessed as years of formal education), we demonstrated that it has a strong positive effect on the FC of a large network. Unlike the aging pattern, this network involves regions and edges located in all lobes and both hemispheres with the exception of the cerebellum. These results are in line with the CR theory (Stern, 2002), in which education level is critical, since a greater FC in this large network is likely to reflect a more finely tuned brain network, easing communication and integration of information, and thus requiring less effort to perform cognitive tasks for those with higher education level (Habeck et al., 2003). Importantly, no interaction between years of education and age was found, providing further evidence to the inexistence of a mediating effect of education level in rates of decline (Tucker-Drob et al., 2009). Rs-fMRI studies have shown education to be a modulator of FC within the DMN in Alzheimer's disease patients, particularly with the posterior cingulate cortex; however they have not indicated significant associations between FC and education in healthy controls (Bozzali et al., 2014). Collectively, it could thus be expected that the posterior cingulate cortex would not be involved in the networks that were here found to display positive associations with years of formal education, which was not the case. However, on this, several aspects must be noted. The sample of healthy controls used in the study from Bozzali and colleagues (2014) was much smaller than the current one and, possibly, their sample size was not enough to achieve statistical significance. Additionally, herein connectivity at the whole brain network level was explored while Bozzali and colleagues explored connectivity, specifically with the DMN.

Intriguingly, here it was found a particular network involving connections (mostly bilateral) linking parts of the cerebellum vermis to cerebral regions in the occipital and temporal lobes, postcentral and precentral regions, rectus and cingulum middle regions, which displayed a negative association with years of education. The classical view that the cerebellum is solely implicated to motor control has long been discarded (Schmahmann and Sherman, 1998); with evidence from several studies involving healthy individuals and patients with cerebellar lesions, indicating the involvement of the cerebellum in cognition and emotion (Schmahmann and Caplan, 2006;Schmahmann, 2010). In the context of these evidences, the finding of associations between FC and education level are not particularly unexpected; here, the intriguing finding concerns the fact that these are negative associations. However, when looking at the mean FC of this network, it can be observed that in absolute values it is actually

positively associated with years of education (meaning that increased education level is associated with increased anti-correlations in this network, rather than the loss of FC). Given that there is evidence for the differential involvement of the cortex and the cerebellum and for education to modulate this functional balance (Bonnet et al., 2009), it is hypothesized that this negative association does not reflect a negative impact but rather a more effective involvement of the cerebrum and cerebellum through this network.

A major limitation of the present study is its cross-sectional design. A longitudinal approach would enable the within-subject analysis of the effect of aging, thus reducing inter-individual variability. This is particularly critical regarding the possible mediating effects of education level in the associations between FC and aging.

In summary, the present work brings further evidence regarding the deleterious effect of aging through the loss of FC in a large sub-network of the brain. Importantly, we show for the first time that a higher educational level is associated with increased FC in a large cortical brain network, possibly reflecting greater neural efficiency, which may contribute to 'alleviate' the deleterious impact of increasing age in brain function.

5. References

Achard, S., and Bullmore, E. (2007). Efficiency and cost of economical brain functional networks. *PLoS Comput Biol* 3**,** e17.

Bonnet, M.C., Dilharreguy, B., Allard, M., Deloire, M.S., Petry, K.G., and Brochet, B. (2009). Differential cerebellar and cortical involvement according to various attentional load: role of educational level. *Hum Brain Mapp* 30**,** 1133-1143.

Bozzali, M., Dowling, C., Serra, L., Spano, B., Torso, M., Marra, C., Castelli, D., Dowell, N.G., Koch, G., Caltagirone, C., and Cercignani, M. (2014). The Impact of Cognitive Reserve on Brain Functional Connectivity in Alzheimer's Disease. *J Alzheimers Dis*.

Bullmore, E., and Sporns, O. (2009). Complex brain networks: graph theoretical analysis of structural and functional systems. *Nat Rev Neurosci* 10**,** 186-198.

Davis, S.W., Dennis, N.A., Buchler, N.G., White, L.E., Madden, D.J., and Cabeza, R. (2009). Assessing the effects of age on long white matter tracts using diffusion tensor tractography. *Neuroimage* 46**,** 530-541.

Davis, S.W., Dennis, N.A., Daselaar, S.M., Fleck, M.S., and Cabeza, R. (2008). Que PASA? The posterior-anterior shift in aging. *Cereb Cortex* 18**,** 1201-1209.

Esposito, G., Kirkby, B.S., Van Horn, J.D., Ellmore, T.M., and Berman, K.F. (1999). Context-dependent, neural system-specific neurophysiological concomitants of ageing: mapping PET correlates during cognitive activation. *Brain* 122 (Pt 5)**,** 963-979.

Guerreiro, M., Silva, A.P., Botelho, M.A., Leitão, O., Castro-Caldas, A., and Garcia, C. (1994). Adaptação à população portuguesa da tradução do Mini Mental State Examination (MMSE). *Revista Portuguesa de Neurologia* 1**,** 9-10.

Habeck, C., Hilton, H.J., Zarahn, E., Flynn, J., Moeller, J., and Stern, Y. (2003). Relation of cognitive reserve and task performance to expression of regional covariance networks in an event-related fMRI study of nonverbal memory. *Neuroimage* 20**,** 1723-1733.

Jernigan, T.L., and Gamst, A.C. (2005). Changes in volume with age–consistency and interpretation of observed effects. *Neurobiol Aging* 26**,** 1271-1274; discussion 1275-1278.

Macdonald, S.W., Hultsch, D.F., and Dixon, R.A. (2003). Performance variability is related to change in cognition: evidence from the Victoria Longitudinal Study. *Psychology and aging* 18**,** 510.

Meunier, D., Achard, S., Morcom, A., and Bullmore, E. (2009). Age-related changes in modular organization of human brain functional networks. *Neuroimage* 44**,** 715-723.

O'sullivan, M., Jones, D.K., Summers, P.E., Morris, R.G., Williams, S.C., and Markus, H.S. (2001). Evidence for cortical "disconnection" as a mechanism of age-related cognitive decline. *Neurology* 57**,** 632-638.

Onoda, K., Ishihara, M., and Yamaguchi, S. (2012). Decreased functional connectivity by aging is associated with cognitive decline. *J Cogn Neurosci* 24**,** 2186-2198.

Sala-Llonch, R., Junque, C., Arenaza-Urquijo, E.M., Vidal-Pineiro, D., Valls-Pedret, C., Palacios, E.M., Domenech, S., Salva, A., Bargallo, N., and Bartres-Faz, D. (2014). Changes in whole-brain functional networks and memory performance in aging. *Neurobiol Aging* 35**,** 2193-2202.

Salthouse, T.A. (2000). Aging and measures of processing speed. *Biol Psychol* 54**,** 35-54.

Salthouse, T.A. (2009). Decomposing age correlations on neuropsychological and cognitive variables. *J Int Neuropsychol Soc* 15**,** 650-661.

Santos, N.C., Costa, P.S., Cunha, P., Cotter, J., Sampaio, A., Zihl, J., Almeida, O.F., Cerqueira, J.J., Palha, J.A., and Sousa, N. (2013). Mood is a key determinant of cognitive performance in community-dwelling older adults: a cross-sectional analysis. *Age (Dordr)* 35**,** 1983-1993.

Santos, N.C., Costa, P.S., Cunha, P., Portugal-Nunes, C., Amorim, L., Cotter, J., Cerqueira, J.J., Palha, J.A., and Sousa, N. (2014). Clinical, physical and lifestyle indicators and relationship with cognition and mood in aging: a cross-sectional analysis of distinct educational groups. *Frontiers in Aging Neuroscience* 6.

Schmahmann, J.D. (2010). The role of the cerebellum in cognition and emotion: personal reflections since 1982 on the dysmetria of thought hypothesis, and its historical evolution from theory to therapy. *Neuropsychol Rev* 20**,** 236-260.

Schmahmann, J.D., and Caplan, D. (2006). Cognition, emotion and the cerebellum. *Brain* 129**,** 290-292.

Schmahmann, J.D., and Sherman, J.C. (1998). The cerebellar cognitive affective syndrome. *Brain* 121 (Pt 4)**,** 561-579.

Sole-Padulles, C., Bartres-Faz, D., Junque, C., Vendrell, P., Rami, L., Clemente, I.C., Bosch, B., Villar, A., Bargallo, N., Jurado, M.A., Barrios, M., and Molinuevo, J.L. (2009). Brain structure and function related to cognitive reserve variables in normal aging, mild cognitive impairment and Alzheimer's disease. *Neurobiol Aging* 30**,** 1114-1124.

Stern, Y. (2002). What is cognitive reserve? Theory and research application of the reserve

concept. *J Int Neuropsychol Soc* 8**,** 448-460.

Tucker-Drob, E.M., Johnson, K.E., and Jones, R.N. (2009). The cognitive reserve hypothesis: a longitudinal examination of age-associated declines in reasoning and processing speed. *Dev Psychol* 45**,** 431-446.

Tzourio-Mazoyer, N., Landeau, B., Papathanassiou, D., Crivello, F., Etard, O., Delcroix, N., Mazoyer, B., and Joliot, M. (2002). Automated anatomical labeling of activations in SPM using a macroscopic anatomical parcellation of the MNI MRI single-subject brain. *Neuroimage* 15**,** 273-289.

Van Der Zwaag, W., Francis, S., Head, K., Peters, A., Gowland, P., Morris, P., and Bowtell, R. (2009). fMRI at 1.5, 3 and 7 T: characterising BOLD signal changes. *Neuroimage* 47**,** 1425-1434.

Zalesky, A. (2011). Moderating registration misalignment in voxelwise comparisons of DTI data: a performance evaluation of skeleton projection. *Magn Reson Imaging* 29**,** 111-125.

Zalesky, A., Fornito, A., and Bullmore, E.T. (2010). Network-based statistic: identifying differences in brain networks. *Neuroimage* 53**,** 1197-1207.

Zhang, J., Wang, J., Wu, Q., Kuang, W., Huang, X., He, Y., and Gong, Q. (2011). Disrupted brain connectivity networks in drug-naive, first-episode major depressive disorder. *Biol Psychiatry* 70**,** 334-342.

The Bounds Of Education In The Human Brain Connectome

Authors: P Marques[123], JM Soares[123], R Magalhães[123], NC Santos[123], N Sousa[123*]

[1]Life and Health Sciences Research Institute (ICVS), School of Health Sciences, University of Minho, Campus Gualtar, 4710-057 Braga, Portugal.

[2]ICVS/3B's - PT Government Associate Laboratory, Braga/Guimarães, Portugal.

[3]Clinical Academic Center – Braga, Braga, Portugal.

*Corresponding author: Nuno Sousa, Life and Health Sciences Research Institute (ICVS), School of Health Sciences, University of Minho, Campus Gualtar, 4710-057 Braga, Portugal. Email: njcsousa@ecsaude.uminho.pt. Phone: +351 253 604 806.

Supplementary Table S1. Degree of the regions comprising the network that evidenced a negative association with age, using a primary threshhold of p < 0.01.

MNI COORDINATES				
X	Y	Z	Degree	AAL Region
14.84	12.07	9.42	28	Caudate_R
-18.45	34.81	42.2	12	Frontal_Sup_L
-41.99	-18.88	9.98	12	Heschl_L
-21.17	-15.95	-20.7	11	ParaHippocampal_L
-11.46	11	9.24	11	Caudate_L
-33.43	32.73	35.46	8	Frontal_Mid_L
48.25	14.75	-16.86	7	Temporal_Pole_Sup_R
8.16	51.67	-7.13	6	Frontal_Med_Orb_R
-35.13	6.65	3.44	6	Insula_L
8.02	-8.83	39.79	6	Cingulum_Mid_R
29.23	-19.78	-10.33	6	Hippocampus_R
-10.85	-17.56	7.98	6	Thalamus_L
21.9	31.12	43.82	5	Frontal_Sup_R
8.46	37.01	15.84	5	Cingulum_Ant_R
9.98	-56.05	43.77	5	Precuneus_R
-53.16	-20.68	7.13	5	Temporal_Sup_L
-38.65	-5.68	50.94	4	Precentral_L
37.59	33.06	34.04	4	Frontal_Mid_R
-5.17	54.06	-7.4	4	Frontal_Med_Orb_L
41.37	-8.21	52.09	3	Precentral_R
-30.65	50.43	-9.62	3	Frontal_Mid_Orb_L
-45.58	29.91	13.99	3	Frontal_Inf_Tri_L
-8.06	15.05	-11.46	3	Olfactory_L
-4.8	49.17	30.89	3	Frontal_Sup_Medial_L
9.1	50.84	30.22	3	Frontal_Sup_Medial_R
-5.08	37.07	-18.14	3	Rectus_L
-5.48	-14.92	41.57	3	Cingulum_Mid_L
25.38	-15.15	-20.47	3	ParaHippocampal_R
27.32	0.64	-17.5	3	Amygdala_R
45.86	-17.15	10.41	3	Heschl_R
-55.52	-33.8	-2.2	3	Temporal_Mid_L
-36.32	14.59	-34.08	3	Temporal_Pole_Mid_L
44.22	14.55	-32.23	3	Temporal_Pole_Mid_R
17.2	-42.86	-18.15	3	Cerebelum_4_5_R
10.43	15.91	-11.26	2	Olfactory_R
-32.39	-80.73	16.11	2	Occipital_Mid_L
-36.36	-78.29	-7.84	2	Occipital_Inf_L
-31.16	-40.3	-20.23	2	Fusiform_L
-42.46	-22.63	48.92	2	Postcentral_L
57.61	-31.5	34.48	2	SupraMarginal_R
-44.14	-60.82	35.59	2	Angular_L
-7.24	-56.07	48.01	2	Precuneus_L
58.15	-21.78	6.8	2	Temporal_Sup_R
-49.77	-28.05	-23.17	2	Temporal_Inf_L
-15	-43.49	-16.93	2	Cerebelum_4_5_L
1.15	-64.43	-34.08	2	Vermis_8
-48.43	12.73	19.02	1	Frontal_Inf_Oper_L

50.2	14.98	21.41	1	Frontal_Inf_Oper_R
-35.98	30.71	-12.11	1	Frontal_Inf_Orb_L
8.35	35.64	-18.04	1	Rectus_R
39.02	6.25	2.08	1	Insula_R
-4.04	35.4	13.95	1	Cingulum_Ant_L
-4.85	-42.92	24.67	1	Cingulum_Post_L
-23.27	-0.67	-17.14	1	Amygdala_L
-7.14	-78.67	6.44	1	Calcarine_L
15.99	-73.15	9.4	1	Calcarine_R
-5.93	-80.13	27.22	1	Cuneus_L
-14.62	-67.56	-4.63	1	Lingual_L
16.29	-66.93	-3.87	1	Lingual_R
38.16	-81.99	-7.61	1	Occipital_Inf_R
33.97	-39.1	-20.18	1	Fusiform_R
-23.45	-59.56	58.96	1	Parietal_Sup_L
26.11	-59.18	62.06	1	Parietal_Sup_R
-55.79	-33.64	30.45	1	SupraMarginal_L
27.78	4.91	2.46	1	Putamen_R
-17.75	-0.03	0.21	1	Pallidum_L
-39.88	15.14	-20.18	1	Temporal_Pole_Sup_L
37.46	-67.14	-29.55	1	Cerebelum_Crus1_R
-23.24	-59.1	-22.13	1	Cerebelum_6_L
24.69	-58.32	-23.65	1	Cerebelum_6_R
-32.36	-59.82	-45.45	1	Cerebelum_7b_L
-22.61	-33.8	-41.76	1	Cerebelum_10_L
1.15	-71.93	-25.14	1	Vermis_7
0.86	-54.87	-34.9	1	Vermis_9
-16.56	47.32	-13.31	0	Frontal_Sup_Orb_L
18.49	48.1	-14.02	0	Frontal_Sup_Orb_R
33.18	52.59	-10.73	0	Frontal_Mid_Orb_R
50.33	30.16	14.17	0	Frontal_Inf_Tri_R
41.22	32.23	-11.91	0	Frontal_Inf_Orb_R
-47.16	-8.48	13.95	0	Rolandic_Oper_L
52.65	-6.25	14.63	0	Rolandic_Oper_R
-5.32	4.85	61.38	0	Supp_Motor_Area_L
8.62	0.17	61.85	0	Supp_Motor_Area_R
7.44	-41.81	21.87	0	Cingulum_Post_R
-25.03	-20.74	-10.13	0	Hippocampus_L
13.51	-79.36	28.23	0	Cuneus_R
-16.54	-84.26	28.17	0	Occipital_Sup_L
24.29	-80.85	30.59	0	Occipital_Sup_R
37.39	-79.7	19.42	0	Occipital_Mid_R
41.43	-25.49	52.55	0	Postcentral_R
-42.8	-45.82	46.74	0	Parietal_Inf_L
46.46	-46.29	49.54	0	Parietal_Inf_R
45.51	-59.98	38.63	0	Angular_R
-7.63	-25.36	70.07	0	Paracentral_Lobule_L
7.48	-31.59	68.09	0	Paracentral_Lobule_R
-23.91	3.86	2.4	0	Putamen_L
21.2	0.18	0.23	0	Pallidum_R
13	-17.55	8.09	0	Thalamus_R
57.47	-37.23	-1.47	0	Temporal_Mid_R
53.69	-31.07	-22.32	0	Temporal_Inf_R

-36.07	-66.72	-28.93	0	Cerebelum_Crus1_L
-28.64	-73.26	-38.2	0	Cerebelum_Crus2_L
32.06	-69.02	-39.95	0	Cerebelum_Crus2_R
-8.8	-37.22	-18.58	0	Cerebelum_3_L
12.32	-34.47	-19.39	0	Cerebelum_3_R
33.14	-63.18	-48.46	0	Cerebelum_7b_R
-25.75	-54.52	-47.68	0	Cerebelum_8_L
25.06	-56.34	-49.47	0	Cerebelum_8_R
-10.95	-48.95	-45.9	0	Cerebelum_9_L
9.46	-49.5	-46.33	0	Cerebelum_9_R
25.99	-33.84	-41.35	0	Cerebelum_10_R
0.76	-38.79	-20.05	0	Vermis_1_2
1.38	-39.93	-11.4	0	Vermis_3
1.22	-52.36	-6.11	0	Vermis_4_5
1.14	-67.06	-15.12	0	Vermis_6
0.36	-45.8	-31.68	0	Vermis_10

Supplementary Table S2. Degree of the regions comprising the network that evidenced a negative association with age, using a primary threshhold of p < 0.005.

MNI COORDINATES				
X	Y	Z	Degree	AAL Region
14.84	12.07	9.42	21	Caudate_R
-41.99	-18.88	9.98	9	Heschl_L
-18.45	34.81	42.2	8	Frontal_Sup_L
-21.17	-15.95	-20.7	8	ParaHippocampal_L
-11.46	11	9.24	7	Caudate_L
-35.13	6.65	3.44	6	Insula_L
21.9	31.12	43.82	4	Frontal_Sup_R
-33.43	32.73	35.46	4	Frontal_Mid_L
8.16	51.67	-7.13	4	Frontal_Med_Orb_R
-53.16	-20.68	7.13	4	Temporal_Sup_L
-38.65	-5.68	50.94	3	Precentral_L
-45.58	29.91	13.99	3	Frontal_Inf_Tri_L
-8.06	15.05	-11.46	3	Olfactory_L
-5.17	54.06	-7.4	3	Frontal_Med_Orb_L
8.02	-8.83	39.79	3	Cingulum_Mid_R
9.1	50.84	30.22	2	Frontal_Sup_Medial_R
-5.08	37.07	-18.14	2	Rectus_L
8.46	37.01	15.84	2	Cingulum_Ant_R
-5.48	-14.92	41.57	2	Cingulum_Mid_L
29.23	-19.78	-10.33	2	Hippocampus_R
25.38	-15.15	-20.47	2	ParaHippocampal_R
-32.39	-80.73	16.11	2	Occipital_Mid_L
-36.36	-78.29	-7.84	2	Occipital_Inf_L
-42.46	-22.63	48.92	2	Postcentral_L
9.98	-56.05	43.77	2	Precuneus_R
45.86	-17.15	10.41	2	Heschl_R
58.15	-21.78	6.8	2	Temporal_Sup_R
48.25	14.75	-16.86	2	Temporal_Pole_Sup_R
-55.52	-33.8	-2.2	2	Temporal_Mid_L
44.22	14.55	-32.23	2	Temporal_Pole_Mid_R
1.15	-64.43	-34.08	2	Vermis_8
41.37	-8.21	52.09	1	Precentral_R
37.59	33.06	34.04	1	Frontal_Mid_R
8.35	35.64	-18.04	1	Rectus_R
27.32	0.64	-17.5	1	Amygdala_R
-7.14	-78.67	6.44	1	Calcarine_L
15.99	-73.15	9.4	1	Calcarine_R
-14.62	-67.56	-4.63	1	Lingual_L
16.29	-66.93	-3.87	1	Lingual_R
-31.16	-40.3	-20.23	1	Fusiform_L
33.97	-39.1	-20.18	1	Fusiform_R
-23.45	-59.56	58.96	1	Parietal_Sup_L
26.11	-59.18	62.06	1	Parietal_Sup_R
-55.79	-33.64	30.45	1	SupraMarginal_L
57.61	-31.5	34.48	1	SupraMarginal_R
-44.14	-60.82	35.59	1	Angular_L
-7.24	-56.07	48.01	1	Precuneus_L

-17.75	-0.03	0.21	1	Pallidum_L
-39.88	15.14	-20.18	1	Temporal_Pole_Sup_L
-36.32	14.59	-34.08	1	Temporal_Pole_Mid_L
-49.77	-28.05	-23.17	1	Temporal_Inf_L
-15	-43.49	-16.93	1	Cerebelum_4_5_L
17.2	-42.86	-18.15	1	Cerebelum_4_5_R
-23.24	-59.1	-22.13	1	Cerebelum_6_L
-22.61	-33.8	-41.76	1	Cerebelum_10_L
1.15	-71.93	-25.14	1	Vermis_7
0.86	-54.87	-34.9	1	Vermis_9
-16.56	47.32	-13.31	0	Frontal_Sup_Orb_L
18.49	48.1	-14.02	0	Frontal_Sup_Orb_R
-30.65	50.43	-9.62	0	Frontal_Mid_Orb_L
33.18	52.59	-10.73	0	Frontal_Mid_Orb_R
-48.43	12.73	19.02	0	Frontal_Inf_Oper_L
50.2	14.98	21.41	0	Frontal_Inf_Oper_R
50.33	30.16	14.17	0	Frontal_Inf_Tri_R
-35.98	30.71	-12.11	0	Frontal_Inf_Orb_L
41.22	32.23	-11.91	0	Frontal_Inf_Orb_R
-47.16	-8.48	13.95	0	Rolandic_Oper_L
52.65	-6.25	14.63	0	Rolandic_Oper_R
-5.32	4.85	61.38	0	Supp_Motor_Area_L
8.62	0.17	61.85	0	Supp_Motor_Area_R
10.43	15.91	-11.26	0	Olfactory_R
-4.8	49.17	30.89	0	Frontal_Sup_Medial_L
39.02	6.25	2.08	0	Insula_R
-4.04	35.4	13.95	0	Cingulum_Ant_L
-4.85	-42.92	24.67	0	Cingulum_Post_L
7.44	-41.81	21.87	0	Cingulum_Post_R
-25.03	-20.74	-10.13	0	Hippocampus_L
-23.27	-0.67	-17.14	0	Amygdala_L
-5.93	-80.13	27.22	0	Cuneus_L
13.51	-79.36	28.23	0	Cuneus_R
-16.54	-84.26	28.17	0	Occipital_Sup_L
24.29	-80.85	30.59	0	Occipital_Sup_R
37.39	-79.7	19.42	0	Occipital_Mid_R
38.16	-81.99	-7.61	0	Occipital_Inf_R
41.43	-25.49	52.55	0	Postcentral_R
-42.8	-45.82	46.74	0	Parietal_Inf_L
46.46	-46.29	49.54	0	Parietal_Inf_R
45.51	-59.98	38.63	0	Angular_R
-7.63	-25.36	70.07	0	Paracentral_Lobule_L
7.48	-31.59	68.09	0	Paracentral_Lobule_R
-23.91	3.86	2.4	0	Putamen_L
27.78	4.91	2.46	0	Putamen_R
21.2	0.18	0.23	0	Pallidum_R
-10.85	-17.56	7.98	0	Thalamus_L
13	-17.55	8.09	0	Thalamus_R
57.47	-37.23	-1.47	0	Temporal_Mid_R
53.69	-31.07	-22.32	0	Temporal_Inf_R
-36.07	-66.72	-28.93	0	Cerebelum_Crus1_L
37.46	-67.14	-29.55	0	Cerebelum_Crus1_R
-28.64	-73.26	-38.2	0	Cerebelum_Crus2_L

32.06	-69.02	-39.95	0	Cerebelum_Crus2_R
-8.8	-37.22	-18.58	0	Cerebelum_3_L
12.32	-34.47	-19.39	0	Cerebelum_3_R
24.69	-58.32	-23.65	0	Cerebelum_6_R
-32.36	-59.82	-45.45	0	Cerebelum_7b_L
33.14	-63.18	-48.46	0	Cerebelum_7b_R
-25.75	-54.52	-47.68	0	Cerebelum_8_L
25.06	-56.34	-49.47	0	Cerebelum_8_R
-10.95	-48.95	-45.9	0	Cerebelum_9_L
9.46	-49.5	-46.33	0	Cerebelum_9_R
25.99	-33.84	-41.35	0	Cerebelum_10_R
0.76	-38.79	-20.05	0	Vermis_1_2
1.38	-39.93	-11.4	0	Vermis_3
1.22	-52.36	-6.11	0	Vermis_4_5
1.14	-67.06	-15.12	0	Vermis_6
0.36	-45.8	-31.68	0	Vermis_10

Supplementary Table S3. Degree of the regions comprising the network that evidenced a positive association with years of formal education using a primary threshhold of p < 0.01.

MNI COORDINATES				
X	Y	Z	Degree	AAL Region
-14.62	-67.56	-4.63	32	Lingual_L
-18.45	34.81	42.2	20	Frontal_Sup_L
41.37	-8.21	52.09	19	Precentral_R
7.48	-31.59	68.09	19	Paracentral_Lobule_R
-5.93	-80.13	27.22	18	Cuneus_L
-5.48	-14.92	41.57	17	Cingulum_Mid_L
44.22	14.55	-32.23	16	Temporal_Pole_Mid_R
24.29	-80.85	30.59	14	Occipital_Sup_R
-38.65	-5.68	50.94	12	Precentral_L
21.9	31.12	43.82	12	Frontal_Sup_R
7.44	-41.81	21.87	12	Cingulum_Post_R
13.51	-79.36	28.23	12	Cuneus_R
41.43	-25.49	52.55	12	Postcentral_R
45.86	-17.15	10.41	12	Heschl_R
8.62	0.17	61.85	11	Supp_Motor_Area_R
8.02	-8.83	39.79	11	Cingulum_Mid_R
-7.14	-78.67	6.44	11	Calcarine_L
37.39	-79.7	19.42	11	Occipital_Mid_R
26.11	-59.18	62.06	11	Parietal_Sup_R
16.29	-66.93	-3.87	10	Lingual_R
-36.36	-78.29	-7.84	10	Occipital_Inf_L
-5.08	37.07	-18.14	9	Rectus_L
-16.54	-84.26	28.17	9	Occipital_Sup_L
33.97	-39.1	-20.18	9	Fusiform_R
-23.45	-59.56	58.96	9	Parietal_Sup_L
-4.85	-42.92	24.67	8	Cingulum_Post_L
-7.24	-56.07	48.01	8	Precuneus_L
-36.32	14.59	-34.08	8	Temporal_Pole_Mid_L
-15	-43.49	-16.93	8	Cerebelum_4_5_L
9.1	50.84	30.22	7	Frontal_Sup_Medial_R
-32.39	-80.73	16.11	7	Occipital_Mid_L
48.25	14.75	-16.86	7	Temporal_Pole_Sup_R
-16.56	47.32	-13.31	6	Frontal_Sup_Orb_L
8.35	35.64	-18.04	6	Rectus_R
-7.63	-25.36	70.07	6	Paracentral_Lobule_L
-36.07	-66.72	-28.93	6	Cerebelum_Crus1_L
-47.16	-8.48	13.95	5	Rolandic_Oper_L
-4.8	49.17	30.89	5	Frontal_Sup_Medial_L
-5.17	54.06	-7.4	5	Frontal_Med_Orb_L
-31.16	-40.3	-20.23	5	Fusiform_L
-53.16	-20.68	7.13	5	Temporal_Sup_L
1.22	-52.36	-6.11	5	Vermis_4_5
-33.43	32.73	35.46	4	Frontal_Mid_L
-5.32	4.85	61.38	4	Supp_Motor_Area_L
-23.27	-0.67	-17.14	4	Amygdala_L
15.99	-73.15	9.4	4	Calcarine_R
58.15	-21.78	6.8	4	Temporal_Sup_R

18.49	48.1	-14.02	3	Frontal_Sup_Orb_R
8.16	51.67	-7.13	3	Frontal_Med_Orb_R
-41.99	-18.88	9.98	3	Heschl_L
-39.88	15.14	-20.18	3	Temporal_Pole_Sup_L
-23.24	-59.1	-22.13	3	Cerebelum_6_L
24.69	-58.32	-23.65	3	Cerebelum_6_R
-42.46	-22.63	48.92	2	Postcentral_L
9.98	-56.05	43.77	2	Precuneus_R
57.47	-37.23	-1.47	2	Temporal_Mid_R
-48.43	12.73	19.02	1	Frontal_Inf_Oper_L
-45.58	29.91	13.99	1	Frontal_Inf_Tri_L
-35.98	30.71	-12.11	1	Frontal_Inf_Orb_L
52.65	-6.25	14.63	1	Rolandic_Oper_R
-4.04	35.4	13.95	1	Cingulum_Ant_L
27.32	0.64	-17.5	1	Amygdala_R
38.16	-81.99	-7.61	1	Occipital_Inf_R
-44.14	-60.82	35.59	1	Angular_L
13	-17.55	8.09	1	Thalamus_R
17.2	-42.86	-18.15	1	Cerebelum_4_5_R
-10.95	-48.95	-45.9	1	Cerebelum_9_L
37.59	33.06	34.04	0	Frontal_Mid_R
-30.65	50.43	-9.62	0	Frontal_Mid_Orb_L
33.18	52.59	-10.73	0	Frontal_Mid_Orb_R
50.2	14.98	21.41	0	Frontal_Inf_Oper_R
50.33	30.16	14.17	0	Frontal_Inf_Tri_R
41.22	32.23	-11.91	0	Frontal_Inf_Orb_R
-8.06	15.05	-11.46	0	Olfactory_L
10.43	15.91	-11.26	0	Olfactory_R
-35.13	6.65	3.44	0	Insula_L
39.02	6.25	2.08	0	Insula_R
8.46	37.01	15.84	0	Cingulum_Ant_R
-25.03	-20.74	-10.13	0	Hippocampus_L
29.23	-19.78	-10.33	0	Hippocampus_R
-21.17	-15.95	-20.7	0	ParaHippocampal_L
25.38	-15.15	-20.47	0	ParaHippocampal_R
-42.8	-45.82	46.74	0	Parietal_Inf_L
46.46	-46.29	49.54	0	Parietal_Inf_R
-55.79	-33.64	30.45	0	SupraMarginal_L
57.61	-31.5	34.48	0	SupraMarginal_R
45.51	-59.98	38.63	0	Angular_R
-11.46	11	9.24	0	Caudate_L
14.84	12.07	9.42	0	Caudate_R
-23.91	3.86	2.4	0	Putamen_L
27.78	4.91	2.46	0	Putamen_R
-17.75	-0.03	0.21	0	Pallidum_L
21.2	0.18	0.23	0	Pallidum_R
-10.85	-17.56	7.98	0	Thalamus_L
-55.52	-33.8	-2.2	0	Temporal_Mid_L
-49.77	-28.05	-23.17	0	Temporal_Inf_L
53.69	-31.07	-22.32	0	Temporal_Inf_R
37.46	-67.14	-29.55	0	Cerebelum_Crus1_R
-28.64	-73.26	-38.2	0	Cerebelum_Crus2_L
32.06	-69.02	-39.95	0	Cerebelum_Crus2_R

-8.8	-37.22	-18.58	0	Cerebelum_3_L
12.32	-34.47	-19.39	0	Cerebelum_3_R
-32.36	-59.82	-45.45	0	Cerebelum_7b_L
33.14	-63.18	-48.46	0	Cerebelum_7b_R
-25.75	-54.52	-47.68	0	Cerebelum_8_L
25.06	-56.34	-49.47	0	Cerebelum_8_R
9.46	-49.5	-46.33	0	Cerebelum_9_R
-22.61	-33.8	-41.76	0	Cerebelum_10_L
25.99	-33.84	-41.35	0	Cerebelum_10_R
0.76	-38.79	-20.05	0	Vermis_1_2
1.38	-39.93	-11.4	0	Vermis_3
1.14	-67.06	-15.12	0	Vermis_6
1.15	-71.93	-25.14	0	Vermis_7
1.15	-64.43	-34.08	0	Vermis_8
0.86	-54.87	-34.9	0	Vermis_9
0.36	-45.8	-31.68	0	Vermis_10

Supplementary Table S4. Degree of the regions comprising the network that evidenced a positive association with years of formal education using a primary threshhold of p < 0.005.

MNI COORDINATES				
X	Y	Z	Degree	AAL Region
-14.62	-67.56	-4.63	28	Lingual_L
-18.45	34.81	42.2	16	Frontal_Sup_L
41.37	-8.21	52.09	14	Precentral_R
44.22	14.55	-32.23	13	Temporal_Pole_Mid_R
-5.48	-14.92	41.57	12	Cingulum_Mid_L
-5.93	-80.13	27.22	12	Cuneus_L
24.29	-80.85	30.59	11	Occipital_Sup_R
7.48	-31.59	68.09	11	Paracentral_Lobule_R
45.86	-17.15	10.41	10	Heschl_R
7.44	-41.81	21.87	8	Cingulum_Post_R
13.51	-79.36	28.23	8	Cuneus_R
-38.65	-5.68	50.94	7	Precentral_L
8.62	0.17	61.85	7	Supp_Motor_Area_R
-5.08	37.07	-18.14	7	Rectus_L
8.02	-8.83	39.79	7	Cingulum_Mid_R
-4.85	-42.92	24.67	7	Cingulum_Post_L
16.29	-66.93	-3.87	7	Lingual_R
26.11	-59.18	62.06	7	Parietal_Sup_R
21.9	31.12	43.82	6	Frontal_Sup_R
9.1	50.84	30.22	6	Frontal_Sup_Medial_R
-7.14	-78.67	6.44	6	Calcarine_L
-16.54	-84.26	28.17	6	Occipital_Sup_L
37.39	-79.7	19.42	6	Occipital_Mid_R
-36.36	-78.29	-7.84	6	Occipital_Inf_L
33.97	-39.1	-20.18	6	Fusiform_R
41.43	-25.49	52.55	6	Postcentral_R
48.25	14.75	-16.86	6	Temporal_Pole_Sup_R
-36.32	14.59	-34.08	6	Temporal_Pole_Mid_L
-16.56	47.32	-13.31	5	Frontal_Sup_Orb_L
-32.39	-80.73	16.11	5	Occipital_Mid_L
-15	-43.49	-16.93	5	Cerebelum_4_5_L
-23.45	-59.56	58.96	4	Parietal_Sup_L
-7.24	-56.07	48.01	4	Precuneus_L
-36.07	-66.72	-28.93	4	Cerebelum_Crus1_L
1.22	-52.36	-6.11	4	Vermis_4_5
-33.43	32.73	35.46	3	Frontal_Mid_L
-7.63	-25.36	70.07	3	Paracentral_Lobule_L
-23.24	-59.1	-22.13	3	Cerebelum_6_L
18.49	48.1	-14.02	2	Frontal_Sup_Orb_R
-4.8	49.17	30.89	2	Frontal_Sup_Medial_L
8.16	51.67	-7.13	2	Frontal_Med_Orb_R
8.35	35.64	-18.04	2	Rectus_R
-23.27	-0.67	-17.14	2	Amygdala_L
-31.16	-40.3	-20.23	2	Fusiform_L
-41.99	-18.88	9.98	2	Heschl_L
-53.16	-20.68	7.13	2	Temporal_Sup_L
-39.88	15.14	-20.18	2	Temporal_Pole_Sup_L

57.47	-37.23	-1.47	2	Temporal_Mid_R
24.69	-58.32	-23.65	2	Cerebelum_6_R
-48.43	12.73	19.02	1	Frontal_Inf_Oper_L
-45.58	29.91	13.99	1	Frontal_Inf_Tri_L
-35.98	30.71	-12.11	1	Frontal_Inf_Orb_L
-47.16	-8.48	13.95	1	Rolandic_Oper_L
-5.17	54.06	-7.4	1	Frontal_Med_Orb_L
-4.04	35.4	13.95	1	Cingulum_Ant_L
15.99	-73.15	9.4	1	Calcarine_R
13	-17.55	8.09	1	Thalamus_R
58.15	-21.78	6.8	1	Temporal_Sup_R
17.2	-42.86	-18.15	1	Cerebelum_4_5_R
37.59	33.06	34.04	0	Frontal_Mid_R
-30.65	50.43	-9.62	0	Frontal_Mid_Orb_L
33.18	52.59	-10.73	0	Frontal_Mid_Orb_R
50.2	14.98	21.41	0	Frontal_Inf_Oper_R
50.33	30.16	14.17	0	Frontal_Inf_Tri_R
41.22	32.23	-11.91	0	Frontal_Inf_Orb_R
52.65	-6.25	14.63	0	Rolandic_Oper_R
-5.32	4.85	61.38	0	Supp_Motor_Area_L
-8.06	15.05	-11.46	0	Olfactory_L
10.43	15.91	-11.26	0	Olfactory_R
-35.13	6.65	3.44	0	Insula_L
39.02	6.25	2.08	0	Insula_R
8.46	37.01	15.84	0	Cingulum_Ant_R
-25.03	-20.74	-10.13	0	Hippocampus_L
29.23	-19.78	-10.33	0	Hippocampus_R
-21.17	-15.95	-20.7	0	ParaHippocampal_L
25.38	-15.15	-20.47	0	ParaHippocampal_R
27.32	0.64	-17.5	0	Amygdala_R
38.16	-81.99	-7.61	0	Occipital_Inf_R
-42.46	-22.63	48.92	0	Postcentral_L
-42.8	-45.82	46.74	0	Parietal_Inf_L
46.46	-46.29	49.54	0	Parietal_Inf_R
-55.79	-33.64	30.45	0	SupraMarginal_L
57.61	-31.5	34.48	0	SupraMarginal_R
-44.14	-60.82	35.59	0	Angular_L
45.51	-59.98	38.63	0	Angular_R
9.98	-56.05	43.77	0	Precuneus_R
-11.46	11	9.24	0	Caudate_L
14.84	12.07	9.42	0	Caudate_R
-23.91	3.86	2.4	0	Putamen_L
27.78	4.91	2.46	0	Putamen_R
-17.75	-0.03	0.21	0	Pallidum_L
21.2	0.18	0.23	0	Pallidum_R
-10.85	-17.56	7.98	0	Thalamus_L
-55.52	-33.8	-2.2	0	Temporal_Mid_L
-49.77	-28.05	-23.17	0	Temporal_Inf_L
53.69	-31.07	-22.32	0	Temporal_Inf_R
37.46	-67.14	-29.55	0	Cerebelum_Crus1_R
-28.64	-73.26	-38.2	0	Cerebelum_Crus2_L
32.06	-69.02	-39.95	0	Cerebelum_Crus2_R
-8.8	-37.22	-18.58	0	Cerebelum_3_L

12.32	-34.47	-19.39	0	Cerebelum_3_R
-32.36	-59.82	-45.45	0	Cerebelum_7b_L
33.14	-63.18	-48.46	0	Cerebelum_7b_R
-25.75	-54.52	-47.68	0	Cerebelum_8_L
25.06	-56.34	-49.47	0	Cerebelum_8_R
-10.95	-48.95	-45.9	0	Cerebelum_9_L
9.46	-49.5	-46.33	0	Cerebelum_9_R
-22.61	-33.8	-41.76	0	Cerebelum_10_L
25.99	-33.84	-41.35	0	Cerebelum_10_R
0.76	-38.79	-20.05	0	Vermis_1_2
1.38	-39.93	-11.4	0	Vermis_3
1.14	-67.06	-15.12	0	Vermis_6
1.15	-71.93	-25.14	0	Vermis_7
1.15	-64.43	-34.08	0	Vermis_8
0.86	-54.87	-34.9	0	Vermis_9
0.36	-45.8	-31.68	0	Vermis_10

Supplementary Table S5. Degree of the regions comprising the network that evidenced a positive association with years of formal education using a primary threshhold of p < 0.001.

MNI COORDINATES				
X	Y	Z	Degree	AAL Region
-14.62	-67.56	-4.63	17	Lingual_L
41.37	-8.21	52.09	6	Precentral_R
-5.93	-80.13	27.22	5	Cuneus_L
-18.45	34.81	42.2	4	Frontal_Sup_L
-5.48	-14.92	41.57	4	Cingulum_Mid_L
44.22	14.55	-32.23	4	Temporal_Pole_Mid_R
21.9	31.12	43.82	3	Frontal_Sup_R
8.62	0.17	61.85	3	Supp_Motor_Area_R
-5.08	37.07	-18.14	3	Rectus_L
-4.85	-42.92	24.67	3	Cingulum_Post_L
7.44	-41.81	21.87	3	Cingulum_Post_R
24.29	-80.85	30.59	3	Occipital_Sup_R
41.43	-25.49	52.55	3	Postcentral_R
45.86	-17.15	10.41	3	Heschl_R
-16.56	47.32	-13.31	2	Frontal_Sup_Orb_L
-7.14	-78.67	6.44	2	Calcarine_L
37.39	-79.7	19.42	2	Occipital_Mid_R
26.11	-59.18	62.06	2	Parietal_Sup_R
-7.24	-56.07	48.01	2	Precuneus_L
7.48	-31.59	68.09	2	Paracentral_Lobule_R
-15	-43.49	-16.93	2	Cerebelum_4_5_L
-38.65	-5.68	50.94	1	Precentral_L
18.49	48.1	-14.02	1	Frontal_Sup_Orb_R
9.1	50.84	30.22	1	Frontal_Sup_Medial_R
8.16	51.67	-7.13	1	Frontal_Med_Orb_R
8.35	35.64	-18.04	1	Rectus_R
8.02	-8.83	39.79	1	Cingulum_Mid_R
16.29	-66.93	-3.87	1	Lingual_R
33.97	-39.1	-20.18	1	Fusiform_R
-23.45	-59.56	58.96	1	Parietal_Sup_L
48.25	14.75	-16.86	1	Temporal_Pole_Sup_R
-23.24	-59.1	-22.13	1	Cerebelum_6_L
1.22	-52.36	-6.11	1	Vermis_4_5
-33.43	32.73	35.46	0	Frontal_Mid_L
37.59	33.06	34.04	0	Frontal_Mid_R
-30.65	50.43	-9.62	0	Frontal_Mid_Orb_L
33.18	52.59	-10.73	0	Frontal_Mid_Orb_R
-48.43	12.73	19.02	0	Frontal_Inf_Oper_L
50.2	14.98	21.41	0	Frontal_Inf_Oper_R
-45.58	29.91	13.99	0	Frontal_Inf_Tri_L
50.33	30.16	14.17	0	Frontal_Inf_Tri_R
-35.98	30.71	-12.11	0	Frontal_Inf_Orb_L
41.22	32.23	-11.91	0	Frontal_Inf_Orb_R
-47.16	-8.48	13.95	0	Rolandic_Oper_L
52.65	-6.25	14.63	0	Rolandic_Oper_R
-5.32	4.85	61.38	0	Supp_Motor_Area_L
-8.06	15.05	-11.46	0	Olfactory_L

10.43	15.91	-11.26	0	Olfactory_R
-4.8	49.17	30.89	0	Frontal_Sup_Medial_L
-5.17	54.06	-7.4	0	Frontal_Med_Orb_L
-35.13	6.65	3.44	0	Insula_L
39.02	6.25	2.08	0	Insula_R
-4.04	35.4	13.95	0	Cingulum_Ant_L
8.46	37.01	15.84	0	Cingulum_Ant_R
-25.03	-20.74	-10.13	0	Hippocampus_L
29.23	-19.78	-10.33	0	Hippocampus_R
-21.17	-15.95	-20.7	0	ParaHippocampal_L
25.38	-15.15	-20.47	0	ParaHippocampal_R
-23.27	-0.67	-17.14	0	Amygdala_L
27.32	0.64	-17.5	0	Amygdala_R
15.99	-73.15	9.4	0	Calcarine_R
13.51	-79.36	28.23	0	Cuneus_R
-16.54	-84.26	28.17	0	Occipital_Sup_L
-32.39	-80.73	16.11	0	Occipital_Mid_L
-36.36	-78.29	-7.84	0	Occipital_Inf_L
38.16	-81.99	-7.61	0	Occipital_Inf_R
-31.16	-40.3	-20.23	0	Fusiform_L
-42.46	-22.63	48.92	0	Postcentral_L
-42.8	-45.82	46.74	0	Parietal_Inf_L
46.46	-46.29	49.54	0	Parietal_Inf_R
-55.79	-33.64	30.45	0	SupraMarginal_L
57.61	-31.5	34.48	0	SupraMarginal_R
-44.14	-60.82	35.59	0	Angular_L
45.51	-59.98	38.63	0	Angular_R
9.98	-56.05	43.77	0	Precuneus_R
-7.63	-25.36	70.07	0	Paracentral_Lobule_L
-11.46	11	9.24	0	Caudate_L
14.84	12.07	9.42	0	Caudate_R
-23.91	3.86	2.4	0	Putamen_L
27.78	4.91	2.46	0	Putamen_R
-17.75	-0.03	0.21	0	Pallidum_L
21.2	0.18	0.23	0	Pallidum_R
-10.85	-17.56	7.98	0	Thalamus_L
13	-17.55	8.09	0	Thalamus_R
-41.99	-18.88	9.98	0	Heschl_L
-53.16	-20.68	7.13	0	Temporal_Sup_L
58.15	-21.78	6.8	0	Temporal_Sup_R
-39.88	15.14	-20.18	0	Temporal_Pole_Sup_L
-55.52	-33.8	-2.2	0	Temporal_Mid_L
57.47	-37.23	-1.47	0	Temporal_Mid_R
-36.32	14.59	-34.08	0	Temporal_Pole_Mid_L
-49.77	-28.05	-23.17	0	Temporal_Inf_L
53.69	-31.07	-22.32	0	Temporal_Inf_R
-36.07	-66.72	-28.93	0	Cerebelum_Crus1_L
37.46	-67.14	-29.55	0	Cerebelum_Crus1_R
-28.64	-73.26	-38.2	0	Cerebelum_Crus2_L
32.06	-69.02	-39.95	0	Cerebelum_Crus2_R
-8.8	-37.22	-18.58	0	Cerebelum_3_L
12.32	-34.47	-19.39	0	Cerebelum_3_R
17.2	-42.86	-18.15	0	Cerebelum_4_5_R

24.69	-58.32	-23.65	0	Cerebelum_6_R
-32.36	-59.82	-45.45	0	Cerebelum_7b_L
33.14	-63.18	-48.46	0	Cerebelum_7b_R
-25.75	-54.52	-47.68	0	Cerebelum_8_L
25.06	-56.34	-49.47	0	Cerebelum_8_R
-10.95	-48.95	-45.9	0	Cerebelum_9_L
9.46	-49.5	-46.33	0	Cerebelum_9_R
-22.61	-33.8	-41.76	0	Cerebelum_10_L
25.99	-33.84	-41.35	0	Cerebelum_10_R
0.76	-38.79	-20.05	0	Vermis_1_2
1.38	-39.93	-11.4	0	Vermis_3
1.14	-67.06	-15.12	0	Vermis_6
1.15	-71.93	-25.14	0	Vermis_7
1.15	-64.43	-34.08	0	Vermis_8
0.86	-54.87	-34.9	0	Vermis_9
0.36	-45.8	-31.68	0	Vermis_10

Supplementary Table S6. Degree of the regions comprising the network that evidenced a negative association with years of formal education using a primary threshhold of p < 0.005.

MNI COORDINATES				
X	Y	Z	Degree	AAL Region
0.36	-45.8	-31.68	36	Vermis_10
0.76	-38.79	-20.05	25	Vermis_1_2
53.69	-31.07	-22.32	4	Temporal_Inf_R
0.86	-54.87	-34.9	4	Vermis_9
-10.95	-48.95	-45.9	3	Cerebelum_9_L
-38.65	-5.68	50.94	2	Precentral_L
41.37	-8.21	52.09	2	Precentral_R
-8.06	15.05	-11.46	2	Olfactory_L
-5.08	37.07	-18.14	2	Rectus_L
8.35	35.64	-18.04	2	Rectus_R
-7.14	-78.67	6.44	2	Calcarine_L
15.99	-73.15	9.4	2	Calcarine_R
-5.93	-80.13	27.22	2	Cuneus_L
13.51	-79.36	28.23	2	Cuneus_R
-14.62	-67.56	-4.63	2	Lingual_L
16.29	-66.93	-3.87	2	Lingual_R
-16.54	-84.26	28.17	2	Occipital_Sup_L
-36.36	-78.29	-7.84	2	Occipital_Inf_L
-31.16	-40.3	-20.23	2	Fusiform_L
33.97	-39.1	-20.18	2	Fusiform_R
41.43	-25.49	52.55	2	Postcentral_R
7.48	-31.59	68.09	2	Paracentral_Lobule_R
-53.16	-20.68	7.13	2	Temporal_Sup_L
44.22	14.55	-32.23	2	Temporal_Pole_Mid_R
17.2	-42.86	-18.15	2	Cerebelum_4_5_R
9.46	-49.5	-46.33	2	Cerebelum_9_R
-16.56	47.32	-13.31	1	Frontal_Sup_Orb_L
18.49	48.1	-14.02	1	Frontal_Sup_Orb_R
52.65	-6.25	14.63	1	Rolandic_Oper_R
8.62	0.17	61.85	1	Supp_Motor_Area_R
10.43	15.91	-11.26	1	Olfactory_R
-5.48	-14.92	41.57	1	Cingulum_Mid_L
8.02	-8.83	39.79	1	Cingulum_Mid_R
24.29	-80.85	30.59	1	Occipital_Sup_R
-32.39	-80.73	16.11	1	Occipital_Mid_L
37.39	-79.7	19.42	1	Occipital_Mid_R
38.16	-81.99	-7.61	1	Occipital_Inf_R
-42.46	-22.63	48.92	1	Postcentral_L
-55.79	-33.64	30.45	1	SupraMarginal_L
-7.63	-25.36	70.07	1	Paracentral_Lobule_L
45.86	-17.15	10.41	1	Heschl_R
58.15	-21.78	6.8	1	Temporal_Sup_R
-55.52	-33.8	-2.2	1	Temporal_Mid_L
57.47	-37.23	-1.47	1	Temporal_Mid_R
-49.77	-28.05	-23.17	1	Temporal_Inf_L
37.46	-67.14	-29.55	1	Cerebelum_Crus1_R
-15	-43.49	-16.93	1	Cerebelum_4_5_L

-22.61	-33.8	-41.76	1	Cerebelum_10_L
-18.45	34.81	42.2	0	Frontal_Sup_L
21.9	31.12	43.82	0	Frontal_Sup_R
-33.43	32.73	35.46	0	Frontal_Mid_L
37.59	33.06	34.04	0	Frontal_Mid_R
-30.65	50.43	-9.62	0	Frontal_Mid_Orb_L
33.18	52.59	-10.73	0	Frontal_Mid_Orb_R
-48.43	12.73	19.02	0	Frontal_Inf_Oper_L
50.2	14.98	21.41	0	Frontal_Inf_Oper_R
-45.58	29.91	13.99	0	Frontal_Inf_Tri_L
50.33	30.16	14.17	0	Frontal_Inf_Tri_R
-35.98	30.71	-12.11	0	Frontal_Inf_Orb_L
41.22	32.23	-11.91	0	Frontal_Inf_Orb_R
-47.16	-8.48	13.95	0	Rolandic_Oper_L
-5.32	4.85	61.38	0	Supp_Motor_Area_L
-4.8	49.17	30.89	0	Frontal_Sup_Medial_L
9.1	50.84	30.22	0	Frontal_Sup_Medial_R
-5.17	54.06	-7.4	0	Frontal_Med_Orb_L
8.16	51.67	-7.13	0	Frontal_Med_Orb_R
-35.13	6.65	3.44	0	Insula_L
39.02	6.25	2.08	0	Insula_R
-4.04	35.4	13.95	0	Cingulum_Ant_L
8.46	37.01	15.84	0	Cingulum_Ant_R
-4.85	-42.92	24.67	0	Cingulum_Post_L
7.44	-41.81	21.87	0	Cingulum_Post_R
-25.03	-20.74	-10.13	0	Hippocampus_L
29.23	-19.78	-10.33	0	Hippocampus_R
-21.17	-15.95	-20.7	0	ParaHippocampal_L
25.38	-15.15	-20.47	0	ParaHippocampal_R
-23.27	-0.67	-17.14	0	Amygdala_L
27.32	0.64	-17.5	0	Amygdala_R
-23.45	-59.56	58.96	0	Parietal_Sup_L
26.11	-59.18	62.06	0	Parietal_Sup_R
-42.8	-45.82	46.74	0	Parietal_Inf_L
46.46	-46.29	49.54	0	Parietal_Inf_R
57.61	-31.5	34.48	0	SupraMarginal_R
-44.14	-60.82	35.59	0	Angular_L
45.51	-59.98	38.63	0	Angular_R
-7.24	-56.07	48.01	0	Precuneus_L
9.98	-56.05	43.77	0	Precuneus_R
-11.46	11	9.24	0	Caudate_L
14.84	12.07	9.42	0	Caudate_R
-23.91	3.86	2.4	0	Putamen_L
27.78	4.91	2.46	0	Putamen_R
-17.75	-0.03	0.21	0	Pallidum_L
21.2	0.18	0.23	0	Pallidum_R
-10.85	-17.56	7.98	0	Thalamus_L
13	-17.55	8.09	0	Thalamus_R
-41.99	-18.88	9.98	0	Heschl_L
-39.88	15.14	-20.18	0	Temporal_Pole_Sup_L
48.25	14.75	-16.86	0	Temporal_Pole_Sup_R
-36.32	14.59	-34.08	0	Temporal_Pole_Mid_L
-36.07	-66.72	-28.93	0	Cerebelum_Crus1_L

-28.64	-73.26	-38.2	0	Cerebelum_Crus2_L
32.06	-69.02	-39.95	0	Cerebelum_Crus2_R
-8.8	-37.22	-18.58	0	Cerebelum_3_L
12.32	-34.47	-19.39	0	Cerebelum_3_R
-23.24	-59.1	-22.13	0	Cerebelum_6_L
24.69	-58.32	-23.65	0	Cerebelum_6_R
-32.36	-59.82	-45.45	0	Cerebelum_7b_L
33.14	-63.18	-48.46	0	Cerebelum_7b_R
-25.75	-54.52	-47.68	0	Cerebelum_8_L
25.06	-56.34	-49.47	0	Cerebelum_8_R
25.99	-33.84	-41.35	0	Cerebelum_10_R
1.38	-39.93	-11.4	0	Vermis_3
1.22	-52.36	-6.11	0	Vermis_4_5
1.14	-67.06	-15.12	0	Vermis_6
1.15	-71.93	-25.14	0	Vermis_7
1.15	-64.43	-34.08	0	Vermis_8

Supplementary Table S7. Degree of the regions comprising the network that evidenced a negative association with years of formal education using a primary threshhold of p < 0.001.

MNI COORDINATES				
X	Y	Z	Degree	AAL Region
0.36	-45.8	-31.68	20	Vermis_10
0.76	-38.79	-20.05	4	Vermis_1_2
-16.54	-84.26	28.17	2	Occipital_Sup_L
-38.65	-5.68	50.94	1	Precentral_L
41.37	-8.21	52.09	1	Precentral_R
52.65	-6.25	14.63	1	Rolandic_Oper_R
8.62	0.17	61.85	1	Supp_Motor_Area_R
-5.08	37.07	-18.14	1	Rectus_L
-5.48	-14.92	41.57	1	Cingulum_Mid_L
8.02	-8.83	39.79	1	Cingulum_Mid_R
-7.14	-78.67	6.44	1	Calcarine_L
-5.93	-80.13	27.22	1	Cuneus_L
13.51	-79.36	28.23	1	Cuneus_R
-14.62	-67.56	-4.63	1	Lingual_L
16.29	-66.93	-3.87	1	Lingual_R
24.29	-80.85	30.59	1	Occipital_Sup_R
-36.36	-78.29	-7.84	1	Occipital_Inf_L
33.97	-39.1	-20.18	1	Fusiform_R
-42.46	-22.63	48.92	1	Postcentral_L
41.43	-25.49	52.55	1	Postcentral_R
-7.63	-25.36	70.07	1	Paracentral_Lobule_L
7.48	-31.59	68.09	1	Paracentral_Lobule_R
-53.16	-20.68	7.13	1	Temporal_Sup_L
44.22	14.55	-32.23	1	Temporal_Pole_Mid_R
-22.61	-33.8	-41.76	1	Cerebelum_10_L
-18.45	34.81	42.2	0	Frontal_Sup_L
21.9	31.12	43.82	0	Frontal_Sup_R
-16.56	47.32	-13.31	0	Frontal_Sup_Orb_L
18.49	48.1	-14.02	0	Frontal_Sup_Orb_R
-33.43	32.73	35.46	0	Frontal_Mid_L
37.59	33.06	34.04	0	Frontal_Mid_R
-30.65	50.43	-9.62	0	Frontal_Mid_Orb_L
33.18	52.59	-10.73	0	Frontal_Mid_Orb_R
-48.43	12.73	19.02	0	Frontal_Inf_Oper_L
50.2	14.98	21.41	0	Frontal_Inf_Oper_R
-45.58	29.91	13.99	0	Frontal_Inf_Tri_L
50.33	30.16	14.17	0	Frontal_Inf_Tri_R
-35.98	30.71	-12.11	0	Frontal_Inf_Orb_L
41.22	32.23	-11.91	0	Frontal_Inf_Orb_R
-47.16	-8.48	13.95	0	Rolandic_Oper_L
-5.32	4.85	61.38	0	Supp_Motor_Area_L
-8.06	15.05	-11.46	0	Olfactory_L
10.43	15.91	-11.26	0	Olfactory_R
-4.8	49.17	30.89	0	Frontal_Sup_Medial_L
9.1	50.84	30.22	0	Frontal_Sup_Medial_R
-5.17	54.06	-7.4	0	Frontal_Med_Orb_L
8.16	51.67	-7.13	0	Frontal_Med_Orb_R

8.35	35.64	-18.04	0	Rectus_R
-35.13	6.65	3.44	0	Insula_L
39.02	6.25	2.08	0	Insula_R
-4.04	35.4	13.95	0	Cingulum_Ant_L
8.46	37.01	15.84	0	Cingulum_Ant_R
-4.85	-42.92	24.67	0	Cingulum_Post_L
7.44	-41.81	21.87	0	Cingulum_Post_R
-25.03	-20.74	-10.13	0	Hippocampus_L
29.23	-19.78	-10.33	0	Hippocampus_R
-21.17	-15.95	-20.7	0	ParaHippocampal_L
25.38	-15.15	-20.47	0	ParaHippocampal_R
-23.27	-0.67	-17.14	0	Amygdala_L
27.32	0.64	-17.5	0	Amygdala_R
15.99	-73.15	9.4	0	Calcarine_R
-32.39	-80.73	16.11	0	Occipital_Mid_L
37.39	-79.7	19.42	0	Occipital_Mid_R
38.16	-81.99	-7.61	0	Occipital_Inf_R
-31.16	-40.3	-20.23	0	Fusiform_L
-23.45	-59.56	58.96	0	Parietal_Sup_L
26.11	-59.18	62.06	0	Parietal_Sup_R
-42.8	-45.82	46.74	0	Parietal_Inf_L
46.46	-46.29	49.54	0	Parietal_Inf_R
-55.79	-33.64	30.45	0	SupraMarginal_L
57.61	-31.5	34.48	0	SupraMarginal_R
-44.14	-60.82	35.59	0	Angular_L
45.51	-59.98	38.63	0	Angular_R
-7.24	-56.07	48.01	0	Precuneus_L
9.98	-56.05	43.77	0	Precuneus_R
-11.46	11	9.24	0	Caudate_L
14.84	12.07	9.42	0	Caudate_R
-23.91	3.86	2.4	0	Putamen_L
27.78	4.91	2.46	0	Putamen_R
-17.75	-0.03	0.21	0	Pallidum_L
21.2	0.18	0.23	0	Pallidum_R
-10.85	-17.56	7.98	0	Thalamus_L
13	-17.55	8.09	0	Thalamus_R
-41.99	-18.88	9.98	0	Heschl_L
45.86	-17.15	10.41	0	Heschl_R
58.15	-21.78	6.8	0	Temporal_Sup_R
-39.88	15.14	-20.18	0	Temporal_Pole_Sup_L
48.25	14.75	-16.86	0	Temporal_Pole_Sup_R
-55.52	-33.8	-2.2	0	Temporal_Mid_L
57.47	-37.23	-1.47	0	Temporal_Mid_R
-36.32	14.59	-34.08	0	Temporal_Pole_Mid_L
-49.77	-28.05	-23.17	0	Temporal_Inf_L
53.69	-31.07	-22.32	0	Temporal_Inf_R
-36.07	-66.72	-28.93	0	Cerebelum_Crus1_L
37.46	-67.14	-29.55	0	Cerebelum_Crus1_R
-28.64	-73.26	-38.2	0	Cerebelum_Crus2_L
32.06	-69.02	-39.95	0	Cerebelum_Crus2_R
-8.8	-37.22	-18.58	0	Cerebelum_3_L
12.32	-34.47	-19.39	0	Cerebelum_3_R
-15	-43.49	-16.93	0	Cerebelum_4_5_L

17.2	-42.86	-18.15	0	Cerebelum_4_5_R
-23.24	-59.1	-22.13	0	Cerebelum_6_L
24.69	-58.32	-23.65	0	Cerebelum_6_R
-32.36	-59.82	-45.45	0	Cerebelum_7b_L
33.14	-63.18	-48.46	0	Cerebelum_7b_R
-25.75	-54.52	-47.68	0	Cerebelum_8_L
25.06	-56.34	-49.47	0	Cerebelum_8_R
-10.95	-48.95	-45.9	0	Cerebelum_9_L
9.46	-49.5	-46.33	0	Cerebelum_9_R
25.99	-33.84	-41.35	0	Cerebelum_10_R
1.38	-39.93	-11.4	0	Vermis_3
1.22	-52.36	-6.11	0	Vermis_4_5
1.14	-67.06	-15.12	0	Vermis_6
1.15	-71.93	-25.14	0	Vermis_7
1.15	-64.43	-34.08	0	Vermis_8
0.86	-54.87	-34.9	0	Vermis_9

CHAPTER IV

Paulo César Gonçalves Marques, Pedro Miguel Silva Moreira, Ricardo José da Silva Magalhães, Patrício Ricardo Soares Costa, Nadine Correia Santos, José Miguel Montenegro Soares, Nuno Jorge Carvalho Sousa

The functional connectome of cognitive reserve

Manuscript to be submitted

The Functional Connectome of Cognitive Reserve

Authors: P Marques[123], PS Moreira[123], R Magalhães[123], P Costa[123], NC Santos[123], JM Soares[123], N Sousa[123]*

[1]Life and Health Sciences Research Institute (ICVS), School of Health Sciences,

[2]ICVS/3B's - PT Government Associate Laboratory, Braga/Guimarães, Portugal.

[3]Clinical Academic Center – Braga, Braga, Portugal.

*Corresponding author: Nuno Sousa, Life and Health Sciences Research Institute (ICVS), School of Health Sciences, University of Minho, Campus Gualtar, 4710-057 Braga, Portugal. Email: njcsousa@ecsaude.uminho.pt. Phone: +351 253 604 806.

Abstract

The Cognitive Reserve (CR) theory postulates that inter-individual differences in cognitive performance can be explained by a more efficient use of the brain resources/networks of those that had a cognitively richer environment throughout life. Typical proxies of CR include education level and intelligence quotient (IQ), but CR actually represents the difference between the cognitive performance expected, taking into account the levels of brain pathology, and the actual performance. In the present study we use a validated latent variable model to estimate CR, from the residual variance in memory and general executive functioning, after accounting for the effects of both structural Magnetic Resonance Imaging (MRI) brain variables (i.e. brain reserve - BR) and demographic variables (sex and years of formal education). Functional connectivity (FC) networks and network topological properties were then explored for associations with the CR variable, using graph theory analysis. Results revealed that demographic characteristics, mainly accounted by education level, were positively associated with higher clustering coefficient, local efficiency and strength in parietal and occipital regions as well as greater global network transitivity. In contrast higher CR associated with a higher FC in a large network, higher global and local efficiency (right occipital) of neuronal networks and increased clustering coefficient of the left putamen. There were no associations between BR and FC or network properties. Altogether, these findings suggest that education level may facilitate the increased ability of the brain to form segregated functional groups of brain regions (clusters or modules), reinforcing the view that higher education level triggers more specialized use of neural processing. Additionally, this study demonstrated for the first time that CR is associated with a more efficient processing of information in the human functional brain network and reinforces the existence of fine balance between segregation and integration in the human brain.

1. Introduction

The concept of "cognitive reserve" (CR) emerged to explain why some aged individuals displaying neuropathologic hallmarks of Alzheimer's disease (AD) in post-mortem brain analysis, never presented any clinical manifestation of the disease in life (Katzman et al., 1988). Given that these subjects presented larger brain volumes than the average, the associated notion of "brain reserve" (BR) arose (Katzman, 1993); with brain size and neuronal

numbers constituting standard proxies for BR (Mortimer et al., 1982;Katzman et al., 1988;Mortimer et al., 2003;Satz et al., 2011). According to the model, brain size determines the amount of damage that can be sustained before it leads to some clinical expression. Specifically, it hypothesizes that bigger brains can sustain more damage, since enough neural substrate remains to support normal functioning. This is a passive model of reserve, since there is a fixed threshold below which functional impairment will be observed (Stern, 2009).

In contrast, several models have been proposed to explain how the brain can actively cope with brain damage through compensatory mechanisms (Stern, 2002;Barulli and Stern, 2013). Thus, the same amount of brain damage may lead to different clinical manifestations, even for individuals with the same BR. CR has been postulated as the reason why higher levels of intelligence (Alexander et al., 1997), education (Stern et al., 1992) and occupational status (Richards and Sacker, 2003), make individuals more capable of sustaining greater brain damage without clinical manifestations. Two distinct mechanisms were proposed to explain the underlying features of CR: neural reserve and neural compensation (Stern et al., 2005). Neural reserve is thought to be related to brain networks that are less susceptible to deterioration, due to their increased efficiency (Neubauer and Fink, 2009). These networks may be recruited when individuals are faced with brain pathology. On the other hand, the neural compensation mechanism relies on the hypothesis that individuals affected by some brain damage recruit networks not usually activated, as a means to compensate the impairments caused by damage.

Altogether, research provides support for both the abovementioned types of reserve. It was demonstrated that several anatomic measures such as brain volume, head circumference, synaptic count and dendritic branching are susceptible to alterations during the lifetime. In fact, it is thought that the underlying mechanisms conducting to these changes are also involved in the development of CR (Stern, 2006). Recently, a latent model was developed as a strategy to obtain a quantitative measure of CR (Reed et al., 2010). Briefly, the authors isolated the variance of episodic memory explained by (1) demographic characteristics and (2) brain pathology, measured by structural MRI. The residual variance (i.e. the variance not explained by any of the abovementioned variables) was defined as CR. The authors observed that this measure correlated with longitudinal cognitive decline and with the degree of brain atrophy attenuation, such that individuals with low CR had an augmented cognitive decline as a result

of brain atrophy. Since then, this model has been replicated and extended (Zahodne et al., 2013). Despite these findings, few researchers have explored the brain networks associated with CR using neuroimaging techniques (Stern et al., 2005;Stern et al., 2008) and, none have explored such properties when individuals are at rest (i.e. independently of a task-performance).

Herein, we used the abovementioned latent model in order to isolate CR and then to assess the brain correlates of CR, by exploring its relationship with FC networks and network topological properties, using graph theory measures (Bullmore and Sporns, 2009). With this strategy, we tested whether CR is associated with higher FC and/or with higher global efficiency of neuronal networks.

2. Methods

2.1 Ethics Statement

The present study was conducted in accordance with the principles expressed in the Declaration of Helsinki and was approved by the local and national ethics committees. The study goals and tests were explained to the participants and all gave informed written consent.

2.2 Participants

The participants included in the present study are part of the sample recruited for the SWITCHBOX Consortium project (www.switchbox-online.eu/). Details regarding participants' selection, neurocognitive assessment and inclusion/exclusion criteria were previously described (Marques et al., 2015). Briefly, 120 subjects were pseudo-randomly recruited from a larger sample, representative of the general Portuguese older population in terms of age, gender, and education [n = 1051, after inclusion/exclusion criteria; subjects were randomly selected from the Guimarães and Vizela local area health authority registries (Costa et al., 2013;Santos et al., 2013;Santos et al., 2014)]. The 120 subjects were selected in order to provide cognitive profiles of overall good cognitive performance (n=60) and overall poor performance (n=60) in a battery of neuropsychological/neurocognitive tests (Marques et al.,

2015). Primary exclusion criteria included inability to understand the informed consent, participant choice to withdraw from the study, incapacity and/or inability to attend the MRI session, dementia and/or diagnosed neuropsychiatric and/or neurodegenerative disorder (medical records). Adjusted thresholds for cognitive impairment were calculated depending on factors such as age and/or education (Grigoletto et al., 1999;Busch and Chapin, 2008). Thus, the applied Mini Mental State Examination (MMSE) test score thresholds were the following: MMSE score < 17 if individual with ≤ 4 years of formal school education and/or ≥ 72 years of age, and MMSE score < 23 otherwise [follows the MMSE validation study for the Portuguese population (Guerreiro et al., 1994)].

From the 120 subjects originally recruited for the main project, nine refused to undergo the MRI acquisition protocol, four had brain lesions/pathology detected at the time of the acquisition and seven presented excessive motion/artifacts, leaving a final sample of 100 older adults that were considered in the present study.

2.3 Magnetic Resonance Imaging Acquisition

The imaging session was performed at Hospital de Braga (Braga, Portugal) on a clinical approved Siemens Magnetom Avanto 1.5 T MRI scanner (Siemens Medical Solutions, Erlangen, Germany) and using a 12-channel receive-only head-coil. The imaging protocol included several different acquisitions. For the present study, only one structural and one rs-fMRI acquisition were considered. For the structural acquisition, a T1-weighted magnetization prepared rapid gradient echo (MPRAGE) sequence with the following parameters was used: 176 sagittal slices, TR/TE= 2730/ 3.48 ms, FA = 7°, slice thickness = 1 mm, slice gap = 0 mm, voxel size= 1x1 mm2, FoV = 256 mm. For the rs-fMRI acquisition, a blood oxygen level dependent (BOLD) sensitive echo-planar imaging (EPI) sequence was used: 30 axial slices, TR/TE = 2000/30 ms, FA = 90°, slice thickness = 3.5, slice gap = 0.48 mm, voxel size = 3.5 x 3.5 mm2, FoV = 1344 mm and 180 volumes. During the resting state scan, the subjects were instructed to remain still, awake, with their eyes closed, as motionless as possible and trying to think of nothing in particular. No participant reported or was noted to fall asleep during the acquisition.

2.4 Structural Segmentation

The structural scans of each subject were segmented with in FreeSurfer toolkit version 5.1 (http://surfer.nmr.mgh.harvard.edu), which implements a semi-automated segmentation workflow. FreeSurfer enables the segmentation of both GM and WM as well as subcortical segmentation. The stages of processing implemented in this pipeline are fully described elsewhere (Fischl et al., 2002;Fischl et al., 2004;Desikan et al., 2006;Destrieux et al., 2010). Validation against manual segmentations has also been described (Fischl et al., 2002) and its results are considered robust across sessions, scanner platforms, updates, and field strengths (Jovicich et al., 2009).

For the present study, only the intracranial volume (ICV), total GM volume (GMV) and white matter hypointensities volume (i.e. WMSA) were considered. This T1-based WMSA volume estimate has been successfully used as a measure of WM lesion volume (Salat et al., 2012), and showed sensitivity in measuring WM lesions in Alzheimer's disease (Salat et al., 2012), as well as to correlate with estimates based on FLAIR acquisitions and to correlate better with clinical symptoms in MS (Bagnato et al., 2010).

2.5 Specification of the Structural Equation Model

A structural equation model was defined in order to estimate the variance of the performance in cognitive dimensions explained by CR. For that, three main latent variables were created: one expressing the variance of cognitive performance uniquely dependent of demographic characteristics (Demographic, DEM); one uniquely associated with MRI variables (Brain Reserve, BR); and, one accounting for the variance not attributed to the other two dimensions (Cognitive Reserve, CR). This model constitutes a replication of a previously validated and replicated model (Reed et al., 2010).

Nevertheless, some modifications were applied to the model proposed by Reed and colleagues in order to address the goals of the current study. Specifically, here, the interest was to study CR as a function of the variance, not only from episodic memory but rather from cognition in

general. In a previous study, using the larger cohort from which the present sample was obtained, a factor structure comprising memory (MEM) and general executive (GENEXEC) functions, obtained from a large a pool of neurocognitive variables, was validated (Santos et al., 2015). Briefly, the MEM factor was composed of the long-term storage (LTS), consistent long-term retrieval (CLTR) and delayed-recall (DR) variables evaluated with the selective reminding test (SRT); while, the GENEXEC factor was composed of the variables Digits Forward (DF), Digits Backward (DB), Stroop words (SW), Stroop colors (SC), Stroop words/colors (SWC), Controlled Oral Word Association Test (COWAT-FAS; admissible words) and MMSE. For further details regarding the exploratory and confirmatory factor analysis please consult (Santos et al., 2015). Another difference to the model proposed by Reed and colleagues concerns the exclusion in the present study of the hippocampal volume as a measure of BR capacity. Indeed, in the present study we did not assess individuals with any diagnosed temporal dementias; furthermore, despite being relevant for memory processing, hippocampal volume does not account for executive functioning, which was also relevant for the purpose of the current study.

GMV was regressed on ICV and a latent variable was specified in reflecting gray matter component (GMC), accounting for ICV. WMSA were included as an observed variable (log-transformed in order to reduce skewness) and was modeled through a latent variable (WMC – White Matter Component). GMC and WMC were regressed on the BR latent variable. DEM was regressed on sex (female as reference) and years of formal education. In order to account for the relevance of each memory and executive functioning component for each dimension, MEM and GENEXEC were defined as latent variables.

In order to achieve the model identification, variances for cognitive dimensions (MEM and GENEXEC) and MRI variables (GMC and WMC) were fixed to account for measurement error. Furthermore, variances for main latent variables were constrained, by fixing residual variances of BR and DEM to 0, and CR to 1. Using this strategy, main latent variables (BR, DEM and CR) are assumed to have an independent contribution to cognitive dimensions (MEM and GENEXEC). Thus, with this model, we were able to estimate the amount of variance attributed to BR, DEM and CR for each subject. In order to achieve this, multiple imputation was performed with Bayesian estimation, resulting in ten complete databases. Values for the

variables of interest were then obtained for each subject, by creating a new database, in which the average of imputed databases for each variable was calculated.

The analytical model is represented in Figure 1. Observed variables are expressed in rectangles and circles represent the latent variables. The specification of the model was conducted using IBM AMOS v22.

2.6 Rs-fMRI Data Preprocessing

RS-fMRI data preprocessing was performed using FMRIB Software Library (FSL v5.07; http://fsl.fmrib.ox.ac.uk/fsl/) tools. The first five volumes of the rs-fMRI acquisition were removed in order to exclude possible magnetic field inhomogeneities at the beginning of the acquisition. The remaining data was corrected for slice timing followed by head motion correction. In order to reduce potential contamination of motion on functional connectivity, motion scrubbing (Power et al., 2012) was also performed in order to identify and further exclude time-points where head motion could be critical. Seven subjects were excluded for having more than 10 motion-contaminated time-points. Each subject functional dataset was then normalized to Montreal Neurological Institute (MNI) standard space through an indirect procedure that included: (i) skull stripping of the mean image of the functional acquisition; ii) rigid-body registration of the mean functional image to the skull stripped structural scan; iii) affine registration of the structural scan to the MNI T1 template; iv) non-linear registration of the structural scan to the MNI T1 template using the affine transformation previously estimated as the initial alignment; v) non-linear transformation of the functional acquisition to MNI standard space trough the sequential application of the rigid-body transformation and the non-linear warp followed by resampling to 2 mm isotropic voxel size. Linear regression of motion parameters, mean WM and cerebrospinal fluid (CSF) signal and motion outliers was performed and the residuals of the regression were band-pass temporal filtered (0.01-0.08Hz) and used for the subsequent analysis.

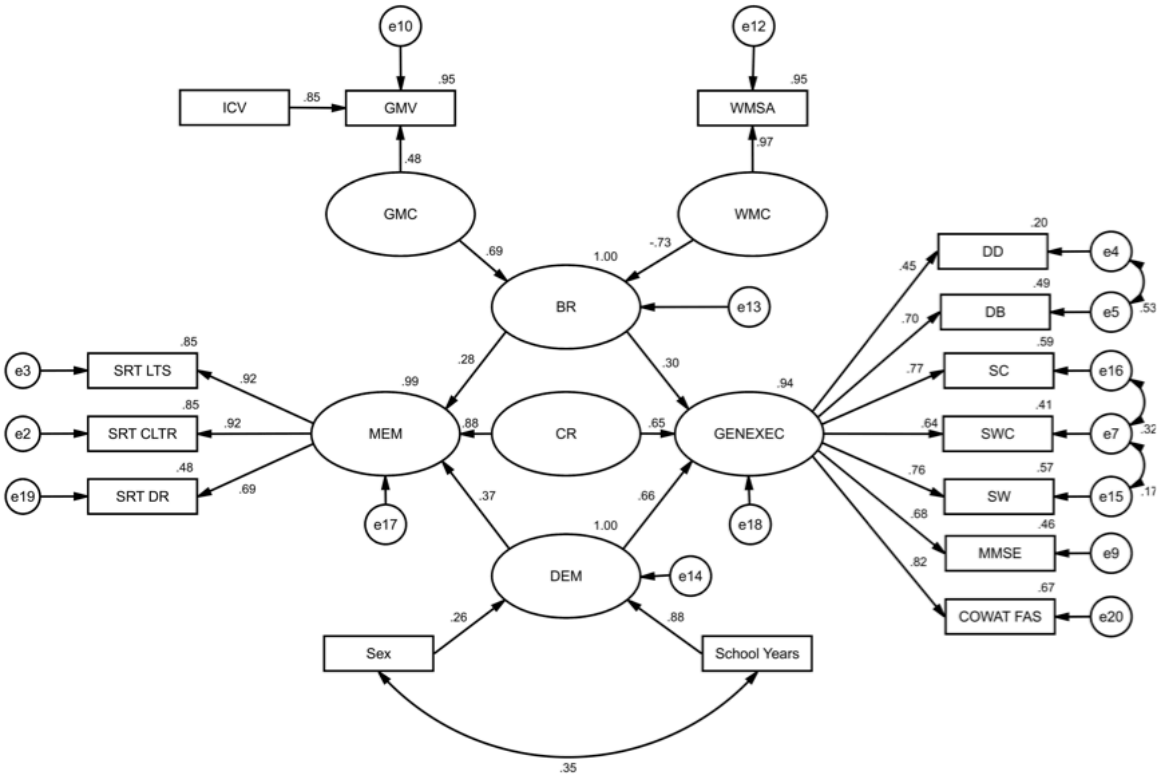


Figure 1. Structural equation model used in order to decompose memory (MEM) and general executive functioning (GENEXEC) factors into independent variables of demographic characteristics influence (DEM), brain reserve capacity measures (BR) and cognitive reserve (CR). DEM was mainly accounted for school years (r = 0.88) but also by sex (r = 0.26). Sex and school years were also correlated (r = 0.35). Intracranial Volume (ICV) correlated strongly (r = 0.85) with gray matter volume (GMV). As expected, the latent gray matter component (GMC) was significantly modeled by GMV (r = 0.48) and the latent white matter component (WMC) was almost entirely (r = 0.97) modeled by the volume of white matter signal abnormalities (WMSA). GMC positively accounted for BR (r = 0.69) and WMC negatively accounted for BR (r = -0.73) due to the inverse relationship between white matter lesioning and BR. BR was the greatest predictor of GENEXEC (r = 0.66), followed by CR (r = 0.65) and then BR (r = 0.30). MEM was mostly predicted by CR (r = 0.88), then by DEM (r = 0.37) and BR (r = 0.28).

2.7 Network Construction

The network nodes were defined as the Anatomical Automatic Labeling (AAL) atlas regions. The mean time-series of the 116 cortical, subcortical and cerebellar regions were extracted and correlations between each possible pair of regions were calculated. This originated a symmetric adjacency matrix R where each entry r_{ij} represents the Pearson correlation coefficient between the time series of region i and j. These matrices were then transformed to Z-score matrices by the application of Fisher's r-to-Z transform to the correlation coefficients. In the present study, only weighted matrices were considered. For the analysis of local and global network metrics the matrices were thresholded at different sparsity thresholds s (from 0.025 to 0.45 in steps of 0.025) and thus the metrics were calculated for the networks composed by different proportions of the strongest edges.

2.8 Network-Based Statistics Analyses

In order to assess if BR and CR measures were associated with functional connectivity at the edge level (i.e. at each individual connection) a General Linear Model (GLM) was applied with each Z-transformed correlation coefficient as the dependent variable and the linear and quadratic effects of age as well as the DEM, BR and CR latent measures as independent variables. Sex and school years were not included in the model since they presented high collinearity with the DM measure. Assessing these effects at the edge level poses a multiple comparisons problem since the networks obtained as described in the previous sections of the manuscript encompassed a total of 116*115/2 = 6670 edges. In order to increase the statistical power of the analysis, the NBS procedure was used (Zalesky et al., 2010). This approach is similar to the cluster-based thresholding approach used in voxel-wise analyses of fMRI data. Instead of considering the null hypothesis at the single edge level, NBS evaluates the null hypothesis at the level of interconnected edges (i.e. sub-networks) surviving a predefined primary threshold. The null hypothesis assumes that a sub-network with similar number of edges, surpassing the primary threshold, occurs by chance. The authors of this procedure recommend the use of different primary thresholds in order to capture different effects. In the present study, three different primary thresholds were used ($p<0.01$, $p<0.005$, $p<0.001$) in order to capture less pronounced but more extent effects (less stringent primary

threshold – $p < 0.01$) as well as localized and pronounced effects (most stringent threshold – $p < 0.001$). 5000 permutations were performed and networks were considered significant at a corrected level of $p < 0.05$ family-wise error (FWE) corrected. BrainNet Viewer (http://www.nitrc.org/projects/bnv/) was used for visualization purposes.

2.9 Graph Theory Analysis

Graph theoretic analyses were performed at the node and the global network metrics level. The metrics were computed with weighted undirected networks, using the Brain Connectivity Toolbox (BCT, http://www.brain-connectivity-toolbox.net) (Rubinov and Sporns, 2010). Some studies involving graph theoretic measures of FC networks discard edges displaying negative FC since such measures cannot be calculated in the presence of negative weights (Achard and Bullmore, 2007;van den Heuvel et al., 2008). In the present study we decided to use absolute values of the network weights for the computation of graph theoretic measures; while we recognize that negative FC might not reflect the same level/kind of meaning as positive FC, we consider this to be less critical than simply neglecting the effect of such edges in network topology.

At the node level, four different metrics were calculated for each region: 1) local efficiency, which is defined as the average of the inverse shortest path length in the neighborhood of the node and, in a weighted network, distinguishes the influence of different paths based on the connection weights of the corresponding neighbors; 2) betweenness centrality that corresponds to the proportion of shortest paths that pass through the node; 3) strength that is the sum of weights of the edges connected to each node; and, 4) clustering coefficient, defined as the average intensity of triangles around a node. At the global network level the following measures were calculated: i) global efficiency, similar to the local efficiency but for the entire network and ii) transitivity which represents a normalized version of the mean of the clustering coefficients of all nodes in the network.

Statistical analysis of graph theoretic metrics computed for different sparsity thresholds were performed with the integrated measures (Tian et al., 2011) of such metrics across the range of sparsities. This methodology has the advantage of reducing the complexity of the analyses and

the number of comparisons. The analyses were performed with a similar GLM to the one described for the NBS analyses, with the dependent variable being replaced by the global or local metrics. For the local measures, results were considered significant at $p < 0.05$ corrected for multiple comparisons using the False Discovery Rate (FDR) criterion across all metrics and nodes. Global measures were considered significant at $p < 0.05$ uncorrected.

3. Results

3.1 Sample characteristics

Table I presents the overall demographic and neuropsychological/cognitive characteristics of the participants.

Table I. Demographic and cognitive characterization of the sample assessed in the study.

	Mean (SD)	**Range**
Demographic measures		
Gender (0=Male)	0.49 (0.5)	[0; 1]
Age	65.12 (8.2)	[51; 82]
School Years	5.47 (3.9)	[0; 17]
MRI measures		
WMSA (log)	3.44 (0.3)	[2.98; 4.37]
GMV	5.62E+05 (4.98E+04)	[4.52E+05; 6.88E+05]
ICV	1.47E+06 (1.58E+05)	[1.13E+06; 1.90E+06]
Cognitive Measures		
SRT LTS	27.33 (13.58)	[0; 58]
SRT CLTR	16.38 (12.73)	[0; 50]
SRT DR	5.25 (3.2)	[0; 12]
DD	7.73 (2.32)	[3; 16]
DB	4.45 (2.66)	[0; 14]
SW	63.48 (21.72)	[0; 103]
SC	48.14 (15.79)	[0; 81]
SWC	28.95 (12.91)	[0; 60]
FAS	18.17 (11.78)	[0; 49]
MMSE	26.63 (3.44)	[17; 30]

3.2 Latent Variable Model

According to the modification indices obtained for the basal model, the covariance between gender and ICV was specified in order to improve model fit. Afterwards, although a significant chi-square statistic was obtained ($\chi^2(83)=138.889$, $p<.001$), based on the remaining fit indices, the specified model was assumed to have a satisfactory fit (CFI=.946 | TLI=.932 | RMSEA=.080). The variance of both cognitive dimensions was significantly predicted by the main latent variables. Of notice, it is relevant to observe that CR revealed to be the most relevant predictor of both cognitive dimensions (MEM: B=.880, p<.001; GENEXEC: B=.658, p<.001).

3.3 Effects of the Cognitive Reserve Latent Variable

Regarding the CR variable, a positive association between CR and FC in a cortical network was found (Figure 2.a-b). This association was significant for the less stringent and intermediate primary thresholds ($p < 0.01$ and $p < 0.005$).

Additionally, at the local metrics level, CR was positively associated with local efficiency in the right occipital middle and occipital inferior regions (Figure 2.d) and with the clustering coefficient of left putamen (Figure 2.f). No significant associations between strength or betweenness centrality and CR were found (Figure 2.e and Figure 2.g). At the global network level, CR was positively associated with global efficiency ($t = 2.93$;$p = 0.004$) (Figure 3.b), but not transitivity ($t = 1.91$; $p = 0.056$).

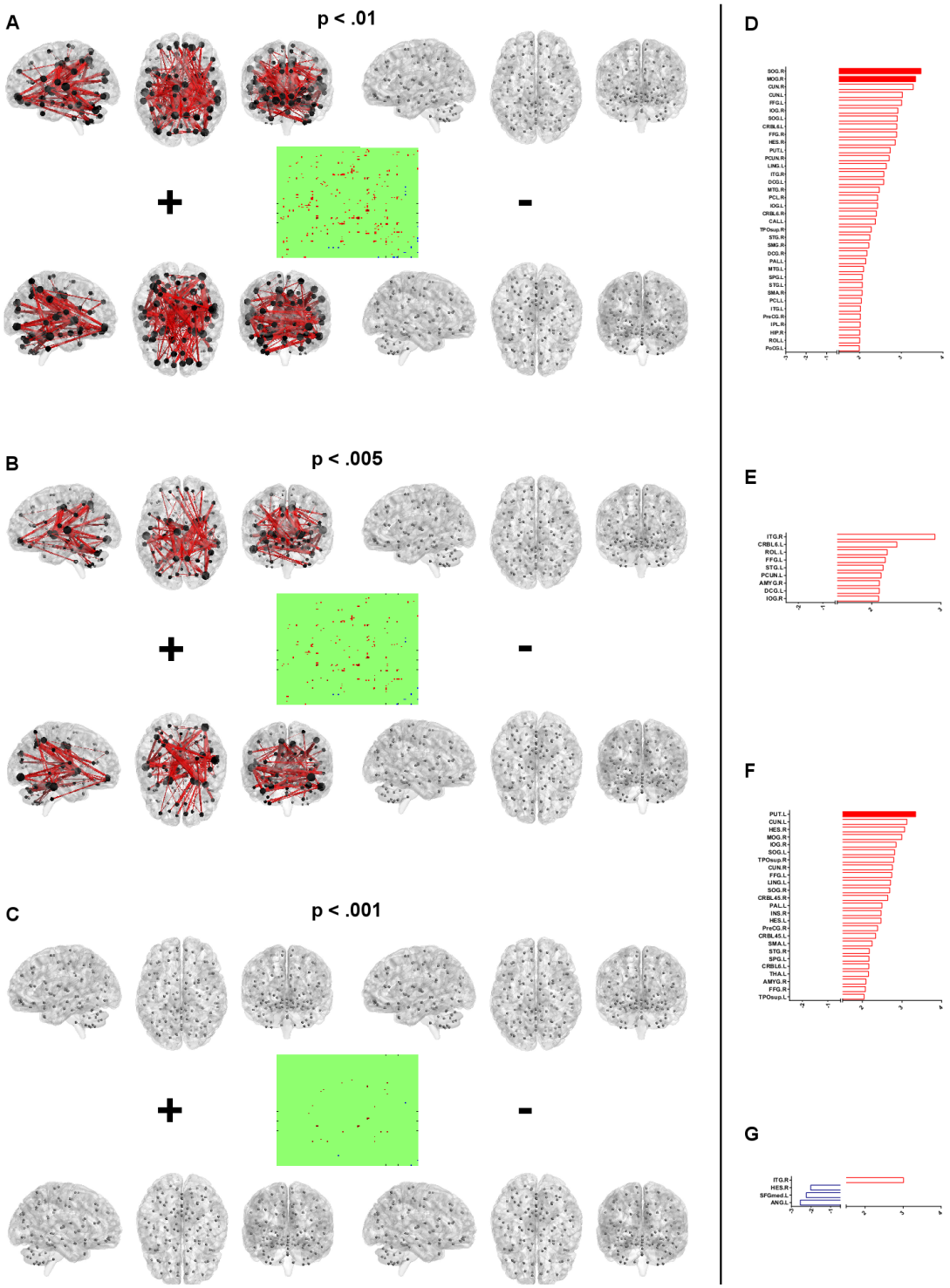


Figure 2. Associations between CR and FC networks using primary thresholds of $p < 0.01$ (a), $p < 0.005$ (b) and $p < 0.001$ (c). Adjacency matrices after the application of the primary thresholds are presented in the middle of each panel. Edges from the networks revealing positive association are presented in red and from negative associations are presented in blue. Associations between CR and local efficiency (d), strength (e), clustering (f) and betweenness centrality (g). Statistically significant associations ($p < 0.05$, FDR corrected) are presented in filled bars and associations surviving an uncorrected threshold of $p < 0.05$ are reported for completeness using unfilled bars.

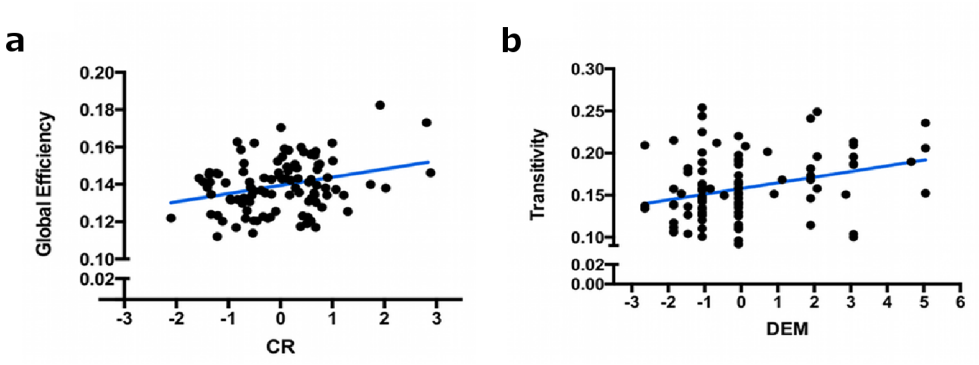


Figure 3. Scatter plots highlighting significant positive associations between CR and network global efficiency (a) and between DEM (b) and network transitivity.

3.4 Effects of the Demographic Latent Variable

Regarding the NBS results, the demographic latent variable (DEM) was positively associated with FC in a large network encompassing connections between several cortical regions. These results were significant for all primary thresholds used (Figure 4.a-c). Additionally, using the intermediate and most strict primary thresholds (i.e. $p < 0.005$ and $p < 0.001$), a network mainly involving connections between the cerebellar vermis and cortical regions evidenced a negative association with the DEM variable (Figure 4.b-c).

Regarding the local network metrics, the DEM variable revealed a significant positive association with local efficiency of the right supplementary motor area, left cingulum middle, bilateral lingual, left occipital middle, left occipital inferior, bilateral fusiform, left precuneus, right paracentral, left cerebellum 4 and 5 and bilateral cerebellum 6 (Figure 4.d). Additionally, DEM was also positively associated with local strength in the right rolandic operculum, left occipital inferior and bilateral cuneus, lingual and fusiform gyrus (Figure 4.e). Positive associations between DEM and local clustering were found in the left calcarine, right Heschl area, left cerebellum 4 and 5, cerebellar vermis 10 and bilateral lingual, occipital inferior, fusiform, precuneus and cerebellum 6 (Figure 4.f). No significant association was found between the DEM variable with betweenness centrality (Figure 4.g).

At the global network level DEM evidenced a positive association with transitivity ($t = 1.64$; $p = 0.104$) but not with global efficiency ($t = 2.73$; $p = 0.008$) (Figure 3.a).

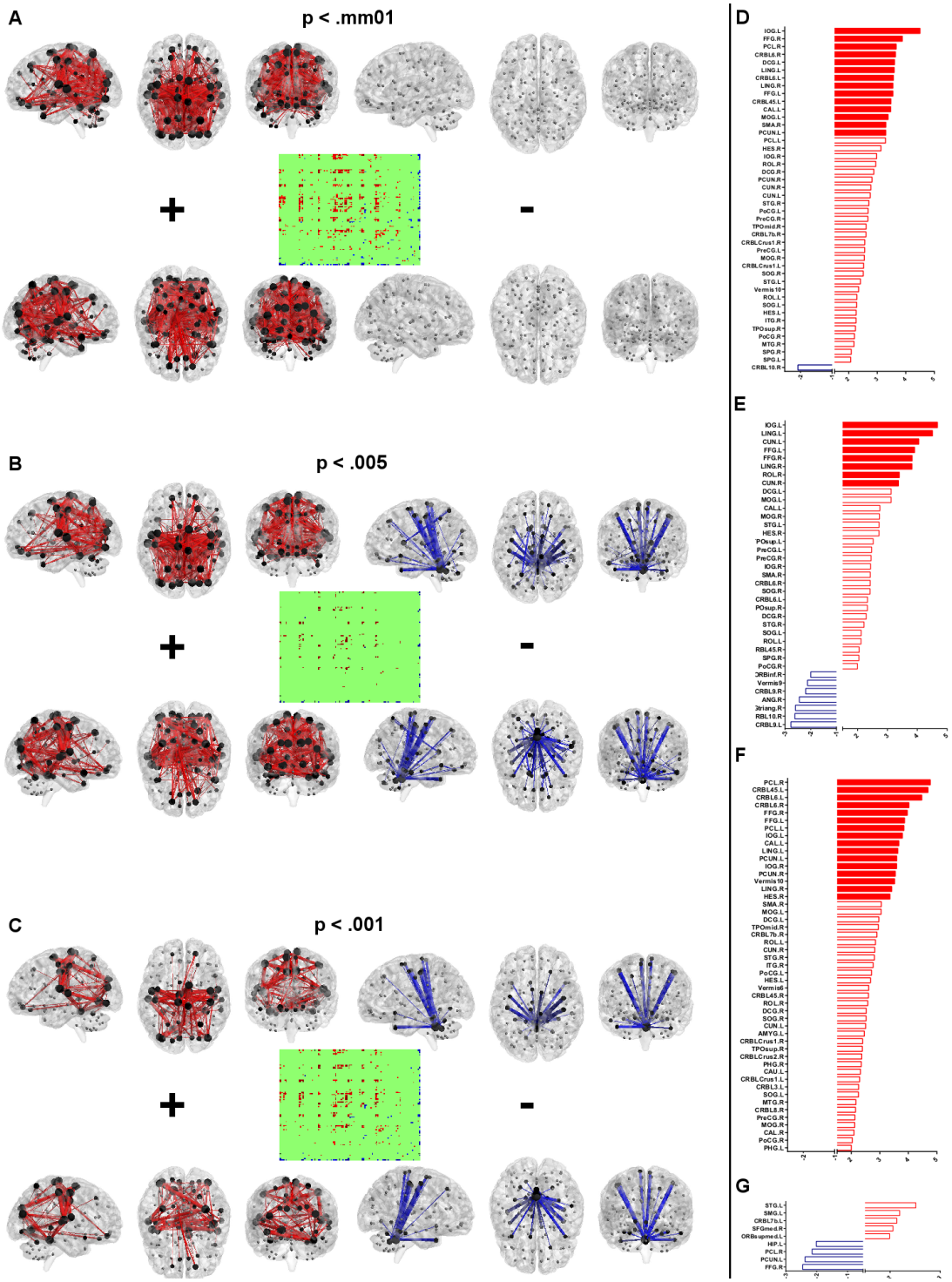


Figure 4. Associations between DEM and FC networks using primary thresholds of $p < 0.01$ (a), $p < 0.005$ (b) and $p < 0.001$ (c). Adjacency matrices after the application of the primary thresholds are presented in the middle of each panel. Edges from the networks revealing positive association are presented in red and edges from negative associations are presented in blue. Associations between DEM and local efficiency (d), strength (e), clustering (f) and betweenness centrality (g). Statistically significant associations ($p < 0.05$, FDR corrected) are presented in filled bars and associations surviving an uncorrected threshold of $p < 0.05$ are reported for completeness using unfilled bars.

3.5 Effects of the Brain Reserve Latent Variable

No significant associations between the BR variable and FC networks (Figure 5.a-c), local network metrics (Figure 5.d-g) or global network metrics were found.

4. Discussion

In the present study we investigated how CR impacts functional connectivity networks, independently of education level. For this purpose CR was quantified as the residual variance in cognitive factors that is not accounted for by the DEM variables (sex and years of formal education) and by the BR capacity variables (brain size and WM lesioning). This type of model was shown to be in line with the CR theory (Reed et al., 2010) and has been, thereafter, validated and extended on (Zahodne et al., 2013). The replication of the latent variable model revealed to be valid for the present study, as proved by the satisfactory fit indices obtained for the model. With this, it was possible to dissect and quantify the effects of CR based on the variance of cognitive functioning not explained either from brain structural pathology variables or by the demographic characteristics. Ultimately, this strategy enabled us to study how CR is manifested at the FC level at rest.

Regarding the demographics variable, the present results closely mimic those obtained in a previous study from our group in which the effects of years of formal education in FC networks were investigated (Marques et al, accepted for publication). Briefly, it was shown that education level was associated with higher FC in a large cortical network and with decreased (i.e. more negative) FC between the cerebellum and cerebrum. This was interpreted as more efficient brain network in individuals with higher number of years of education and a more effective differential involvement of the cerebrum and cerebellum. This finding is not surprising since the DEM variable is mainly accounted for by the number of years of formal education. However, in the present study it is further demonstrated that this demographic variable DEM was also associated with particular topological characteristics of the brain FC network. At the local metric level, the DEM variable was associated with higher local efficiency, nodal strength and clustering coefficient in several brain regions spanning most of the occipital and parietal lobes. Associations in some sensorimotor regions and the cerebellum were also found. This

suggests that these regions are more tightly connected between themselves and more segregated from the rest of the brain, facilitating the communication within these networks and revealing the positive effects, mainly of years of formal education, in posterior brain regions. Additionally, at the global network level, DEM was associated with the network transitivity but not global efficiency. Transitivity is a well-known measure of functional segregation (Watts and Strogatz, 1998;Rubinov and Sporns, 2010). This suggests that demographic variables, especially education level, are associated with the increased ability of the brain to form segregated groups of brain regions (clusters or modules), reinforcing the view that higher education level triggers more specialized use of neural processing.

Furthermore, the present results provide evidence that CR impacts on the brain FC network architecture, even when education level is accounted for. As expected, CR was associated with a large and sparse network displaying higher FC in individuals with higher CR. Similarly to the associations found for education level, this is likely to reflect the positive effect in brain functioning facilitating communication and integration. Higher CR was also associated with higher local efficiency of the right superior and middle occipital regions. This suggests that connections involving these regions display higher FC in subjects with higher CR, highlighting their importance in creating tighter functional connections within the brain network. Additionally, we found that the left putamen presented higher clustering coefficient in individuals with higher CR, revealing the importance of the putamen in the formation of clusters of interconnected regions. The putamen is known for playing an important role in learning and decision-making and has been associated to habitual behaviors learned through repetitive training (Soares et al., 2012;Wunderlich et al., 2012). Thus, our results bring evidence that CR might be associated with an increased involvement of the putamen in the functional brain network, mediating other connections within the network that might be associated with the “better” learning and decision-making performance commonly associated with higher CR as a result of extensively trained actions/behaviors.

Of particular interest is the association between CR and global efficiency. FC networks have weaker connections between modules, when compared to structural networks, and thus global efficiency values are typically low (Rubinov and Sporns, 2010). Despite this, here we show that individuals with higher CR displayed higher global efficiency values compared to those with lower CR. Global efficiency is a measure of functional integration, where higher values mean

that shorter and more efficient paths are available in order to connect every possible pair of nodes (Rubinov and Sporns, 2010). This means that individuals with higher cognitive performance, controlling for BR and demographic differences, present a more tightly connected network likely to reflect an increase capacity for parallel information transfer and integrated processing (Bullmore and Sporns, 2012). This is closely related to the concept of a more efficient use of the brain's resources, one of the hallmarks of CR (Stern, 2002). Previous studies have found similar associations in structural (Li et al., 2009) and functional (van den Heuvel et al., 2009) brain networks with IQ, a proxy of CR.

The present study presents some limitations. Micro-structural measures of white matter integrity such as the ones derived from Diffusion Tensor Imaging (DTI) could be useful for quantifying BR capacity as it might add important information on brain structure. Additionally, since the proposed latent model has the potential to provide longitudinal trajectories of CR, longitudinal studies should be carried out in order to investigate if CR can be a moderator of age related cognitive decline in older individuals as proposed by others (Tucker-Drob et al., 2009;Bozzali et al., 2015). Finally, it would be of interest to consider other demographic characteristics (such as primary occupation) and/or cohorts characterized by high education levels to have a broader picture of the impact of FC in brain functional connectivity.

In conclusion, the present study reveals that CR is associated with increased FC in a large network and with a better organization of the network topology. It is also shown that demographic characteristics, mainly accounted for by years of formal education, are also associated with brain network reorganizations. More importantly we brought evidence that while years of education are likely to be associated with a higher specialization of the brain network, CR is associated with higher network efficiency.

5. References

Achard, S., and Bullmore, E. (2007). Efficiency and cost of economical brain functional networks. *PLoS Comput Biol* 3**,** e17.

Alexander, G.E., Furey, M.L., Grady, C.L., Pietrini, P., Brady, D.R., Mentis, M.J., and Schapiro,

M.B. (1997). Association of premorbid intellectual function with cerebral metabolism in Alzheimer's disease: implications for the cognitive reserve hypothesis. *Am J Psychiatry* 154**,** 165-172.

Bagnato, F., Salman, Z., Kane, R., Auh, S., Cantor, F.K., Ehrmantraut, M., Gallo, A., Ikonomidou, V.N., Ohayon, J., Pellicano, C., Stern, S.K., and Mcfarland, H.F. (2010). T1 cortical hypointensities and their association with cognitive disability in multiple sclerosis. *Mult Scler* 16**,** 1203-1212.

Barulli, D., and Stern, Y. (2013). Efficiency, capacity, compensation, maintenance, plasticity: emerging concepts in cognitive reserve. *Trends in Cognitive Sciences* 17**,** 502-509.

Bozzali, M., Dowling, C., Serra, L., Spano, B., Torso, M., Marra, C., Castelli, D., Dowell, N.G., Koch, G., Caltagirone, C., and Cercignani, M. (2015). The impact of cognitive reserve on brain functional connectivity in Alzheimer's disease. *J Alzheimers Dis* 44**,** 243-250.

Bullmore, E., and Sporns, O. (2009). Complex brain networks: graph theoretical analysis of structural and functional systems. *Nat Rev Neurosci* 10**,** 186-198.

Bullmore, E.T., and Sporns, O. (2012). The economy of brain network organization. *Nature Reviews Neuroscience* 13**,** 336-349.

Busch, R.M., and Chapin, J.S. (2008). Review of normative data for common screening measures used to evaluate cognitive functioning in elderly individuals. *Clin Neuropsychol* 22**,** 620-650.

Costa, P.S., Santos, N.C., Cunha, P., Palha, J.A., and Sousa, N. (2013). The use of bayesian latent class cluster models to classify patterns of cognitive performance in healthy ageing. *PLoS One* 8**,** e71940.

Desikan, R.S., Segonne, F., Fischl, B., Quinn, B.T., Dickerson, B.C., Blacker, D., Buckner, R.L., Dale, A.M., Maguire, R.P., Hyman, B.T., Albert, M.S., and Killiany, R.J. (2006). An automated labeling system for subdividing the human cerebral cortex on MRI scans into gyral based regions of interest. *Neuroimage* 31**,** 968-980.

Destrieux, C., Fischl, B., Dale, A., and Halgren, E. (2010). Automatic parcel- lation of human

cortical gyri and sulci using standard anatomical nomenclature. *Neuroimage*.

Fischl, B., Salat, D.H., Busa, E., Albert, M., Dieterich, M., Haselgrove, C., Van Der Kouwe, A., Killiany, R., Kennedy, D., Klaveness, S., Montillo, A., Makris, N., Rosen, B., and Dale, A.M. (2002). Whole brain segmentation: automated labeling of neuroanatomical structures in the human brain. *Neuron* 33**,** 341-355.

Fischl, B., Salat, D.H., Van Der Kouwe, A.J., Makris, N., Segonne, F., Quinn, B.T., and Dale, A.M. (2004). Sequence-independent segmentation of magnetic resonance images. *Neuroimage* 23 Suppl 1**,** S69-84.

Grigoletto, F., Zappala, G., Anderson, D.W., and Lebowitz, B.D. (1999). Norms for the Mini-Mental State Examination in a healthy population. *Neurology* 53**,** 315-320.

Guerreiro, M., Silva, A.P., Botelho, M.A., Leitão, O., Castro-Caldas, A., and Garcia, C. (1994). Adaptação à população portuguesa da tradução do Mini Mental State Examination (MMSE). *Revista Portuguesa de Neurologia* 1**,** 9-10.

Jovicich, J., Czanner, S., Han, X., Salat, D., Van Der Kouwe, A., Quinn, B., Pacheco, J., Albert, M., Killiany, R., Blacker, D., Maguire, P., Rosas, D., Makris, N., Gollub, R., Dale, A., Dickerson, B.C., and Fischl, B. (2009). MRI-derived measurements of human subcortical, ventricular and intracranial brain volumes: Reliability effects of scan sessions, acquisition sequences, data analyses, scanner upgrade, scanner vendors and field strengths. *NeuroImage* 46**,** 177-192.

Katzman, R. (1993). Education and the prevalence of dementia and Alzheimer's disease. *Neurology*.

Katzman, R., Terry, R., Deteresa, R., Brown, T., Davies, P., Fuld, P., Renbing, X., and Peck, A. (1988). Clinical, pathological, and neurochemical changes in dementia: a subgroup with preserved mental status and numerous neocortical plaques. *Ann Neurol* 23**,** 138-144.

Li, Y.H., Liu, Y., Li, J., Qin, W., Li, K.C., Yu, C.S., and Jiang, T.Z. (2009). Brain Anatomical Network and Intelligence. *Plos Computational Biology* 5.

Marques, P.C., Soares, J.M., Magalhaes, R.J., Santos, N.C., and Sousa, N.J. (2015). Macro- and micro-structural white matter differences correlate with cognitive performance in healthy aging. *Brain Imaging Behav*.

Marques, P.C., Soares, J.M., Magalhaes, R.J., Santos, N.C., and Sousa, N.J. (accepted for publication). The bounds of education in the human brain connectome *Scientific Reports*.

Mortimer, J.A., Schuman, L.M., and Kuller, L.H. (1982). The Epidemiology of Dementia. *Journal of Neuropathology & Experimental Neurology* 41**,** 105.

Mortimer, J.A., Snowdon, D.A., and Markesbery, W.R. (2003). Head circumference, education and risk of dementia: findings from the Nun Study. *Journal of Clinical and Experimental Neuropsychology* 25**,** 671-679.

Neubauer, A.C., and Fink, A. (2009). Intelligence and neural efficiency. *Neuroscience & Biobehavioral Reviews* 33**,** 1004-1023.

Power, J.D., Barnes, K.A., Snyder, A.Z., Schlaggar, B.L., and Petersen, S.E. (2012). Spurious but systematic correlations in functional connectivity MRI networks arise from subject motion. *Neuroimage* 59**,** 2142-2154.

Reed, B.R., Mungas, D., Farias, S.T., Harvey, D., Beckett, L., Widaman, K., Hinton, L., and Decarli, C. (2010). Measuring cognitive reserve based on the decomposition of episodic memory variance. *Brain* 133**,** 2196-2209.

Richards, M., and Sacker, A. (2003). Lifetime antecedents of cognitive reserve. *J Clin Exp Neuropsychol* 25**,** 614-624.

Rubinov, M., and Sporns, O. (2010). Complex network measures of brain connectivity: uses and interpretations. *Neuroimage* 52**,** 1059-1069.

Salat, D.H., Williams, V.J., Leritz, E.C., Schnyer, D.M., Rudolph, J.L., Lipsitz, L.A., Mcglinchey, R.E., and Milberg, W.P. (2012). Inter-individual variation in blood pressure is associated with regional white matter integrity in generally healthy older adults. *Neuroimage* 59**,** 181-192.

Santos, N.C., Costa, P.S., Amorim, L., Moreira, P.S., Cunha, P., Cotter, J., and Sousa, N. (2015). Exploring the factor structure of neurocognitive measures in older individuals. *PLoS One* 10**,** e0124229.

Santos, N.C., Costa, P.S., Cunha, P., Cotter, J., Sampaio, A., Zihl, J., Almeida, O.F., Cerqueira, J.J., Palha, J.A., and Sousa, N. (2013). Mood is a key determinant of cognitive performance in community-dwelling older adults: a cross-sectional analysis. *Age (Dordr)* 35**,** 1983-1993.

Santos, N.C., Costa, P.S., Cunha, P., Portugal-Nunes, C., Amorim, L., Cotter, J., Cerqueira, J.J., Palha, J.A., and Sousa, N. (2014). Clinical, physical and lifestyle indicators and relationship with cognition and mood in aging: a cross-sectional analysis of distinct educational groups. *Frontiers in Aging Neuroscience* 6.

Satz, P., Cole, M.A., Hardy, D.J., and Rassovsky, Y. (2011). Brain and cognitive reserve: Mediator(s) and construct validity, a critique. *Journal of Clinical and Experimental Neuropsychology* 33**,** 121-130.

Soares, J.M., Sampaio, A., Ferreira, L.M., Santos, N.C., Marques, F., Palha, J.A., Cerqueira, J.J., and Sousa, N. (2012). Stress-induced changes in human decision-making are reversible. *Transl Psychiatry* 2**,** e131.

Stern, Y. (2002). What is cognitive reserve? Theory and research application of the reserve concept. *J Int Neuropsychol Soc* 8**,** 448-460.

Stern, Y. (2006). Cognitive reserve and Alzheimer disease. *Alzheimer Disease & Associated Disorders* 20**,** 112-117.

Stern, Y. (2009). Cognitive reserve: A catalyst for research. *Journal of the Neurological Sciences* 283**,** 256-256.

Stern, Y., Alexander, G.E., Prohovnik, I., and Mayeux, R. (1992). Inverse relationship between education and parietotemporal perfusion deficit in Alzheimer's disease. *Ann Neurol* 32**,** 371-375.

Stern, Y., Habeck, C., Moeller, J., Scarmeas, N., Anderson, K.E., Hilton, H.J., Flynn, J.,

Sackeim, H., and Van Heertum, R. (2005). Brain networks associated with cognitive reserve in healthy young and old adults. *Cerebral Cortex* 15**,** 394-402.

Stern, Y., Zarahn, E., Habeck, C., Holtzer, R., Rakitin, B.C., Kumar, A., Flynn, J., Steffener, J., and Brown, T. (2008). A common neural network for cognitive reserve in verbal and object working memory in young but not old. *Cerebral Cortex* 18**,** 959-967.

Tian, L., Wang, J., Yan, C., and He, Y. (2011). Hemisphere-and gender-related differences in small-world brain networks: a resting-state functional MRI study. *Neuroimage* 54**,** 191-202.

Tucker-Drob, E.M., Johnson, K.E., and Jones, R.N. (2009). The cognitive reserve hypothesis: a longitudinal examination of age-associated declines in reasoning and processing speed. *Dev Psychol* 45**,** 431-446.

Van Den Heuvel, M.P., Stam, C.J., Boersma, M., and Pol, H.E.H. (2008). Small-world and scale-free organization of voxel-based resting-state functional connectivity in the human brain. *Neuroimage* 43**,** 528-539.

Van Den Heuvel, M.P., Stam, C.J., Kahn, R.S., and Pol, H.E.H. (2009). Efficiency of Functional Brain Networks and Intellectual Performance. *Journal of Neuroscience* 29**,** 7619-7624.

Watts, D.J., and Strogatz, S.H. (1998). Collective dynamics of 'small-world' networks. *Nature* 393**,** 440-442.

Wunderlich, K., Dayan, P., and Dolan, R.J. (2012). Mapping value based planning and extensively trained choice in the human brain. *Nat Neurosci* 15**,** 786-791.

Zahodne, L.B., Manly, J.J., Brickman, A.M., Siedlecki, K.L., Decarli, C., and Stern, Y. (2013). Quantifying cognitive reserve in older adults by decomposing episodic memory variance: replication and extension. *Journal of the International Neuropsychological Society* 19**,** 854-862.

Zalesky, A., Fornito, A., and Bullmore, E.T. (2010). Network-based statistic: identifying differences in brain networks. *Neuroimage* 53**,** 1197-1207.

CHAPTER V

Paulo César Gonçalves Marques, Pedro Miguel Silva Moreira, Ricardo José da Silva Magalhães, Liliana Patrícia Carvalho Amorim, Teresa de Jesus da Costa Castanho, Nadine Correia Santos, José Miguel Montenegro Soares, Nuno Jorge Carvalho Sousa

Connectomic functional brain changes in healthy aging and age-related cognitive decline

Manuscript to be submitted

Connectomic functional brain changes in healthy aging and age-related cognitive decline

Authors: P Marques[123], PS Moreira[123], R Magalhães[123], L Amorim[123], T Castanho[123], JM Soares[123], NC Santos[123], N Sousa[123]

[1]Life and Health Sciences Research Institute (ICVS), School of Health Sciences,

[2]ICVS/3B's - PT Government Associate Laboratory, Braga/Guimarães, Portugal.

[3]Clinical Academic Center – Braga, Braga, Portugal.

*Corresponding author: Nuno Sousa, Life and Health Sciences Research Institute (ICVS), School of Health Sciences, University of Minho, Campus Gualtar, 4710-057 Braga, Portugal. Email: njcsousa@ecsaude.uminho.pt. Phone: +351 253 604 806.

Abstract

Healthy aging is a dynamic process characterized by declines in several cognitive dimensions, inter-individual variability and brain structural and functional changes. Network approaches to brain functioning have provided new insights on how the human brain is impacted by illness or natural conditions. Yet, few studies have used such methods to study the impact of aging in the human brain functional connectome and even less using a longitudinal design. In this study we followed a group of healthy older adults, previously categorized as overall good and poor cognitive performers, for a period 18 months. Functional connectivity (FC) networks' properties were analyzed with graph theory methods and associations between changes in network properties and changes in learning and memory scores were explored. Our data shows that good cognitive performance is associated with higher FC, higher functional segregation spanning the majority of the brain (with the exception of the prefrontal cortex) and higher network efficiency. We also show that aging is associated with both decreases and increases in FC, accompanied by rearrangements in local network properties such as decreased strength, segregation and "hubness" in prefrontal regions and increases in strength and "hubness" of the hippocampus. Finally, we show that increases in local clustering of the left hippocampus were associated with decreases in recall performance associated with aging while changes in the local clustering of the left putamen correlated positively with changes in learning performance. Our findings suggest that: (1) good cognitive performance in older adults is associated with brain network differences that seem to be maintained through aging; (2) age is characterized by rearrangements in local brain network properties, and compensatory mechanisms seem to take place to maintain global network properties; (3) changes in local clustering of key regions for learning and memory capture differences in cognitive performance in those domains.

1. Introduction

Healthy aging, namely at brain level, is a dynamic process characterized by a heterogeneous pattern of structure and function preservation and deterioration. Specifically, gray and white matter volume alterations (Lemaitre et al., 2012;Fjell et al., 2013;Soares et al., 2014;Jancke

et al., 2015), cortical thinning (Salat et al., 2004;Pacheco et al., 2015), functional reorganization (Cabeza, 2002;Dennis and Cabeza, 2008) and functional connectivity (FC) (Allen et al., 2011;Mowinckel et al., 2012;Ferreira and Busatto, 2013), are all hallmarks of the aging process. These brain changes have also been associated with the common variability on cognitive functioning across the lifespan (Davis et al., 2008;Meunier et al., 2014;Reuter-Lorenz and Park, 2014). Several domains become less efficient, including executive and speed processing, working memory ability, episodic memory, long-term memory and attention (Salthouse et al., 1991;Salthouse, 2000;Nyberg et al., 2003;Salthouse and Madden, 2008) while at the same time, others, such as knowledge storage, semantic memory (Ronnlund et al., 2005;Singh-Manoux et al., 2012), and language comprehension are more resistant to age-induced alterations (Tyler et al., 2010).

Most studies in aging and cognition focused on region-specific analyses, precluding a global and wider picture on how the brain is being constantly adapted and re-organized. The human brain is a complex system of interconnected and synchronized regions spontaneously organized into several networks (Sporns et al., 2005;Hagmann et al., 2008). Recently, graph theory approaches have been employed to study the connectivity properties of these structural (Gong et al., 2009) and functional (Goni et al., 2014) brain specialized networks (Park and Friston, 2013). Graph approaches provide ideal means to study alterations in global architecture and within local specialized networks, offer the possibility to establish relationships between neural changes and cognitive functions.

Several recent studies have shown that connectivity between separate brain regions is essential for effective cognitive functioning (Onoda et al., 2012;Wen et al., 2012;Meunier et al., 2014;Strenziok et al., 2014) and that it is critically affected by the age (Ferreira and Busatto, 2013). Both structural and FC reorganizations occur along aging, impacting significantly on cognitive functioning: decreased integrity in grey matter is associated with decreased connectivity in language regions and with increased overall FC (Meunier et al., 2014); increased FC is associated with faster responding and older adults exhibit a lower association strength, varying also as a function of task demands (Chou et al., 2013); global structural brain network properties and general intelligence are correlated in advanced elderly (Fischer et al., 2014); decreased connectivity within functional networks is related with poorer cognitive functioning in elderly, pointing to a decrease in the specificity of functional networks in older

ages (Geerligs et al., 2014); longitudinal analysis shows that the structural brain networks develop into a fast distribution from young to middle age and became eventually a fast localization in the old age and in terms of the regional nodal properties, significant positive quadratic correlations were found in the brain regions predominately associated with the default-mode, attention, and memory systems (Wu et al., 2013).

One of the most affected cognitive domains by advanced aging is memory (Nyberg et al., 2012). However, this decline is heterogeneous, with some older individuals presenting a relatively well-preserved memory functioning. Studies have revealed that in older participants the entorhinal thinning may occur before a decreased default-mode FC and hippocampal volume loss, which in turn lead to deficits in memory performance (Ward et al., 2015). However, most studies investigating associations between FC and memory in aging are cross-sectional and thus, fail to provide a direct link between cognitive decline and connectivity measures. One exception is a study from Persson and colleagues showing that declines in memory over a six-year interval are associated with decreased hippocampal activation and volume (Persson et al., 2012). Another recent study suggested that associations between memory performance and brain structural/functional changes are not either simultaneous or consequential, but a mixture of effects (Fjell et al., 2015). In this study decreased FC between the hippocampus and cortical regions was associated with better performance in recall in young adults while in older adults, a less pronounced but positive association was found.

However, to the best of our knowledge, no longitudinal study has yet been conducted in order to demonstrate the impact of aging in graph theory metrics derived from FC networks and how changes in these metrics relate to changes in memory performance. In the present study we aimed at describing these effects in a longitudinal setting and further explore if they differ between individuals with contrasting cognitive profiles (i.e. good cognitive performers vs poor cognitive performers).

2. Methods

2.1 Ethics Statement

The present study was conducted in accordance with the principles expressed in the Declaration of Helsinki and was approved by the local and national ethics committees. The study goals and tests were explained to the participants and all gave informed written consent.

2.2 Participants

The subjects that participated in the present study were recruited based on cognitive data obtained on a previous study and form the sample recruited for the Switchbox Consortium project (www.switchbox-online.eu/). For the Switchbox project, 120 subjects initially recruited were selected from a larger sample, representative of the general Portuguese older population in terms of age, gender, and education [n = 1051, after inclusion/exclusion criteria; subjects randomly selected from the Guimarães and Vizela local area health authority registries (Costa et al., 2013;Santos et al., 2013;Santos et al., 2014)]. These 120 subjects were selected in order to provide cognitive profiles of overall good cognitive performance (n=60) and overall poor performance (n=60) (Marques et al., 2015). Details regarding the neurocognitive assessment and categorization into the two opposite cognitive profiles are provided below. Primary exclusion criteria for both time points included inability to understand the informed consent, participant choice to withdraw from the study, incapacity and/or inability to attend the Magnetic Resonance Imaging (MRI) session, dementia and/or diagnosed neuropsychiatric and/or neurodegenerative disorder (medical records). Following previous recommendations, adjusted thresholds for cognitive impairment were calculated depending on factors such as age and/or education (Grigoletto et al., 1999;Busch and Chapin, 2008). Thus, the applied Mini Mental State Examination (MMSE) test score thresholds were the following: MMSE score < 17 if individual with ≤ 4 years of formal school education and/or ≥ 72 years of age, and MMSE score < 23 otherwise [follows the MMSE validation study for the Portuguese population (Guerreiro et al., 1994)].

In the first assessment, from the 120 subjects originally recruited for the main project, nine participants refused to undergo the MRI acquisition protocol, four undiagnosed brain lesions/pathology detected during the MRI assessment and seven were excluded for having excessive motion/artifacts in the resting-state fMRI (rs-fMRI) scan. In the second neuropsychological/cognitive and MRI assessments, two individuals could not be reached, six could not attend the assessment within the time-frame of the study due to scheduling conflicts, nine met exclusion criteria, 17 declined to participate and 86 accepted to participate. From the 86 participants re-assessed three declined to undergo the MRI scan on the assessment day, nine had either not completed the first MRI assessment or had met the exclusion criteria for inclusion in the data analysis for the first MRI scan. Additionally, one individual had brain lesions and another was excluded due to excessive head motion in the second MRI scan.

A total of 75 individuals met all the inclusion criteria for the present study. From these, 48 were good cognitive performers and 29 were poor cognitive performers. The mean time interval between assessments was 18 months and the groups of cognitive performance differed significantly in all cognitive tests in both assessments.

2.3 Neurocognitive assessment

A team of trained psychologists performed all neurocognitive/neuropsychological assessments. The initial neurocognitive assessment was performed for the larger sample (n=1051) from which the present sample was derived. A large test battery was applied and included the following instruments: digit-span forward and backward test, Stroop color and word test, controlled oral word association test (COWAT, letters F-A-S), selective reminding test (SRT), digit symbol substitution test (DSST), mini-mental state examination (MMSE), geriatric depression scale (GDS, long-version) and the Graffar socio-demographic scale (Santos et al. 2014).

The SRT was used to assess memory trajectories from the baseline assessment to the follow-up assessment. This test consists in a list of 12 words that is read to the participant and then, in the following five trials, the participant is asked to immediately recall the 12 words. In each trial, the words that the participant failed to recall are reminded to the participant. After 15

minutes of finishing the fifth trial, participants are asked once more to recall the list of words. For the present study, the Consistent Long-Term Retrieval (CLTR – words consistently recalled on at least the three last trials, without reminding) and the Delayed Recall (DR – words correctly recalled 20 minutes after the fifth trial) scores were considered. CLTR represents a measure of short-term memory/learning while DR is assumed to represent a measure of memory, namely recall.

2.4 Magnetic Resonance Imaging Acquisition

The MRI assessments were performed on a 1.5 T clinical approved Siemens Magnetom Avanto MRI scanner (Siemens Medical Solutions, Erlangen, Germany) with a 12-channel receive-only head-coil, at Hospital de Braga (Braga, Portugal). The imaging protocol included several different acquisitions. An anatomical scan was initially acquired using a T1-weighted magnetization prepared rapid gradient echo (MPRAGE) sequence with the following imaging parameters: 176 sagittal slices, TR/TE= 2730/3.48 ms, FA = 7°, slice thickness = 1 mm, slice gap = 0 mm, voxel size= 1x1 mm^2, FoV = 256 mm. An rs-fMRI acquisition was also acquired using a blood oxygen level dependent (BOLD) sensitive echo-planar imaging (EPI) sequence: 30 axial slices, TR/TE = 2000/30 ms, FA = 90°, slice thickness = 3.5, slice gap = 0.48 mm, voxel size = 3.5 x 3.5 mm^2, FoV = 1344 mm and 180 volumes. During the resting state scan, the subjects were instructed to remain still, awake, with their eyes closed, as immobile as possible and trying to think of nothing in particular. No participant fell asleep during the acquisition.

2.5 Preprocessing of rs-fMRI data

Preprocessing of rs-fMRI data was performed with FMRIB Software Library (FSL v5.07; http://fsl.fmrib.ox.ac.uk/fsl/) tools. The first five volumes of the rs-fMRI acquisition were removed to allow for signal stabilization. The data underwent the following data pre-processing pipeline: (1) slice timing correction, (2) head motion correction and motion scrubbing (Power et al., 2012) to identify and further exclude time-points where head motion could be critical, (3) removal of non-brain tissue, (4) nonlinear spatial normalization to Montreal Neurological

Institute (MNI) standard space, (5) linear regression of motion parameters, motion outliers, mean white matter and cerebrospinal fluid signal, (6) band-pass temporal filtering (0.01-0.08Hz). The spatial normalization was performed as follows: co-registration of the mean functional image with the structural image of the same individual using a rigid-body registration; affine registration of the structural image to the MNI T1 template; non-linear normalization of the structural image to MNI standard space using the previous affine registration as the initial alignment; final non-linear normalization of the functional data to MNI standard space trough the combined application of the rigid-body transformation matrix and the non-linear warp, followed by resampling to 2 mm isotropic voxel size.

2.6 Network construction

The nodes of the FC networks were defined as the 116 cortical, subcortical and cerebellar regions from the Anatomical Automatic Labeling (AAL) atlas. The mean time-series of each region were extracted and the edges of the networks were defined as the Z-transformed correlation coefficients between the time-series of each possible pair of regions, resulting in an 116x116 FC matrix for each subject and moment of assessment. For the graph theory analysis, instead of binarizing the FC matrices, the absolute values of the weights were used so that negative weights were not excluded. Some studies involving graph theoretic measures of FC networks discard edges displaying negative FC since such measures cannot be calculated in the presence of negative weights (Achard and Bullmore, 2007;van den Heuvel et al., 2008). However anti-correlations between brain regions metabolism are known to exist (Keller et al., 2013) and we considered attributing the same importance to negative and positive correlations of the same magnitude to be less critical than simply neglecting the effect of such edges in network topology.

2.7 Graph theory analysis

Graph theory analysis was performed in order to investigate possible effects in the properties of each node as well as in the global network properties. The Brain Connectivity Toolbox (BCT, http://www.brain-connectivity-toolbox.net)(Rubinov and Sporns, 2010) was used to calculate

both nodal and global network properties. Three different metrics were calculated for each node: i) strength that is defined as the sum of weights of the edges connected to each node and represents a measure of density of connections around the node; ii) betweenness centrality, a measure of centrality (i.e. importance of the node in functional integration – "hubness") and corresponds to the proportion of all shortest paths that contain the node and iii) clustering coefficient, defined as the average intensity of triangles around a node, measures how tightly the neighbors of a node are connected among themselves.

At the global network level the following measures were calculated: i) global efficiency, a measure of integration, is defined as the average of the inverse shortest path length; ii) mean clustering coefficient that represents the mean of the clustering coefficients of all nodes and thus provide a measure of segregation and iii) assortativity that indicates if network nodes tend to be connected with nodes of similar strength, assessed trough correlation coefficients between strengths of all nodes.

Graph theory metrics are typically computed for different sparsities of the FC matrix. However different thresholds may yield different results, there is no consensus for the range of sparsities to be considered and it increases the complexity number of comparisons of the analysis. In order to overcome this, these metrics were initially computed for a range of sparsities (0.1 – 0.4, in increments of 0.025) and their integrated measure (i.e. area under the curve) was used for the analysis, resulting in one value for each metric (Tian et al., 2011).

2.8 Statistical Analysis

The statistical analyses were performed at the edge, node and global network level. In each level, two different analyses were performed. Initially, a mixed-design Analysis of Covariance (ANCOVA) was performed with group of performance as the between-subjects factor and time of assessment as the within-subjects factor. This model enabled the investigation of group differences in FC networks (group effect), the investigation of age-related trajectories (within-subjects effect) and the examination of group differences in age-related trajectories (interaction between group and within-subjects effects). Then, associations between changes in FC variables and changes in CLTR and DR scores were assessed with regression analyses with the

change in cognitive score as the dependent variable and change in FC variables as the independent variable.

At the edge level, the Network-Based Statistic (NBS) procedure was used to increase the statistical power of the analysis. This allows the identification of connected sub-networks whose edges display similar associations the independent variables (Zalesky et al., 2010). This procedure is similar to the cluster-based thresholding approach used in voxel-wise analyses of fMRI data. Firstly a General Linear Model (GLM) is applied independently for each edge, considering the edge weight as the dependent variable. Then, instead of considering the null hypothesis at the single edge level, NBS evaluates the null hypothesis at the level of interconnected edges (i.e. sub-networks) surviving the application of a predefined primary threshold for a given effect of interest. The null hypothesis assumes that a sub-network with similar number of edges, surpassing the primary threshold, occurs by chance. In accordance with the established guidelines for the use of this procedure, three primary thresholds were used ($p < 0.01$, $p < 0.005$, $p < 0.001$) so that less pronounced but more extent effects (less stringent primary threshold – $p < 0.01$) as well as localized and pronounced effects (most stringent threshold – $p < 0.001$) could be captured. Five thousand permutations were performed and networks were considered significant at a level of $p<0.05$ family-wise error (FWE) corrected. BrainNet viewer (http://www.nitrc.org/projects/bnv/) was used for visualization purposes.

At the nodal and global metric level, the models were fitted using Matlab. Results of the ANCOVA model were considered significant at $p<0.05$ corrected for multiple comparisons using the False Discovery Rate (FDR) criterion across all metrics/nodes. Regarding the associations between changes in local metrics and changes in memory variables, results were considered significant at $p<0.05$ uncorrected for a group of subcortical nodes known to be involved in complementary learning and memory systems, namely the caudate (Brovelli et al., 2011), putamen (Brovelli et al., 2011) and hippocampus (Burgess et al., 2002). For the remaining nodes, results were considered significant at $p < 0.05$ FDR corrected.

At the global network level, results were considered significant at $p<0.05$.

3. Results

3.1 Demographic and cognitive characterization

Table I presents the sample demographic and neurocognitive characteristics. Groups of cognitive performance did not differ significantly in the proportion of males versus females and age. Good cognitive performers presented significantly higher number of years of education and scored higher in all cognitive measures (MMSE, CLTR and DR). Regarding cognitive trajectories from the baseline assessment to the follow-up, participants declined significantly in MMSE and DR scores, but not in CLTR. However, a significant interaction was found for CLTR scores. Interestingly, post-hoc t-tests revealed that while good performers had a trend for a decrease in CLTR scores, the opposite was found in poor performers.

Table I. Sample demographic and cognitive characteristics.

	Baseline		Follow-up		Good - Poor	Baseline - Follow-up	Interaction
	Good	Poor	Good	Poor	F (p-value)	F (p-value)	F (p-value)
Sex	27M/19F	12M/17F	27M/19F	12M/17F	ns	-	-
Education	7.3 (4.48)	3.55 (1.74)	7.3 (4.48)	3.55 (1.74)	4.30 (< 0.001)	-	-
Age	64.57 (8.80)	65.37 (6.85)	66.15 (8.73)	67.03 (6.77)	0.20 (0.658)	-	-
MMSE	27.78 (2.30)	25.72 (3.70)	26.70 (2.72)	24.41 (3.78)	10.63 (0.002)	18.30 (< 0.001)	0.16 (0.691)
CLTR	25.74 (8.94)	4.24 (5.94)	22.22 (12.97)	7.59 (7.73)	94.55 (< 0.001)	0.004 (0.950)	6.30 (0.014)
DR	7.24 (2.83)	3.58 (1.89)	5.52 (3.10)	2.79 (2.54)	36.2 (< 0.001)	11.87 (< 0.001)	1.64 (0.200)

3.2 Differences in network properties between groups of cognitive performance

No group differences were found at the edge level, using the NBS procedure.

At the node level, good performers presented higher strength in 19 nodes when compared to poor performers, mainly comprising regions from the temporal lobe and regions from the occipital lobe (Figure 1.a). Regarding local clustering, 43 nodes exhibited significantly higher values in good performers when compared to poor performers (Figure 1.b); these nodes span all the brain lobes with the exception of the frontal lobe. The most significant results were

found in the right superior and middle occipital, right parahippocampal, right Heschl and left cerebellum 4 5 and 6 (Figure 1.b). The right cuneus and occipital superior, left temporal superior and the bilateral rolandic operculum exhibited higher betweenness centrality in good performers when compared to poor performers, while poor performers exhibited higher values in the left angular and right cerebellum crus 2.

Table II presents the results for group comparisons of the nodal properties.

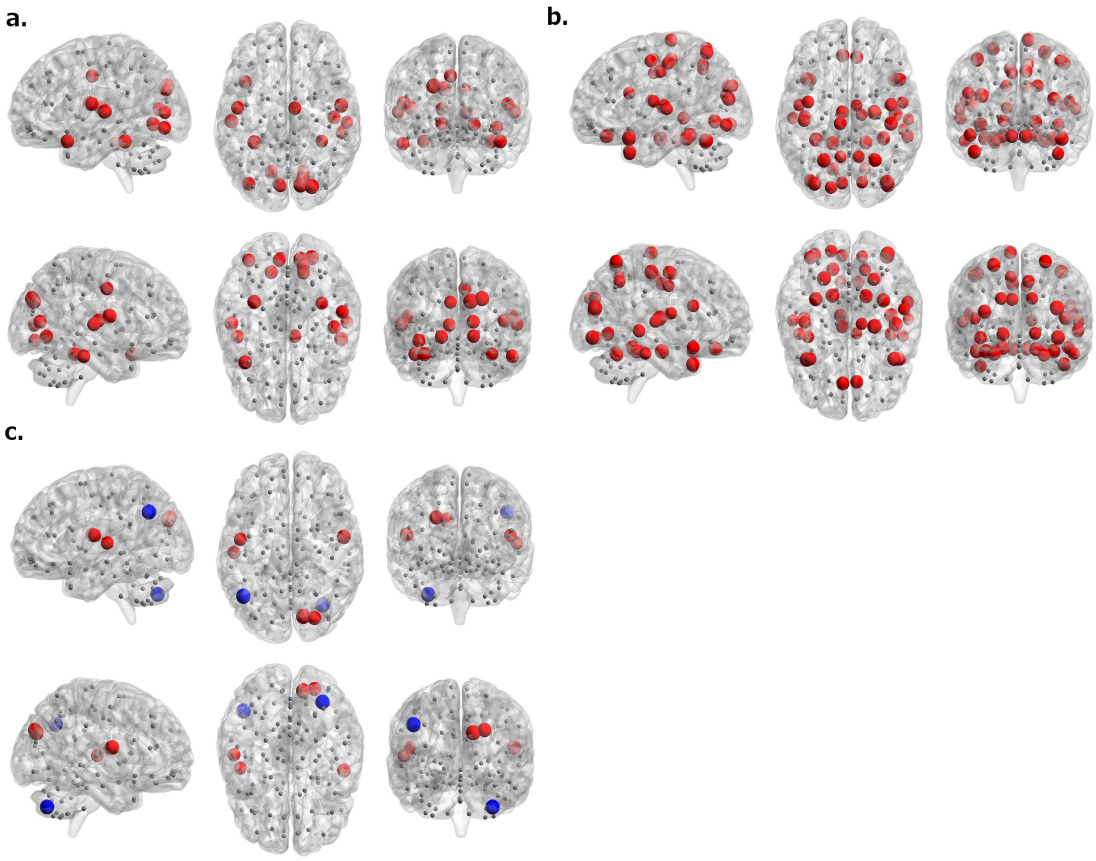


Figure 1. Significant group differences between good and poor cognitive performers in nodal network metrics. AAL regions showing significant ($p < 0.05$, FDR corrected for multiple comparisons) group effects in strength (a), clustering coefficient (b) and betweenness centrality (c). Red dots represent nodes where the metric is higher in good than poor cognitive performers and blue dots represent nodes where the metric is lower in good performers compared to poor performers. Grey dots represent nodes without a significant effect.

Table II. Comparison of nodal properties between groups. The table presents the direction of the results for each metric, the node label, F-statistic and corresponding uncorrected p-value. Results fully corrected for multiple comparisons using the FDR criterion (p<0.05).

Effect	Node	F	p-value	Node	F	p-value
Strength						
Good > Poor	Cuneus R	15.85	0.0002	Occipital Sup R	15.34	0.0002
	Rolandic Oper R	13.58	0.0004	Temporal Sup L	12.90	0.0006
	Fusiform L	12.46	0.0007	Temporal Pole Sup L	11.68	0.0010
	Heschl R	10.96	0.0015	Rolandic Oper L	10.89	0.0015
	Lingual L	10.88	0.0015	Calcarine R	10.69	0.0016
	Occipital Inf L	10.49	0.0018	Cingulum Mid R	9.82	0.0025
	Temporal Inf R	9.72	0.0026	Calcarine L	9.57	0.0028
	Lingual R	9.52	0.0029	Temporal Sup R	9.13	0.0035
	Fusiform R	8.69	0.0043	Cuneus L	8.41	0.0049
	Cerebellum 6 L	7.38	0.0082			
Good < Poor	NA					
Clustering						
Good> Poor	Occipital Mid R	21.17	< 0.0001	ParaHippocampal R	19.34	<0.0001
	Heschl R	18.45	0.0001	Cerebellum 6 L	17.86	0.0001
	Occipital Inf R	17.34	0.0001	Cerebellum 4 5 L	17.24	0.0001
	Temporal Pole Sup L	17.15	0.0001	Postcentral R	16.38	0.0001
	Fusiform L	15.74	0.0002	Fusiform R	15.56	0.0002
	Cerebellum 4 5 R	15.48	0.0002	Occipital Mid L	15.19	0.0002
	Parietal Sup L	15.07	0.0002	Temporal Pole Mid R	14.48	0.0003
	Rectus L	13.81	0.0004	Lingual L	13.64	0.0004
	Parietal Sup R	12.86	0.0006	Precentral R	12.61	0.0007
	Rectus R	12.56	0.0007	Cingulum Mid L	12.42	0.0007
	Temporal Pole Sup R	12.29	0.0008	Paracentral Lobule L	12.05	0.0009
	Occipital Inf L	11.94	0.0009	Temporal Mid R	11.73	0.0010
	Postcentral L	11.23	0.0013	Cerebellum 6 R	11.16	0.0013
	Cuneus L	10.60	0.0017	Precentral L	10.41	0.0019
	Precuneus R	10.30	0.0020	Temporal Pole Mid L	10.30	0.0020
	Occipital Sup L	10.09	0.0022	Frontal Inf Oper R	10.03	0.0022
	Lingual R	9.91	0.0024	Heschl L	9.80	0.0025
	Temporal Sup L	9.40	0.0030	Precuneus L	9.37	0.0031
	Cuneus R	9.17	0.0034	Temporal Inf R	9.17	0.0034
	Rolandic Oper L	8.97	0.0038	Thalamus R	8.75	0.0042
	Cingulum Mid R	8.47	0.0048	Rolandic Oper R	8.44	0.0049
	Temporal Sup R	8.12	0.0057			
Good<Poor	NA					
Betweenness						
Good > Poor	Cuneus R	13.85	0.0003	Rolandic Oper R	11.80	0.0010
	Occipital Sup R	10.94	0.0015	Rolandic Oper L	8.75	0.0042
	Temporal Sup L	8.62	0.0044			
Good < Poor	Angular L	13.91	0.0004	Cerebellum Crus2 R	12.99	0.0006

At global network level, good performers presented higher global efficiency ($F = 14.72$; $p < 0.001$) and mean clustering coefficient ($F = 13.41$; $p < 0.001$) than poor performers, while no significant difference was found in assortativity ($F = 0.123$; $p = 0.727$). Figure 2 presents scatter plots highlighting these differences.

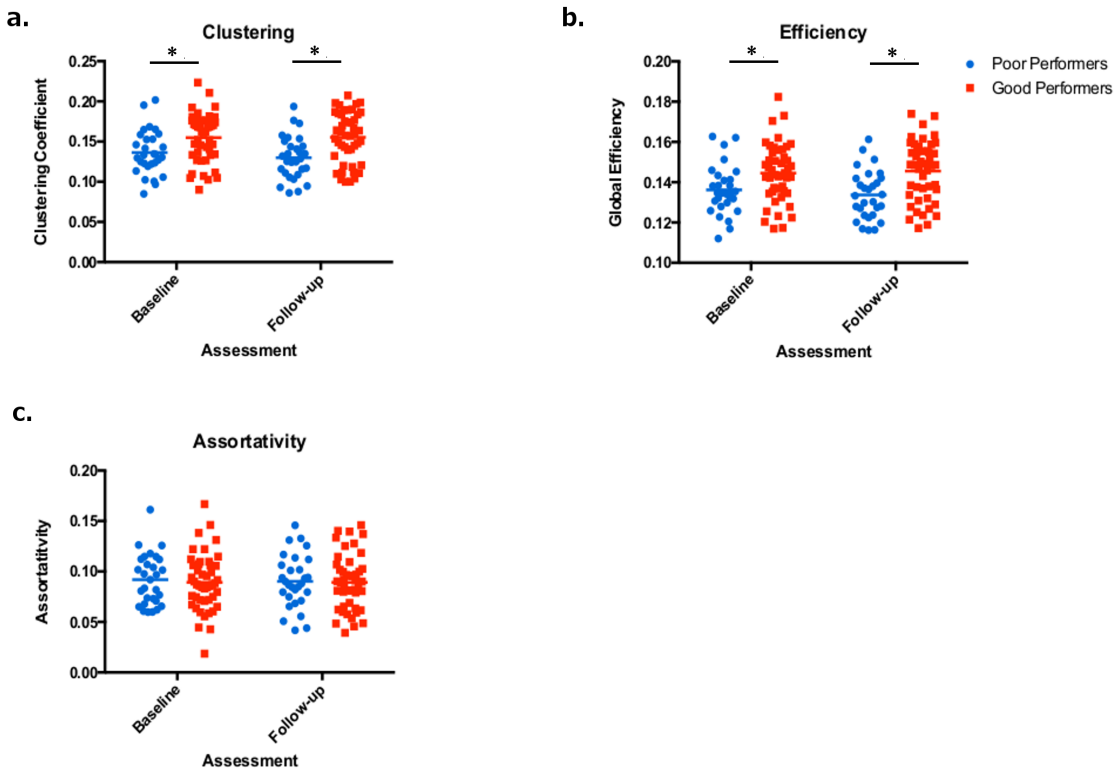


Figure 2. Scatter plots of global network measures of each group at each assessment. Good performers presented (a) higher mean clustering coefficient and (b) global efficiency than poor performers, while (c) no differences were found in assortativity (c). Good performers are represented in red, poor performers are represented in blue. Asterisks (*) denote significant group differences at $p < 0.001$.

3.3 Age-related trajectories in network properties

From the baseline assessment to the follow-up, two brain sub-networks revealed significant changes with time. These effects were significant across the three primary thresholds used for

the NBS analysis; however, only the results obtained with the strictest primary threshold ($p < 0.001$) are presented. A large sub-network revealed decreases in FC between the baseline and follow-up assessments. This network encompassed 297 edges and 70 nodes (Figure 3.b). Most of this sub-network's edges interconnected several prefrontal regions and the temporal poles, as well as some connections from/to parietal and cerebellar regions. In contrast, there was a small sub-network, composed by 66 edges that were connecting 47 different nodes, that display significant increases in FC between the two time-points of assessment (Figure 3.a). This network was mainly composed by edges interconnecting the pallidum, hippocampus, lingual gyrus and temporal superior gyrus to other temporal, frontal and cerebellar regions.

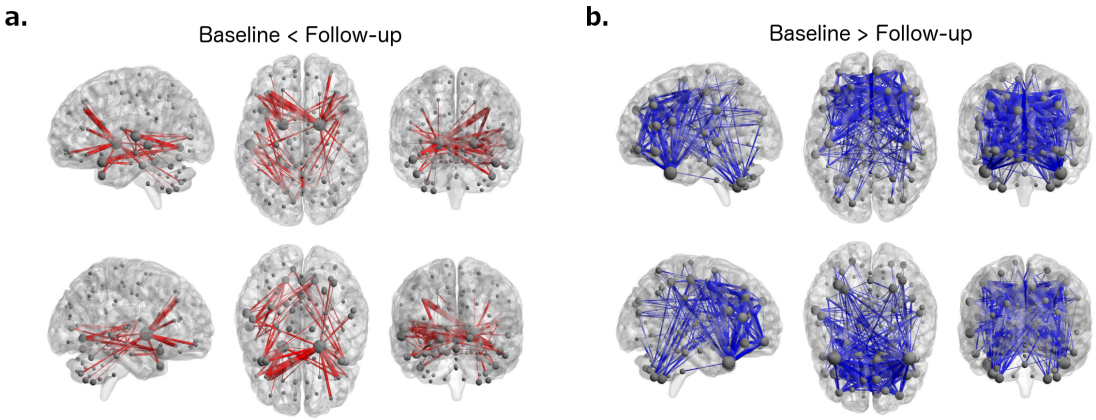


Figure 3. Significant differences in sub-networks of FC. From the baseline assessment to the follow-up, a small sub-network evidenced increased FC (a) while another sub-network evidenced decreases in FC (b). Red lines represent connections showing increased FC and blue lines represent connections evidencing decreased FC. The size of each node is proportional to the number of connections involving that particular node.

Regarding local network properties, we found increases in strength in the bilateral hippocampus and lingual gyrus, right amygdala, left cerebellum (3, 4 and 5) in between the two-time points. Significant decreases in strength were observed in frontal nodes (bilateral frontal superior, frontal middle, frontal middle orbital, right frontal superior orbital, right frontal superior medial and right frontal inferior operculum) and in right precentral and right parietal inferior (Figure 4.a). As for clustering coefficient, significant increases were only observed in

left cerebellum 3. On the other hand, the bilateral frontal superior and frontal middle, right frontal middle orbital, frontal inferior operculum and left parietal inferior evidenced significant decreases in clustering coefficient (Figure 4.b). Decreases in betweenness centrality were found in the bilateral frontal superior and frontal middle, right frontal superior orbital, right frontal middle orbital, right frontal superior medial and left parietal inferior. In contrast, increases in centrality were found in the bilateral hippocampus, lingual and cerebellum 3, right amygdala, right putamen and right cerebellum 6 (Figure 4.c).

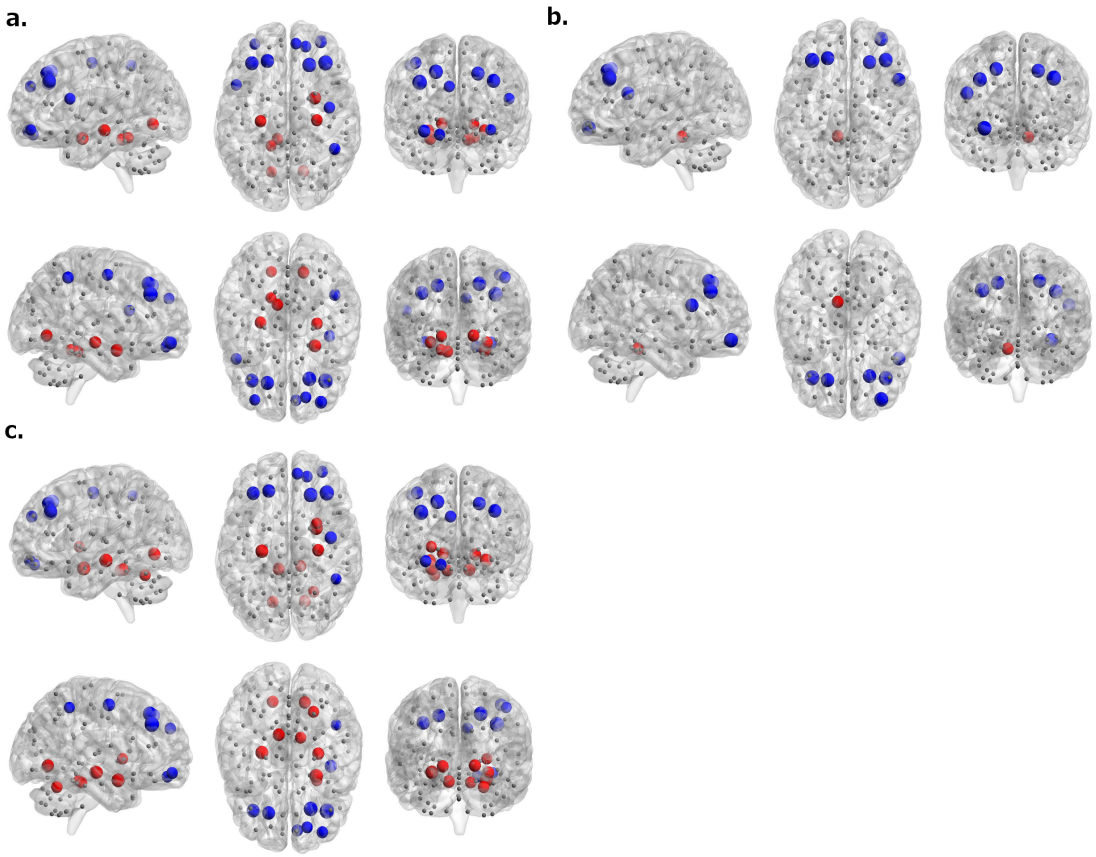


Figure 4. Significant differences in local metrics between moments of assessment. Significant decreases ($p < 0.05$, FDR corrected for multiple comparisons) in (a) strength, (b) clustering coefficient, (c) local efficiency and (d) betweenness centrality (d) were found in several nodes. Red dots represent nodes showing increases in local metrics and blue dots represent nodes evidencing decreases in the same metrics from baseline to the follow-up assessment. Grey dots represent nodes without a significant effect.

Table III summarizes the results for the comparisons between assessments in local network properties.

Table III. Comparison of local metrics between the baseline (M0) and the follow-up assessments (M1). The table presents the direction of the results for each metric, the node label, F-statistic and corresponding uncorrected p-value. Results fully corrected for multiple comparisons using the FDR criterion ($p<0.05$).

Effect	Node	F	p-value	Node	F	p-value
Strength						
M0 < M1	Amygdala R	14.98	0.0002	Lingual R	11.29	0.0012
	Hippocampus L	11.25	0.0013	Cerebellum 3 L	11.16	0.0013
	Hippocampus R	10.94	0.0015	Lingual L	8.86	0.0040
	Cerebellum 4 5 L	8.49	0.0047			
M0 > M1	Frontal Mid R	29.99	0.0000	Frontal Sup R	24.25	0.0000
	Frontal Mid L	21.01	0.0000	Frontal Sup L	20.49	0.0000
	Frontal Mid Orb R	14.06	0.0004	Parietal Inf R	10.69	0.0016
	Precentral R	10.27	0.0020	Frontal Sup Orb R	9.79	0.0025
	Frontal Inf Oper L	9.35	0.0031	Frontal Sup Medial R	9.12	0.0035
	Frontal Mid Orb L	8.27	0.0053			
Clustering						
M0 > M1	Frontal Mid Orb R	17.26	0.0001	Frontal Mid R	10.46	0.0018
	Frontal Inf Oper R	10.35	0.0019	Frontal Sup R	10.24	0.0020
	Frontal Mid L	10.11	0.0022	Frontal Sup L	8.75	0.0042
	Parietal Inf L	8.47	0.0048			
M0 < M1	Cerebellum 3 L	8.34	0.0051			
Betweenness						
M0 > M1	Frontal Mid R	28.91	0.0000	Frontal Sup R	23.30	0.0000
	Frontal Mid L	17.76	0.0001	Frontal Sup L	16.90	0.0001
	Precentral R	13.65	0.0004	Frontal Mid Orb R	10.24	0.0020
	Frontal Sup Medial R	9.90	0.0024	Frontal Sup Orb R	9.67	0.0027
	Parietal Inf R	8.17	0.0056			
M0 < M1	Amygdala R	18.81	0.0000	Hippocampus L	17.09	0.0001
	Cerebellum 3 L	13.21	0.0005	Lingual R	12.40	0.0007
	Hippocampus R	12.15	0.0008	Lingual L	11.42	0.0012
	Cerebellum 6 R	9.90	0.0024	Cerebellum 3 R	9.62	0.0027
	Putamen R	8.99	0.0037			

No significant alterations were found in global network properties between assessments.

3.4 Group differences in network properties' trajectories

No significant interactions were found at any level of analysis, indicating that the rates of change of any of the variables assessed, from baseline to the follow-up, did not differ significantly between groups of cognitive performance.

3.5 Associations with cognitive decline

After assessing the group differences and changes in network properties we explored if the longitudinal changes in network properties of key regions to learning and memory were associated with the longitudinal trajectories in a measure of learning (CLTR) and recall (DR). Changes in strength and betweenness centrality of the nodes considered were not significantly associated with changes in learning or memory/recall. However, changes in clustering coefficient of the left putamen revealed a significant positive correlation with changes in leaning scores (Figure 5.a), while changes in the clustering coefficient of the left hippocampus evidenced a negative correlation with changes in recall (Figure 5.b).

No significant correlations were found at the edge, node and global network level using the fully exploratory approach.

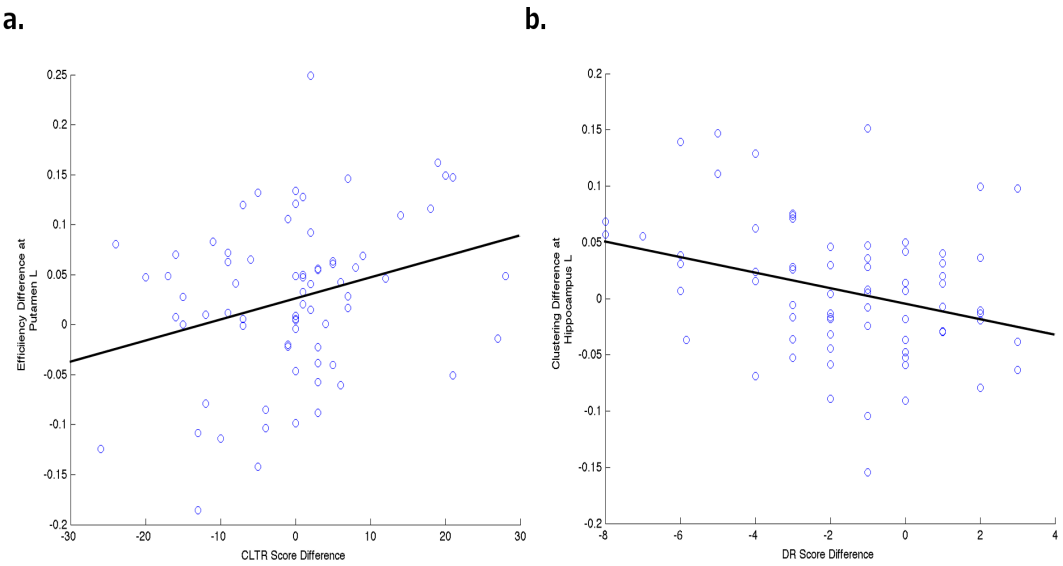


Figure 5. Associations between changes in local clustering and changes cognitive dimensions. Changes in clustering coefficient of left putamen correlated positively with changes in Consistent Long-Term Retrieval (CLTR) (a) while reductions in Delayed Recall (DR) scores correlated negatively with changes in the clustering coefficient of the left hippocampus.

4. Discussion

Several studies show that the human functional brain connectome follows a non-random network topology enabling the human brain to continuously process and integrate information. In a previous cross-sectional study with this cohort, poor cognitive performers revealed increased white matter macro- and micro-structural damage/degeneration and the effects of age were more pronounced in these individuals (Marques et al., 2015). These findings led us to expect that poor performers would present a worse functioning brain network, reflected by alteration in local and global properties. Our results are in line with these expectations since several differences were found in local metrics spanning different lobes and also in global metrics. Good performers presented higher nodal strength in several nodes compared to poor performers, pointing to a higher FC around those particular nodes and, thus, reflecting stronger functional connections with neighboring nodes. Similarly, higher clustering coefficient was found in several brain regions suggesting that higher local processing around those nodes is associated with better cognitive performance in older individuals. These rearrangements are

accompanied by increased importance of certain brain regions (e.g., the rolandic operculum, temporal superior, cuneus and occipital superior gyrus) for the network formation.

The above-described differences span a large portion of the cortex with the exception of the prefrontal cortex. The prefrontal cortex is known to play an important role in top-down control being essential for the representation of goals and the means to achieve them (Kane and Engle, 2002). Our results suggest that differences in cognition between groups are independent of prefrontal contributions for the functional brain network. This is somehow unexpected, since executive functioning is highly dependent on prefrontal cortex integrity and connectivity (Badre and Wagner, 2007). Yet, the good performers' brain network reveled higher global efficiency and mean clustering coefficient than poor performers'. This is suggestive of a fine-tuned and efficient brain network in good cognitive performers, which simultaneously present a higher segregation and integration pattern. A fine balance between specialized functional units (clusters) and information transfer across the whole brain network is a well-known characteristic (Bullmore and Sporns, 2012), and our results suggest that higher levels of both properties are associated with better cognitive functioning.

The most interesting results of the present study concern the connectome-level longitudinal trajectories as these directly point to the effects of aging. Since each individual serves as his own control (baseline assessment), this approach is not influenced by cohort effects, as occurs in cross-sectional approaches. To the best of our knowledge, this is the first study to investigate age-related trajectories in the functional brain network with a connectomic analysis. Aging studies exploring FC typically report decreases in FC between some brain regions and resting-state networks (RSNs), mainly the Default Mode Network (DMN) but also other RSNs (Damoiseaux et al., 2008); however, most of these studies are cross-sectional. In the present study, we found a large sub-network whose connections displayed decreases in FC within 18 months. These results are in accordance with the majority of the aging studies that reported decreases in FC with aging, including a recent study from our group in which a negative correlation between age and FC in a large brain sub-network was found (Marques et al., accepted for publication). However, in the present study we also found that a smaller sub-network revealed increases in FC within the 18 months between the assessments. Interestingly, this network was mainly composed by connections between subcortical regions and the prefrontal cortex or the temporal cortex. We found these changes to be accompanied

by decreases in local strength, clustering and betweenness centrality in prefrontal regions and increases in local strength and betweenness centrality in the hippocampus and lingual gyrus. No net change in global network properties was found. Although with the current design no causal link can be established, our results seem to corroborate the PASA theory of cognitive aging (Davis et al., 2008). This model proposes that an increased recruitment of frontal regions in older adults takes place as a compensatory mechanism that the brain uses to face age related impairments. We propose that these decreases in strength and hubness in prefrontal regions reflect such impairments and, thus, greater activation would be necessary to achieve the necessary levels of FC for the performance of a given task.

Another interesting finding is that changes in local clustering in key regions to leaning and memory seem to be accompanied with the longitudinal changes in these particular functions. The changes in clustering coefficient of the left putamen were positively associated with changes in learning. This is in accordance with the previously described role of putamen in learning, particularly during the initial acquisition (Brovelli et al., 2011). The negative association between changes in left hippocampus' clustering coefficient and recall scores points to the well-established role of this region in memory functioning (Squire, 1992). While, at first hand, a positive association between changes in the clustering coefficient of the hippocampus and changes in memory could be expected, some studies report a negative association between hippocampal FC and memory scores (Salami et al., 2014). A recent FC longitudinal study revealed that decreased hippocampal-cortical FC was associated with better performance in recall in young adults, while and the opposite occurred in older subjects (Fjell et al., 2015). Our results demonstrate that increases in local processing around the neighboring nodes of the hippocampus and the hippocampus itself are related with decreases in recall, while changes in local processing around the putamen's neighbors are positively associated to changes in learning.

The present study confirms that connectomic approaches have the potential to capture several aspects of the functional brain differences and reorganizations that occur with aging and their associations with cognition. These approaches have the advantage that are subject-specific, enabling the extraction of metrics for each individual, independently of the remaining sample under study. This contrasts for example with Independent Component Analysis (ICA) based studies, where study-specific RSNs need to be identified in order to estimate the each subject's

spatial maps. Additionally, the major advantage of this study relies on its longitudinal design. With this, we were able to demonstrate, for the first time, that both increases and decreases in FC and local network properties occur with aging and that changes in local network properties are associated with changes in cognitive dimensions; this clearly extends the limited information that can be extracted for cross-sectional studies.

Some limitations may be raised to this work. The aging process is continuous and not limited to older individuals. Thus, in future studies, it would be relevant to include younger individuals to assess the specificity of functional connectivity alterations during different aging phases. In addition, it would be interesting to add further assessments to these individuals. These would enable us to test whether the alterations herein detected are linear throughout time. Integrative analysis combining both functional and structural connectivity data could also further distinguish if the results here presented are mainly driven by the underlying network structure or by independent functional changes.

5. References

Allen, E.A., Erhardt, E.B., Damaraju, E., Gruner, W., Segall, J.M., Silva, R.F., Havlicek, M., Rachakonda, S., Fries, J., Kalyanam, R., Michael, A.M., Caprihan, A., Turner, J.A., Eichele, T., Adelsheim, S., Bryan, A.D., Bustillo, J., Clark, V.P., Feldstein Ewing, S.W., Filbey, F., Ford, C.C., Hutchison, K., Jung, R.E., Kiehl, K.A., Kodituwakku, P., Komesu, Y.M., Mayer, A.R., Pearlson, G.D., Phillips, J.P., Sadek, J.R., Stevens, M., Teuscher, U., Thoma, R.J., and Calhoun, V.D. (2011). A baseline for the multivariate comparison of resting-state networks. *Front Syst Neurosci* 5**,** 2.

Badre, D., and Wagner, A.D. (2007). Left ventrolateral prefrontal cortex and the cognitive control of memory. *Neuropsychologia* 45**,** 2883-2901.

Brovelli, A., Nazarian, B., Meunier, M., and Boussaoud, D. (2011). Differential roles of caudate nucleus and putamen during instrumental learning. *Neuroimage* 57**,** 1580-1590.

Bullmore, E.T., and Bassett, D.S. (2011). Brain graphs: graphical models of the human brain connectome. *Annu Rev Clin Psychol* 7**,** 113-140.

Bullmore, E.T., and Sporns, O. (2012). The economy of brain network organization. *Nature Reviews Neuroscience* 13**,** 336-349.

Burgess, N., Maguire, E.A., and O'keefe, J. (2002). The human hippocampus and spatial and episodic memory. *Neuron* 35**,** 625-641.

Busch, R.M., and Chapin, J.S. (2008). Review of normative data for common screening measures used to evaluate cognitive functioning in elderly individuals. *Clin Neuropsychol* 22**,** 620-650.

Cabeza, R. (2002). Hemispheric asymmetry reduction in older adults: the HAROLD model. *Psychol Aging* 17**,** 85-100.

Chou, Y.H., Chen, N.K., and Madden, D.J. (2013). Functional brain connectivity and cognition: effects of adult age and task demands. *Neurobiol Aging* 34**,** 1925-1934.

Costa, P.S., Santos, N.C., Cunha, P., Palha, J.A., and Sousa, N. (2013). The use of bayesian latent class cluster models to classify patterns of cognitive performance in healthy ageing. *PLoS One* 8**,** e71940.

Damoiseaux, J.S., Beckmann, C.F., Arigita, E.J., Barkhof, F., Scheltens, P., Stam, C.J., Smith, S.M., and Rombouts, S.A. (2008). Reduced resting-state brain activity in the "default network" in normal aging. *Cerebral cortex* 18**,** 1856-1864.

Davis, S.W., Dennis, N.A., Daselaar, S.M., Fleck, M.S., and Cabeza, R. (2008). Que PASA? The posterior-anterior shift in aging. *Cereb Cortex* 18**,** 1201-1209.

Dennis, A.N., and Cabeza, R. (2008). "Neuroimaging of Healthy Cognitive Aging," in *Handbook of aging and cognition,* ed. F.I.M.C.T.A. Salthouse. Mahwah, NJ: Erlbaum).

Ferreira, L.K., and Busatto, G.F. (2013). Resting-state functional connectivity in normal brain aging. *Neurosci Biobehav Rev* 37**,** 384-400.

Fischer, F.U., Wolf, D., Scheurich, A., and Fellgiebel, A. (2014). Association of structural global brain network properties with intelligence in normal aging. *PLoS One* 9**,** e86258.

Fjell, A.M., Sneve, M.H., Storsve, A.B., Grydeland, H., Yendiki, A., and Walhovd, K.B. (2015).

Brain Events Underlying Episodic Memory Changes in Aging: A Longitudinal Investigation of Structural and Functional Connectivity. *Cereb Cortex*.

Fjell, A.M., Westlye, L.T., Grydeland, H., Amlien, I., Espeseth, T., Reinvang, I., Raz, N., Holland, D., Dale, A.M., and Walhovd, K.B. (2013). Critical ages in the life course of the adult brain: nonlinear subcortical aging. *Neurobiol Aging* 34**,** 2239-2247.

Geerligs, L., Maurits, N.M., Renken, R.J., and Lorist, M.M. (2014). Reduced specificity of functional connectivity in the aging brain during task performance. *Hum Brain Mapp* 35**,** 319-330.

Gong, G., He, Y., Concha, L., Lebel, C., Gross, D.W., Evans, A.C., and Beaulieu, C. (2009). Mapping anatomical connectivity patterns of human cerebral cortex using in vivo diffusion tensor imaging tractography. *Cereb Cortex* 19**,** 524-536.

Goni, J., Van Den Heuvel, M.P., Avena-Koenigsberger, A., Velez De Mendizabal, N., Betzel, R.F., Griffa, A., Hagmann, P., Corominas-Murtra, B., Thiran, J.P., and Sporns, O. (2014). Resting-brain functional connectivity predicted by analytic measures of network communication. *Proc Natl Acad Sci U S A* 111**,** 833-838.

Grigoletto, F., Zappala, G., Anderson, D.W., and Lebowitz, B.D. (1999). Norms for the Mini-Mental State Examination in a healthy population. *Neurology* 53**,** 315-320.

Guerreiro, M., Silva, A.P., Botelho, M.A., Leitão, O., Castro-Caldas, A., and Garcia, C. (1994). Adaptação à população portuguesa da tradução do Mini Mental State Examination (MMSE). *Revista Portuguesa de Neurologia* 1**,** 9-10.

Hagmann, P., Cammoun, L., Gigandet, X., Meuli, R., Honey, C.J., Wedeen, V., and Sporns, O. (2008). Mapping the structural core of human cerebral cortex. *Plos Biology* 6**,** 1479-1493.

Jancke, L., Merillat, S., Liem, F., and Hanggi, J. (2015). Brain size, sex, and the aging brain. *Hum Brain Mapp* 36**,** 150-169.

Kane, M.J., and Engle, R.W. (2002). The role of prefrontal cortex in working-memory capacity, executive attention, and general fluid intelligence: an individual-differences perspective.

Psychon Bull Rev 9**,** 637-671.

Keller, C.J., Bickel, S., Honey, C.J., Groppe, D.M., Entz, L., Craddock, R.C., Lado, F.A., Kelly, C., Milham, M., and Mehta, A.D. (2013). Neurophysiological investigation of spontaneous correlated and anticorrelated fluctuations of the BOLD signal. *J Neurosci* 33**,** 6333-6342.

Lemaitre, H., Goldman, A.L., Sambataro, F., Verchinski, B.A., Meyer-Lindenberg, A., Weinberger, D.R., and Mattay, V.S. (2012). Normal age-related brain morphometric changes: nonuniformity across cortical thickness, surface area and gray matter volume? *Neurobiol Aging* 33**,** 617 e611-619.

Marques, P.C., Soares, J.M., Magalhaes, R.J., Santos, N.C., and Sousa, N.J. (2015). Macro- and micro-structural white matter differences correlate with cognitive performance in healthy aging. *Brain Imaging Behav*.

Marques, P.C., Soares, J.M., Magalhaes, R.J., Santos, N.C., and Sousa, N.J. (accepted for publication). The bounds of education in the human brain connectome *Scientific Reports*.

Meunier, D., Stamatakis, E.A., and Tyler, L.K. (2014). Age-related functional reorganization, structural changes, and preserved cognition. *Neurobiol Aging* 35**,** 42-54.

Mowinckel, A.M., Espeseth, T., and Westlye, L.T. (2012). Network-specific effects of age and in-scanner subject motion: a resting-state fMRI study of 238 healthy adults. *Neuroimage* 63**,** 1364-1373.

Nyberg, L., Lovden, M., Riklund, K., Lindenberger, U., and Backman, L. (2012). Memory aging and brain maintenance. *Trends Cogn Sci* 16**,** 292-305.

Nyberg, L., Maitland, S.B., Ronnlund, M., Backman, L., Dixon, R.A., Wahlin, A., and Nilsson, L.G. (2003). Selective adult age differences in an age-invariant multifactor model of declarative memory. *Psychology and Aging* 18**,** 149-160.

Onoda, K., Ishihara, M., and Yamaguchi, S. (2012). Decreased functional connectivity by aging is associated with cognitive decline. *J Cogn Neurosci* 24**,** 2186-2198.

Pacheco, J., Goh, J.O., Kraut, M.A., Ferrucci, L., and Resnick, S.M. (2015). Greater cortical thinning in normal older adults predicts later cognitive impairment. *Neurobiol Aging* 36**,** 903-908.

Park, H.J., and Friston, K. (2013). Structural and functional brain networks: from connections to cognition. *Science* 342**,** 1238411.

Persson, J., Pudas, S., Lind, J., Kauppi, K., Nilsson, L.G., and Nyberg, L. (2012). Longitudinal structure-function correlates in elderly reveal MTL dysfunction with cognitive decline. *Cereb Cortex* 22**,** 2297-2304.

Power, J.D., Barnes, K.A., Snyder, A.Z., Schlaggar, B.L., and Petersen, S.E. (2012). Spurious but systematic correlations in functional connectivity MRI networks arise from subject motion. *Neuroimage* 59**,** 2142-2154.

Reuter-Lorenz, P.A., and Park, D.C. (2014). How does it STAC up? Revisiting the scaffolding theory of aging and cognition. *Neuropsychol Rev* 24**,** 355-370.

Ronnlund, M., Nyberg, L., Backman, L., and Nilsson, L.G. (2005). Stability, growth, and decline in adult life span development of declarative memory: Cross-sectional and longitudinal data from a population-based study. *Psychology and Aging* 20**,** 3-18.

Rubinov, M., and Sporns, O. (2010). Complex network measures of brain connectivity: uses and interpretations. *Neuroimage* 52**,** 1059-1069.

Salami, A., Pudas, S., and Nyberg, L. (2014). Elevated hippocampal resting-state connectivity underlies deficient neurocognitive function in aging. *Proc Natl Acad Sci U S A* 111**,** 17654-17659.

Salat, D.H., Buckner, R.L., Snyder, A.Z., Greve, D.N., Desikan, R.S., Busa, E., Morris, J.C., Dale, A.M., and Fischl, B. (2004). Thinning of the cerebral cortex in aging. *Cereb Cortex* 14**,** 721-730.

Salthouse, T.A. (2000). Aging and measures of processing speed. *Biol Psychol* 54**,** 35-54.

Salthouse, T.A., Babcock, R.L., and Shaw, R.J. (1991). Effects of adult age on structural and

operational capacities in working memory. *Psychol Aging* 6**,** 118-127.

Salthouse, T.A., and Madden, D.J. (2008). Information processing speed and aging.

Santos, N.C., Costa, P.S., Cunha, P., Cotter, J., Sampaio, A., Zihl, J., Almeida, O.F., Cerqueira, J.J., Palha, J.A., and Sousa, N. (2013). Mood is a key determinant of cognitive performance in community-dwelling older adults: a cross-sectional analysis. *Age (Dordr)* 35**,** 1983-1993.

Santos, N.C., Costa, P.S., Cunha, P., Portugal-Nunes, C., Amorim, L., Cotter, J., Cerqueira, J.J., Palha, J.A., and Sousa, N. (2014). Clinical, physical and lifestyle indicators and relationship with cognition and mood in aging: a cross-sectional analysis of distinct educational groups. *Frontiers in Aging Neuroscience* 6.

Singh-Manoux, A., Kivimaki, M., Glymour, M.M., Elbaz, A., Berr, C., Ebmeier, K.P., Ferrie, J.E., and Dugravot, A. (2012). Timing of onset of cognitive decline: results from Whitehall II prospective cohort study. *British Medical Journal* 344.

Soares, J.M., Marques, P., Magalhães, R., Santos, N.C., and Sousa, N. (2014). Brain structure across the lifespan: the influence of stress and mood. *Frontiers in Aging Neuroscience* 6**,** 330.

Sporns, O., Tononi, G., and Kotter, R. (2005). The human connectome: A structural description of the human brain. *PLoS Comput Biol* 1**,** e42.

Squire, L.R. (1992). Memory and the hippocampus: a synthesis from findings with rats, monkeys, and humans. *Psychol Rev* 99**,** 195-231.

Strenziok, M., Parasuraman, R., Clarke, E., Cisler, D.S., Thompson, J.C., and Greenwood, P.M. (2014). Neurocognitive enhancement in older adults: comparison of three cognitive training tasks to test a hypothesis of training transfer in brain connectivity. *Neuroimage* 85 Pt 3**,** 1027-1039.

Tian, L., Wang, J., Yan, C., and He, Y. (2011). Hemisphere-and gender-related differences in small-world brain networks: a resting-state functional MRI study. *Neuroimage* 54**,** 191-202.

Tyler, L.K., Shafto, M.A., Randall, B., Wright, P., Marslen-Wilson, W.D., and Stamatakis, E.A. (2010). Preserving syntactic processing across the adult life span: the modulation of the frontotemporal language system in the context of age-related atrophy. *Cereb Cortex* 20**,** 352-364.

Ward, A.M., Mormino, E.C., Huijbers, W., Schultz, A.P., Hedden, T., and Sperling, R.A. (2015). Relationships between default-mode network connectivity, medial temporal lobe structure, and age-related memory deficits. *Neurobiol Aging* 36**,** 265-272.

Wen, X., Yao, L., Liu, Y., and Ding, M. (2012). Causal interactions in attention networks predict behavioral performance. *J Neurosci* 32**,** 1284-1292.

Wu, K., Taki, Y., Sato, K., Qi, H., Kawashima, R., and Fukuda, H. (2013). A longitudinal study of structural brain network changes with normal aging. *Front Hum Neurosci* 7**,** 113.

Zalesky, A., Fornito, A., and Bullmore, E.T. (2010). Network-based statistic: identifying differences in brain networks. *Neuroimage* 53**,** 1197-1207.

CHAPTER VI

General Discussion

1. Discussion

Normal aging is a heterogeneous and inevitable process characterized by declines in several cognitive abilities and also by several structural (Kaup et al., 2011) and functional brain changes/alterations (Eyler et al., 2011). Even though age induced changes seem to be irreversible (or at least difficult to revert), some individuals seem to present rather preserved cognitive abilities, while others reveal marked declines in the same cognitive domains (Salthouse, 2009;Singh-Manoux et al., 2012;Meunier et al., 2014). Several factors such as stress, mood, life experiences and genetic factors among many others have been proposed as mediators in the aging process, ultimately contributing for the heterogeneity in age-related cognitive decline (Grady, 2012;Santos et al., 2014). In an aged society, such as the current one, the search for mechanisms that can ultimately promote healthy cognitive aging has outstanding potential social and economic benefits. Cognition is intrinsically related to brain functioning and brain functioning itself is dependent on the underlying brain structure. Better understanding on how all of these factors interact and their correlates in the complex brain network may reveal targets/means for intervention and promotion of healthier aging.

The main scope of the present thesis was to bring new evidence of brain network biomarkers of healthy cognitive aging. In order to achieve this, a sample of older individuals (52+), derived from a large representative cohort of the Portuguese population, was studied. These individuals have been previously categorized as presenting overall good cognitive performance (n=60) or poor cognitive performance (n=60), and were screened with a multimodal brain MRI protocol. These procedures were repeated 18 months after the baseline assessment, thus providing the unique opportunity to understand how changes in brain function/structure relate to changes in cognition. Within the scope of this Thesis, three cross-sectional studies, using the data from the baseline assessment, and one larger longitudinal study, were performed.

In the first study, we compared different aspects of WM structure between groups of cognitive performance and how WM structural indices correlate with age. WM can be perceived as the "wiring" of the brain networks since it comprises mainly the axonal fibers that interconnect the different brain regions. Several white matter alterations, such as volumetric shrinkage, ischemic lesions and microstructural alterations, are known to occur in aging and have been associated with cognitive alterations (Brickman et al., 2006;Madden et al., 2011;Maillard et

al., 2012). Herein we revealed that, while WM volume negatively correlates with age, it does not distinguish good from poor cognitive performers, suggesting that WM volumetry per se is not associated with cognition; interestingly, this is in accordance with a previous study (Taki et al., 2011).

We also revealed that overall good cognitive performance is associated with lower loads of white matter lesioning (i.e. WMSA). WMSA are known to increase with aging, mainly due to accumulation of ischemic lesions that are associated with axonal loss and demyelination, ultimately, resulting in declines in cognitive functioning (Wang et al., 2011;Maillard et al., 2012). Our results also suggest that this aging pattern of higher WMSA volume is more pronounced in poor performers than good performers, which in turn could be interpreted has having a greater impact in poor performers than in good performers. Additionally, we revealed that cognitive performance is also associated with "better" WM microstructural properties (i.e. higher FA, lower RD and AD), even after accounting for the previously described macro-structural differences. Although no direct link between these measures and axonal loss or degradation can be established (Jones et al., 2013), the pattern identified fits that reported for the majority of the aging studies which has been associated with axonal loss and demyelination (Klawiter et al., 2011). The more significant association of these metrics with age in poor performers, similarly to WMSA, suggests once again that aging has greater impact in poor performers' WM. This study provided evidence that both macro- and micro-structural aspects of WM structure should be taken into account when considering possible associations with cognition in aging. We also hypothesize that overall cognitive performance, and possibly age-related cognitive decline, in older adults, are in part the result of differences in the rates of the normal WM degradation that accompanies the aging process and that this degradation does not seem to be uniquely attributed to a single process. However, inferences regarding rates of decline/increase should be taken cautiously as such associations cannot be fully established without longitudinal data.

After showing that overall good cognitive performance was associated with preserved WM macro- and micro-structure, we explored the effects of education in the human brain functional connectome. Education was one of the significant predicators of groups of general cognitive performance (Santos et al., 2013). Education level has also been proposed and widely used as a proxy of CR, a theoretical construct according to which individuals that have the capacity to

optimize the use of the available brain resources/networks tend to present better cognitive performance (Stern, 2002). In fact, researchers have shown that individuals with higher levels of education not only consistently score higher in neurocognitive tests (Plassman et al., 1995;Wilson et al., 2009) but also present lower risk of dementia (Meng and D'Arcy, 2012). Albeit all these evidences on the positive effects of education in cognition, no study had yet characterized its impact in the human brain functional connectome. Filling a gap in neuroscience literature, we revealed that, while age correlated negatively with FC in a large brain sub-network, years of education correlated positively with FC in another large cortical sub-network and also with more significant anti-correlations between the cerebellum and several cortical regions. Besides providing further evidence that aging is associated with decreases in FC, in line with the disconnection theory of aging, particularly in frontal regions (O'Sullivan et al., 2001;Davis et al., 2008), this was the first study to actually associate years of education with a model of brain functional networks and that revealed that higher FC in a particular network is likely to reflect a more efficient brain, as suggested by the CR theory (Habeck et al., 2003;Barulli and Stern, 2013). This study also demonstrated that the cerebellum is likely to play an important role in cognition, mainly through the differential interactions with cortical regions (Bonnet et al., 2009) and that these effects are reflected in anti-correlations in FC. These effects of education may have the potential to counterbalance the deleterious impact of aging and thus provide clear evidence of the benefits of formal education at brain level, which in turn could have an impact on promoting education policies.

Several proxies, other that education level, such as intelligence quotient (IQ) (Stern et al., 2003), occupational attainment (Ghaffar et al., 2012), cognitive stimulating leisure activities (Scarmeas et al., 2003) and cognitive engagement (Zihl et al., 2014), have been used in order to assess CR. However, since it is a theoretical construct, none of these proxies truly represents or measures CR. Although it correlates with CR, education is also associated with higher income ((Winkleby et al., 1992)) and access to healthcare (Cutler and Lleras-Muney, 2010). Reed and colleagues (2010) proposed an alternative multifactorial latent model that measured CR as the variance in cognitive dimensions that is not explained by measures of brain pathology (e.g. brain size, volume of WM lesions) nor demographic variables (e.g. sex, education or ethnicity). This reflects a better approximation to the concept of CR and overcomes most of the limitations of the use of proxies. We used a similar model in order to

obtain an estimate CR and investigated what was its impact in brain networks using a graph theory approach. We reveled that demographic characteristics, mostly accounted for by years of formal education, were associated with sub-networks closely resembling the sub-networks identified for education level. We also confirmed that these were associated with higher clustering coefficient, local efficiency and strength in parietal and occipital regions as well as greater global network transitivity. Taken together, these findings indicate that the positive effects of education level in cognition may be due to the increased ability of the brain to form segregated functional groups of brain regions (clusters or modules), reinforcing the view that higher education level triggers more specialized use of neural processing. Finally, we confirmed that CR, independently of education, is associated with higher FC, higher local efficiency in the right occipital regions, higher clustering coefficient in the left putamen and higher global efficiency. This was the first study to reveal that CR is actually associated with a more efficient brain network, as proposed by Barulli and Stern (2013). Interestingly, this also seems to be related with higher participation of putamen in network communication, a key region in decision making and learning brain systems (Soares et al., 2012;Wunderlich et al., 2012) and might be a biomarker of "better" learning and decision-making performance commonly associated to higher CR. The findings that a proxy of CR (i.e. education) and CR itself (independently of education) are associated with higher segregation and integration, respectively, are remarkable examples of the existence of a fine balance between specialized functional units (clusters) and information transfer across the whole brain network (Bullmore and Sporns, 2012).

In the studies presented in Chapters 2-4 effects of aging were analyzed through correlations with age. The cross-sectional approach is the most common in neuroimaging studies where a single imaging session is performed. However, "snapshot" approaches do not enable researchers to establish rates of change in brain function and relate these changes with aging or cognitive decline. For this purpose, longitudinal designs, where the same individual is evaluated multiple times along their lifespan, are required. In the last study performed under the scope of the present Thesis, we performed a follow-up neurocognitive and imaging assessment of the groups of cognitive performance assessed in the previous studies after a period of 18 months. We demonstrated that, independently of the moment of assessment, overall good cognitive performance is associated with more efficient brain networks with higher

functional segregation due to higher FC around nodes spanning the vast majority of the cortex and cerebellum with the exception of the prefrontal cortex. We also demonstrated that aging was associated not only with decreases in FC but also with increases in a specific sub-network. This is a novel finding that challenges the majority of the aging studies, including our previous cross-sectional analysis described in Chapter 3, that mostly report decreases in FC (Ferreira and Busatto, 2013). Although there are some exceptions suggesting that some increases in FC also occur with aging (Tomasi and Volkow, 2012;Sala-Llonch et al., 2014), these findings are still controversial and this is the first study to demonstrate it in a longitudinal setting where inter-individual differences are accounted for since each subject serves as his own control. The net effect of these increases and decreases in FC seem to have no impact in the global network properties, suggesting that compensatory mechanisms occur with aging, and these enable individuals to cope with the adverse effects of this dynamic process. Even though this finding challenges previous results of decreased global efficiency in older adults (Achard and Bullmore, 2007), it is possible that, in a longer timeframe, the negative impact of aging would overcome the ability of the individuals to compensate for those impairments. Cross-sectional studies suggested that rearrangements in local efficiency also occur with aging (Sala-Llonch et al., 2014;Song et al., 2014). We also demonstrated that rearrangements do occur in local network properties, where decreases in strength and clustering in frontal regions were accompanied by increases in strength and hubness of the hippocampus and lingual gyrus. These findings are in line with the PASA theory, since prefrontal regions seem to suffer more deleterious effects with aging than other brain regions (Davis et al., 2008). This is also the first longitudinal study to report changes in local network properties. Importantly, our results did not suggest that longitudinal trajectories differed between groups of cognitive performance, which in turn, suggests that both groups are equally affected by aging. Taking this into account, differences in network properties associated with cognitive performance in older adults probably reflect previously acquired differences rather than differential rates of age-related decline.

As already stated, aging is commonly accompanied by cognitive decline and memory seems to be one the most affected cognitive domains (Nyberg et al., 2003). There are two complementary systems that play important roles in memory involving subcortical regions: while the caudate and the putamen are part of a learning system important in acquiring and

associating information, the hippocampus has been established as key region for memory consolidation (Atallah et al., 2004). In our study, we brought new evidence that changes in clustering coefficient of the putamen correlated positively with learning while increases in hippocampal clustering coefficient where associated with declines in recall. A recent longitudinal study revealed that changes in cortical-striatal connectivity were related with learning and short-term memory changes while changes in long-term consolidation were associated with hippocampal-cortical FC changes (Fjell et al., 2015). Our findings neither contradict nor confirm the findings from Fjell and colleagues, since local clustering changes do not imply changes in FC in the same or opposite direction. Instead these must be seen as complementary results. Indeed, our findings suggest that increases in local processing around the neighbors of the hippocampus are related with decreases in recall while changes in local processing around the putamen's neighbors are positively correlated to changes in learning.

In conclusion, within this thesis we demonstrated that overall good cognitive performance is associated with alterations in WM structure as well as more efficient functional brain networks and simultaneously with higher functional segregation. We also revealed which functional brain sub-networks are associated with key contributors for inter-individual variability in cognition among older adults (education and CR) and that individuals with higher CR present more efficient brain networks with potential to counterbalance the detrimental effects of aging. Regarding aging, our longitudinal results clarified that both increases and decreases in FC occur in aging (contrarily to what was suggested by the cross-sectional analysis), that the deleterious impact of aging mainly affect frontal regions and that local reorganizations occur, possibly as a compensatory mechanism, resulting in no alterations in global network properties. Finally, local clustering in key brain regions seems to be a viable biomarker of longitudinal trajectories of learning and recall.

Another major contribution of the present work concerns the use of connectomic approaches. These approaches, combined with graph theory analysis seem to capture important aspects of brain aging and cognition and provide crucial information regarding brain functioning. In our studies they have proven useful not only in capturing previously described and expected effects but also in revealing novel findings (e.g. network efficiency) impossible to obtain with more traditional analysis. Furthermore, they provide a wider integrative view of brain functioning where both local and global aspects of the brain networks can be analyzed. Additionally, our

results highlight the importance of longitudinal studies for the establishment of which brain alterations are in fact associated with cognitive decline.

2. Future perspectives

The work presented in this thesis not only contributed to the better understanding of aging, cognition and their inter-relationships but also raised new questions that we aim at addressing in future studies. Specifically, a longitudinal analysis on WM macro- and micro-structure will be conducted in order to clarify if cognitive performance is in fact associated differences in the rates of WM degradation with aging. Structural connectivity analysis complementary to the FC analyses here reported should be performed in order to provide insights regarding structure-function relationships in aging and cognitive decline. Additionally, multifactorial predictive models should be built combining the results from all the reported studies in order to establish which effects have similar sources (i.e. explain the same variance in cognition) or are independent in predicting cognitive performance in aging, purely from neuroimaging biomarkers.

3. References

Achard, S., and Bullmore, E. (2007). Efficiency and cost of economical brain functional networks. *PLoS Comput Biol* 3**,** e17.

Atallah, H.E., Frank, M.J., and O'reilly, R.C. (2004). Hippocampus, cortex, and basal ganglia: insights from computational models of complementary learning systems. *Neurobiol Learn Mem* 82**,** 253-267.

Barulli, D., and Stern, Y. (2013). Efficiency, capacity, compensation, maintenance, plasticity: emerging concepts in cognitive reserve. *Trends in Cognitive Sciences* 17**,** 502-509.

Bonnet, M.C., Dilharreguy, B., Allard, M., Deloire, M.S., Petry, K.G., and Brochet, B. (2009). Differential cerebellar and cortical involvement according to various attentional load: role of educational level. *Hum Brain Mapp* 30**,** 1133-1143.

Brickman, A.M., Zimmerman, M.E., Paul, R.H., Grieve, S.M., Tate, D.F., Cohen, R.A., Williams, L.M., Clark, C.R., and Gordon, E. (2006). Regional white matter and neuropsychological functioning across the adult lifespan. *Biol Psychiatry* 60**,** 444-453.

Bullmore, E.T., and Sporns, O. (2012). The economy of brain network organization. *Nature Reviews Neuroscience* 13**,** 336-349.

Conforti, L., Gilley, J., and Coleman, M.P. (2014). Wallerian degeneration: an emerging axon death pathway linking injury and disease. *Nature Reviews Neuroscience* 15**,** 394-409.

Cutler, D.M., and Lleras-Muney, A. (2010). Understanding differences in health behaviors by education. *J Health Econ* 29**,** 1-28.

Davis, S.W., Dennis, N.A., Daselaar, S.M., Fleck, M.S., and Cabeza, R. (2008). Que PASA? The posterior-anterior shift in aging. *Cereb Cortex* 18**,** 1201-1209.

Eyler, L.T., Sherzai, A., Kaup, A.R., and Jeste, D.V. (2011). A review of functional brain imaging correlates of successful cognitive aging. *Biol Psychiatry* 70**,** 115-122.

Ferreira, L.K., and Busatto, G.F. (2013). Resting-state functional connectivity in normal brain aging. *Neurosci Biobehav Rev* 37**,** 384-400.

Fjell, A.M., Sneve, M.H., Storsve, A.B., Grydeland, H., Yendiki, A., and Walhovd, K.B. (2015). Brain Events Underlying Episodic Memory Changes in Aging: A Longitudinal Investigation of Structural and Functional Connectivity. *Cereb Cortex*.

Ghaffar, O., Fiati, M., and Feinstein, A. (2012). Occupational attainment as a marker of cognitive reserve in multiple sclerosis. *PLoS One* 7**,** e47206.

Grady, C. (2012). The cognitive neuroscience of ageing. *Nat Rev Neurosci* 13**,** 491-505.

Habeck, C., Hilton, H.J., Zarahn, E., Flynn, J., Moeller, J., and Stern, Y. (2003). Relation of cognitive reserve and task performance to expression of regional covariance networks in an event-related fMRI study of nonverbal memory. *Neuroimage* 20**,** 1723-1733.

Jones, D.K., Knosche, T.R., and Turner, R. (2013). White matter integrity, fiber count, and other fallacies: the do's and don'ts of diffusion MRI. *Neuroimage* 73**,** 239-254.

Kaup, A.R., Mirzakhanian, H., Jeste, D.V., and Eyler, L.T. (2011). A review of the brain structure correlates of successful cognitive aging. *The Journal of neuropsychiatry and clinical neurosciences* 23**,** 6-15.

Klawiter, E.C., Schmidt, R.E., Trinkaus, K., Liang, H.F., Budde, M.D., Naismith, R.T., Song, S.K., Cross, A.H., and Benzinger, T.L. (2011). Radial diffusivity predicts demyelination in ex vivo multiple sclerosis spinal cords. *Neuroimage* 55**,** 1454-1460.

Madden, D.J., Bennett, I.J., Burzynska, A., Potter, G.G., Chen, N.K., and Song, A.W. (2011). Diffusion tensor imaging of cerebral white matter integrity in cognitive aging. *Biochimica et biophysica acta*.

Maillard, P., Carmichael, O., Fletcher, E., Reed, B., Mungas, D., and Decarli, C. (2012). Coevolution of white matter hyperintensities and cognition in the elderly. *Neurology* 79**,** 442-448.

Meng, X., and D'arcy, C. (2012). Education and dementia in the context of the cognitive reserve hypothesis: a systematic review with meta-analyses and qualitative analyses. *PLoS One* 7**,** e38268.

Meunier, D., Stamatakis, E.A., and Tyler, L.K. (2014). Age-related functional reorganization, structural changes, and preserved cognition. *Neurobiol Aging* 35**,** 42-54.

Nyberg, L., Maitland, S.B., Ronnlund, M., Backman, L., Dixon, R.A., Wahlin, A., and Nilsson, L.G. (2003). Selective adult age differences in an age-invariant multifactor model of declarative memory. *Psychology and Aging* 18**,** 149-160.

O'sullivan, M., Jones, D.K., Summers, P.E., Morris, R.G., Williams, S.C., and Markus, H.S. (2001). Evidence for cortical "disconnection" as a mechanism of age-related cognitive decline. *Neurology* 57**,** 632-638.

Plassman, B.L., Welsh, K.A., Helms, M., Brandt, J., Page, W.F., and Breitner, J.C. (1995). Intelligence and education as predictors of cognitive state in late life: a 50-year follow-up. *Neurology* 45**,** 1446-1450.

Reed, B.R., Mungas, D., Farias, S.T., Harvey, D., Beckett, L., Widaman, K., Hinton, L., and

Decarli, C. (2010). Measuring cognitive reserve based on the decomposition of episodic memory variance. *Brain* 133**,** 2196-2209.

Sala-Llonch, R., Junque, C., Arenaza-Urquijo, E.M., Vidal-Pineiro, D., Valls-Pedret, C., Palacios, E.M., Domenech, S., Salva, A., Bargallo, N., and Bartres-Faz, D. (2014). Changes in whole-brain functional networks and memory performance in aging. *Neurobiol Aging* 35**,** 2193-2202.

Salthouse, T.A. (2009). Decomposing age correlations on neuropsychological and cognitive variables. *J Int Neuropsychol Soc* 15**,** 650-661.

Santos, N.C., Costa, P.S., Cunha, P., Cotter, J., Sampaio, A., Zihl, J., Almeida, O.F., Cerqueira, J.J., Palha, J.A., and Sousa, N. (2013). Mood is a key determinant of cognitive performance in community-dwelling older adults: a cross-sectional analysis. *Age (Dordr)* 35**,** 1983-1993.

Santos, N.C., Costa, P.S., Cunha, P., Portugal-Nunes, C., Amorim, L., Cotter, J., Cerqueira, J.J., Palha, J.A., and Sousa, N. (2014). Clinical, physical and lifestyle indicators and relationship with cognition and mood in aging: a cross-sectional analysis of distinct educational groups. *Frontiers in Aging Neuroscience* 6.

Scarmeas, N., Zarahn, E., Anderson, K.E., Habeck, C.G., Hilton, J., Flynn, J., Marder, K.S., Bell, K.L., Sackeim, H.A., Van Heertum, R.L., Moeller, J.R., and Stern, Y. (2003). Association of life activities with cerebral blood flow in Alzheimer disease: implications for the cognitive reserve hypothesis. *Arch Neurol* 60**,** 359-365.

Singh-Manoux, A., Kivimaki, M., Glymour, M.M., Elbaz, A., Berr, C., Ebmeier, K.P., Ferrie, J.E., and Dugravot, A. (2012). Timing of onset of cognitive decline: results from Whitehall II prospective cohort study. *British Medical Journal* 344.

Soares, J.M., Sampaio, A., Ferreira, L.M., Santos, N.C., Marques, F., Palha, J.A., Cerqueira, J.J., and Sousa, N. (2012). Stress-induced changes in human decision-making are reversible. *Transl Psychiatry* 2**,** e131.

Song, J., Birn, R.M., Boly, M., Meier, T.B., Nair, V.A., Meyerand, M.E., and Prabhakaran, V.

(2014). Age-related reorganizational changes in modularity and functional connectivity of human brain networks. *Brain Connect* 4**,** 662-676.

Stern, Y. (2002). What is cognitive reserve? Theory and research application of the reserve concept. *J Int Neuropsychol Soc* 8**,** 448-460.

Stern, Y., Zarahn, E., Hilton, H.J., Flynn, J., Delapaz, R., and Rakitin, B. (2003). Exploring the neural basis of cognitive reserve. *J Clin Exp Neuropsychol* 25**,** 691-701.

Sun, S.W., Liang, H.F., Cross, A.H., and Song, S.K. (2008). Evolving Wallerian degeneration after transient retinal ischemia in mice characterized by diffusion tensor imaging. *Neuroimage* 40**,** 1-10.

Taki, Y., Kinomura, S., Sato, K., Goto, R., Wu, K., Kawashima, R., and Fukuda, H. (2011). Correlation between gray/white matter volume and cognition in healthy elderly people. *Brain Cogn* 75**,** 170-176.

Tomasi, D., and Volkow, N.D. (2012). Aging and functional brain networks. *Mol Psychiatry* 17**,** 471, 549-458.

Wang, L., Goldstein, F.C., Levey, A.I., Lah, J.J., Meltzer, C.C., Holder, C.A., and Mao, H. (2011). White matter hyperintensities and changes in white matter integrity in patients with Alzheimer's disease. *Neuroradiology* 53**,** 373-381.

Wilson, R.S., Hebert, L.E., Scherr, P.A., Barnes, L.L., Mendes De Leon, C.F., and Evans, D.A. (2009). Educational attainment and cognitive decline in old age. *Neurology* 72**,** 460-465.

Winkleby, M.A., Jatulis, D.E., Frank, E., and Fortmann, S.P. (1992). Socioeconomic status and health: how education, income, and occupation contribute to risk factors for cardiovascular disease. *Am J Public Health* 82**,** 816-820.

Wunderlich, K., Dayan, P., and Dolan, R.J. (2012). Mapping value based planning and extensively trained choice in the human brain. *Nat Neurosci* 15**,** 786-791.

Zihl, J., Fink, T., Pargent, F., Ziegler, M., and Buhner, M. (2014). Cognitive reserve in young

and old healthy subjects: differences and similarities in a testing-the-limits paradigm with DSST. PLoS One 9, e84590.